

**INVESTIGATION OF THE MECHANICAL AND
PHYSICAL PROPERTIES OF BARIUM GLASS
AND ZIRCONIA NANOPARTICLE FILLED RESIN-
BASED DENTAL COMPOSITES**

**A Thesis Submitted to
the Graduate School of
İzmir Institute of Technology
in Partial Fulfillment of the Requirements for the Degree of**

MASTER OF SCIENCE

in Mechanical Engineering

**by
Nazife ÇERÇİ**

**JUNE 2024
İZMİR**

We approve the thesis of **Nazife ÇERCI**

Examining Committee Members:

Prof. Dr. Metin TANOĞLU

Department of Mechanical Engineering, İzmir Institute of Technology

Prof. Dr. Ekrem ÖZDEMİR

Department of Chemical Engineering, İzmir Institute of Technology

Assoc. Prof. Dr. Aylin ZİYLAN

Department of Metallurgical and Materials Engineering, Dokuz Eylül University

11 June 2024

Prof. Dr. Metin TANOĞLU

Supervisor, Department of Mechanical Engineering, İzmir Institute of Technology

Prof. Dr. M. İ. Can DEDE

Head of the Department of Mechanical Engineering

Prof. Dr. Mehtap EANES

Dean of the Graduate School

ACKNOWLEDGEMENTS

I would like to express gratitude to my advisor, Prof. Dr. Metin TANOĞLU for his guidance, support, motivation, and encouragement during my thesis. I would also like to thank to my committee members Prof. Dr. Ekrem ÖZDEMİR and Assoc. Prof. Dr. Aylin ZİYLAN for their constructive review of the final manuscript.

I would like to thank Mustafa İlker AKTAŞ from Gülsa Medical Devices and Materials Industry and Trade Inc. and Elçin ÜNVER from Atlas-Enta Dentistry Industry and Trade Inc. for providing the materials and for their advice throughout my thesis.

I would like to thank Dr. Aref CEVAHİR for his valuable contributions, understanding, encouragement, and also his advice throughout my study.

I am grateful to my project members Senagül TUNCA TAŞKIRAN and Büşra Öykü ALAN for their help, support and contributions. My laboratory friends and colleagues, who helped and supported me during my thesis; Ahmet Ayberk GÜRBÜZ, Ceren TÜRKDOĞAN DAMAR, Gözde ESENOĞLU, Hande İPLİKÇİ, Seçkin MARTİN, Muhammet Erdal ULAŞLI and Onur ÖZCAN.

And also, I would like to thank IZTECH Center for Materials Research (MAM) and Biotechnology and Bioengineering Application and Research Center for their contribution to the analysis in this thesis.

Last, but most importantly, I offer sincere thanks to my mother Serbay ÇERCİ, my father Sedat ÇERCİ and especially my dear little sister Sinem ÇERCİ for their support, continuous advice, motivation, inspiration, encouragement throughout my life and believing in me. I feel very lucky to have them in my life. I would not have been able to achieve my goals without their support.

ABSTRACT

INVESTIGATION OF THE MECHANICAL AND PHYSICAL PROPERTIES OF BARIUM GLASS AND ZIRCONIA NANOPARTICLE FILLED RESIN-BASED DENTAL COMPOSITES

The amalgams traditionally used in dental fillings cause a number of serious health problems, largely due to the mercury they contain. Furthermore, amalgam fillings, which do not match the colour of the tooth, also have a negative effect on aesthetics. On the other hand, the development of resin-based dental composites, which have a good aesthetic appearance due to their compatibility with tooth colour, high mechanical properties, high radiopacity, low polymerisation shrinkage and ease of application, have become the preferred alternative to amalgam fillings in dentistry.

In this thesis, the effects of different concentrations (wt.%) of zirconia and barium glass nanoparticles on the mechanical and physical properties of the resin based composite were studied. The total filler concentration of the composites was 65 wt.%. The composites were prepared by dispersing 20 wt.% and 30 wt.% surface modified barium glass, 1 wt.% and 2 wt.% surface modified zirconia nanoparticles in the monomer mixture containing 40 wt.%, 30 wt.% and 30 wt.% Bis-GMA, UDMA and TEGDMA, respectively. The mechanical properties; flexural strength and compressive strength, depth of cure, polymerization shrinkage and water sorption and solubility of the resin based composites were examined. The fracture surface of composites was investigated using scanning electron microscopy (SEM).

Three point bending and compression test results showed that barium glass and zirconia nanoparticles noticeably enhanced the mechanical properties of the composites. The Ba30Z1 sample containing 30 wt.% barium glass and 1 wt.% zirconia achieved the highest flexural strength of 79.09 ± 3.32 MPa with a 37% increase over the reference sample. The Ba20Z2 sample containing 20 wt.% barium glass and 2 wt.% zirconia achieved the highest compressive strength of 250.05 ± 8.01 MPa with a 41% increase over the reference sample.

ÖZET

BARYUM CAMI VE ZİRKONYA NANOPARTİKÜL DOLGULU REÇİNE BAZLI DENTAL KOMPOZİTLERİN MEKANİK VE FİZİKSEL ÖZELLİKLERİNİN ARAŞTIRILMASI

Geleneksel olarak diş dolgularında kullanılan amalgamlar, büyük ölçüde içerdikleri cıva nedeniyle bir dizi ciddi sağlık sorununa neden olmaktadır. Ayrıca dişin rengine uymayan amalgam dolgular estetiği de olumsuz etkilemektedir. Öte yandan, diş rengiyle uyumu, yüksek mekanik özellikleri, yüksek radyopasitesi, düşük polimerizasyon büzülmesi ve uygulama kolaylığı nedeniyle iyi bir estetik görünüme sahip olan reçine bazlı dental kompozitlerin geliştirilmesi, diş hekimliğinde amalgam dolgulara tercih edilen alternatif haline gelmiştir.

Bu tezde, farklı konsantrasyonlardaki (ağ.%) zirkonya ve baryum cam nanopartiküllerinin reçine esaslı kompozitin mekanik ve fiziksel özellikleri üzerindeki etkileri incelenmiştir. Kompozitlerin toplam dolgu maddesi konsantrasyonu ağ.% 65'tir. Kompozitler, sırasıyla ağ.% 40, ağ.% 30 ve ağ.%30 Bis-GMA, UDMA ve TEGDMA içeren bir monomer karışımında ağ.% 20 ve ağ.% 30 yüzey modifiye baryum camı, ağ.% 1 ve ağ.% 2 yüzey modifiye zirkonya nanopartiküllerinin dağıtılmasıyla hazırlanmıştır. Reçine esaslı kompozitlerin mekanik özellikleri; eğilme mukavemeti ve basınç mukavemeti, kürlenme derinliği, polimerizasyon büzülmesi ve su sorpsiyonu ve çözünürlüğü incelenmiştir. Kompozitlerin kırılma yüzeyi taramalı elektron mikroskobu (SEM) kullanılarak incelenmiştir.

Üç nokta eğme ve sıkıştırma testi sonuçları, baryum camı ve zirkonya nanopartiküllerinin kompozitlerin mekanik özelliklerini belirgin şekilde geliştirdiğini göstermiştir. ağ.% 30 baryum camı ve ağ.% 1 zirkonya içeren Ba30Z1 numunesi, referans numuneye göre %37'lik bir artışla $79,09 \pm 3,32$ MPa ile en yüksek eğilme dayanımına ulaşmıştır. ağ.% 20 baryum camı ve ağ.% 2 zirkonya içeren Ba20Z2 numunesi, referans numuneye göre %41'lik bir artışla $250,05 \pm 8,01$ MPa ile en yüksek basınç dayanımına ulaşmıştır.

TABLE OF CONTENTS

LIST OF FIGURES	viii
LIST OF TABLES	x
CHAPTER 1. INTRODUCTION	1
CHAPTER 2. DENTAL COMPOSITE MATERIALS.....	4
2.1. Structure of the Human Tooth.....	4
2.2. Dental Composites	5
2.3. Structure of the Resin-Based Composites.....	7
2.3.1. Organic Phase (Resin Matrix).....	7
2.3.2. Inorganic Phase (Reinforcement)	10
2.3.2.1. Silica (SiO ₂).....	11
2.3.2.1.1. Fumed Silica	12
2.3.2.1.2. Colloidal Silica.....	12
2.3.2.2. Zirconia (ZrO ₂)	13
2.3.2.3. Barium Glass	13
2.4. Initiator and Accelerator System.....	14
2.4.1. Chemically cured Composites	15
2.4.2. Light-cured Composites.....	15
2.4.3. Dual cured Composites	18
2.5. Coupling Agent	18
2.6. Properties of Resin Based Composites	20
2.6.1. Degree of conversion	20
2.6.2. Polymerization Shrinkage.....	21
2.6.3. Mechanical Properties.....	22
2.6.4. Colour stability & Aesthetic Properties	22
2.6.5. Water Sorption and Solubility	23
2.6.6. Optical Properties	24
2.6.7. Radiopacity	25

CHAPTER 3. LITERATURE REVIEW	26
CHAPTER 4. EXPERIMENTAL.....	30
4.1. Materials.....	30
4.2. Surface Modification of Inorganic Particles	32
4.3. Preparation of Dental Composites	33
4.4. Characterization of Particles and Dental Composites.....	36
4.4.1. Scanning Electron Microscopy (SEM) and EDS Analysis.....	36
4.4.2. Dynamic Light Scattering (DLS) Analysis of Nanoparticles	37
4.4.3. Fourier Transform Infrared Spectroscopy (FT-IR).....	37
4.5. Mechanical Tests of Dental Composites.....	38
4.5.1. Three Point Bending Test	38
4.5.2. Compression Test	40
4.6. Depth of Cure Determination of Dental Composite	42
4.7. Water Sorption and Solubility Test of Dental Composites.....	42
4.8. Polymerization Shrinkage Measurement of Dental Composites	44
CHAPTER 5. RESULTS AND DISCUSSION.....	46
5.1. Characterization Results.....	46
5.1.1. Scanning Electron Microscopy (SEM) and EDS Analysis.....	46
5.1.2. Dynamic Light Scattering (DLS) Analysis of Nanoparticles	55
5.1.3. Fourier Transform Infrared Spectroscopy (FT-IR).....	58
5.2. Mechanical Test Results	61
5.2.1. Three-Point Bending Test Results	61
5.2.2. Compression Test Results.....	64
5.3. Depth of Cure Determination Results of Dental Composites	66
5.4. Water Sorption and Solubility Test Results of Dental Composites	68
5.5. Polymerization Shrinkage Test Results of Dental Composites.....	70
CHAPTER 6. CONCLUSION	73
6.1. Future Works.....	75
REFERENCES	76

LIST OF FIGURES

<u>Figure</u>	<u>Page</u>
Figure 2.1. General structure of a human tooth	4
Figure 2.2. Schematic illustration of a composite	6
Figure 2.3. Structure of dental composite resin materials	7
Figure 2.4. Chemical Structure of the monomers	9
Figure 2.5. Photoinitiator mechanism of CQ in the presence of tertiary amine	16
Figure 2.6. Polymerization steps (a)free radicals formation,(b) initiation step, (c)polymer chain propagation step of the polymerization by addition of the monomer units,(d)chain termination step of polymerization by monomer radical collision	16
Figure 2.7. Molecular structure of widely used initiators; a)CQ, b)TPO, c)PPD.....	17
Figure 2.8. Molecular structure of widely used co-initiators; (a) DMAEMA, (b) DMPT, (c) EDAB (Source : B.Pratap et.al.2019).....	18
Figure 2.9. (a) structure of γ -MPS, (b) process of surface threated fillers with γ -MPS	19
Figure 2.10. Radio-opacity image of dental composite	25
Figure 4.1. (a) Colloidal silica 40 wt.% SiO ₂ -60 wt.% water, (b) colloidal silica after pre-drying	32
Figure 4.2. Surface modification process of the nanoparticles; (a) chemical mixture, (b) particle addition to chemical mixture, (c) remove the volatile chemicals at 80°C for 24 hours, (d) surface modified particles	33
Figure 4.3. (a) Resin mixture with CQ&EDMA,(b) ZrO ₂ ,Ba glass particles addition,(c) colloidal SiO ₂ addition,(d) fumed SiO ₂ by hand mixing, (e) after mixing in mortar mill,(f) fumed SiO ₂ addition in the mortar mill,(g) composite mixing in mortar mill, (h) final state	35
Figure 4.4. Automatic mortar mill for homogeneous dispersion of the particles	35
Figure 4.5. Light curing unit used in the curing process	36
Figure 4.6. Mould used in the preparation of bending specimens: (a) open, (b) close.....	38
Figure 4.7. The top view of the curing zones of flexural strength test specimen	38
Figure 4.8. The test setup for three-point bending test	39
Figure 4.9. The specimens were tested using a three-point bending method	39
Figure 4.10. Mould used in the preparation of compression specimens: (a)open, (b) close.....	40
Figure 4.11. Compression test setup.....	41
Figure 4.12. Compression test specimens.....	41
Figure 4.13. View of the mould and curing zones used for water absorption and solubility samples.....	42
Figure 4.14. Water sorption and solubility test specimens	43
Figure 4.15. Measuring the mass of a sample in (a) air, (b) water.	44

<u>Figure</u>	<u>Page</u>
Figure 5.1. SEM image of untreated fumed silica nanoparticles at 100000X magnification	46
Figure 5.2. SEM image of untreated colloidal silica nanoparticles: (a) at 100000X magnification,(b) average particle size at 400000X magnification	47
Figure 5.3. SEM image of untreated zirconia nanoparticles: (a) at 100000X magnification, (b) average particle size at 200000X magnification	47
Figure 5.4. SEM image of modified barium glass particles: (a) at 50000X magnification, (b) average particle size at 100000X magnification	48
Figure 5.5. SEM images in the secondary electron mode of the fracture surface of composites: (a) Ref., (b) Z1, (c) Z2, (d) Ba20, (e) Ba20Z1, (f) Ba20Z2, (g) Ba30, (h) Ba30Z1, (i) Ba30Z2	48
Figure 5.6. SEM images in the backscattered electron mode of the fracture surface of composites: (a) Ref., (b) Z1, (c) Z2, (d) Ba20, (e) Ba20Z1, (f) Ba20Z2, (g) Ba30, (h) Ba30Z1, (i) Ba30Z2	50
Figure 5.7. Morphological structure image shows spectrum 1 of Z2 composite.....	52
Figure 5.8. Elemental analysis of Z2 composite results for spectrum 1	52
Figure 5.9. Morphological structure image shows spectrum 2 of Z2 composite.....	53
Figure 5.10. Elemental analysis of Z2 composite results for spectrum 2	53
Figure 5.11. EDS mapping analysis of Z2 composite	54
Figure 5.12. Morphological structure image of Ba20Z2 composite.....	55
Figure 5.13. Elemental analysis of Ba20Z2 composite results for spectrum 10	55
Figure 5.14. Particle size distribution of fumed silica	56
Figure 5.15. Particle size distribution of colloidal silica	56
Figure 5.16. Particle size distribution of zirconia	57
Figure 5.17. Particle size distribution of barium glass	57
Figure 5.18. FTIR spectra of fumed silica particles with and without surface modification	59
Figure 5.19. FTIR spectra of colloidal silica particles with and without surface modification	59
Figure 5.20. FTIR spectra of zirconia particles with and without surface modification	60
Figure 5.21. FTIR spectra of barium glass particles with and without surface modification	60
Figure 5.22. Flexural strength results of dental composites with their standard deviation.....	62
Figure 5.23. Flexural modulus results of dental composites with their standard deviation.....	64
Figure 5.24. Compressive strength results of dental composites with their standard deviation.....	65
Figure 5.25. Curing depth of dental composites with their standard deviation	67
Figure 5.26. Water sorption results of dental composites with their standard deviation.....	69
Figure 5.27. Water solubility results of dental composites with their standard deviation.....	69
Figure 5.28. Polymerization shrinkage results of dental composites	71

LIST OF TABLES

<u>Table</u>	<u>Page</u>
Table 2.1. Component of enamel, dentin and cementum of tooth structure.....	5
Table 2.2. Detailed properties of the monomers.....	9
Table 2.3. Basic Properties of widely preferred initiators	17
Table 2.4. Basic properties of widely preferred cointiators.....	18
Table 2.5. Refractive indices of resin monomers and fillers	24
Table 4.1. The molecular weight and supplier of the chemicals used for resin matrix	30
Table 4.2. Detailed properties of the fillers used in resin-based dental composites	31
Table 4.3. Details of the chemicals used for surface modification.....	31
Table 4.4. Inorganic nanoparticles concentration of the composite groups produced.....	34
Table 5.1. Flexural strength and modulus of dental composites	61
Table 5.2. Compressive strength of dental composites	65
Table 5.3. Curing depth of the composites	66
Table 5.4. Water sorption and water solubility of the dental composites.....	68
Table 5.5. Polymerization shrinkage of dental composites	71

CHAPTER 1

INTRODUCTION

Teeth play a significant role in chewing, speech and human health. They are of great importance for both the aesthetic appearance and the quality of life. Dental problems are one of the common problems experienced by the majority of the population.¹

Teeth are one of the hardest parts of the human body, like bones and inorganic and organic materials are found in the compositions of bones and teeth. However, even if their structural components are similar, the bone can heal by producing new cells on its own when it is injured or broken while it is not possible for the tooth to heal on its own after damage. External intervention is required to repair a damage to the tooth.²

Tooth decay and cavities are a common and leading problem that people suffer from when it comes to dental issues. This problem is quite widespread in society, and affects both adults and children, in particular, between 60% and 90% children of school age are faced with the problem of tooth deterioration, which is mainly caused by the build-up of bacteria from food and drink.³ This problem has been solved by removing the decay from the tooth surface of the tooth and filling the gaps that have formed. Amalgam has been used as a dental filling material over 150 years in this situation.^{4,5}

Dental amalgam fillings are made up of two main components: mercury and the commonly used metals silver, copper and tin. The content of these components is 50% mercury, 50% silver, zinc, tin and other metals (less than 3%). Amalgam fillings have been widely used for more than a century due to several advantages. These advantages include affordability, durability, longevity, ease of application and good strength. In addition to these advantages, there are also some disadvantages. Because it contains toxic mercury, amalgam is harmful to the health of both the patient and the dentist.⁶ Another disadvantage is the amount of mercury it contains, and the mercury that is released from the amalgam over the years is dangerous to the environment. Also, aesthetic appearance is very important to people nowadays, and amalgam fillings have disadvantages for the aesthetic appearance of the tooth.⁷

In recent years, resin-based composite materials which were discovered by Bowen. Bowen's inorganic particle formulation of Bis-GMA (2,2-bis[4-(2-hydroxy-3-

methacryloxypropoxy) phenyl] propane) is an important step for contemporary dental composites in the early 1960s⁸ have been developed to overcome these negative effects of amalgam and have been commonly used as a replacement for amalgam fillings.⁹

Dental composite materials have become popular in dentistry due to their unique properties, such as higher mechanical properties, low polymerisation shrinkage, high radiopacity, good aesthetics and easy application. Another important feature of resin-based composite fillings is that they are highly compatible with the tooth surface and do not contain toxic metals like mercury.¹⁰

Resin composites consist of three main components, an organic phase (resin matrix), an inorganic phase (inert fillers) and a coupling agent. Initiators and accelerators are used for the polymerisation and pigments are also included in the compositions.⁵

Commonly, Bis-GMA (bisphenol a glycidyl methacrylate), TEGDMA (triethylene glycol dimethacrylate), UDMA (urethane dimethacrylate) and BisEMA (ethoxylated bisphenol a dimethacrylate) are used in resin composites. In resin-based composites, Bis-GMA is the most commonly used monomer as a matrix. It is used in combination with TEGDMA monomer to reduce its high viscosity. Bis-EMA is the ethoxylated version of Bis-GMA and UDMA is another alternative monomer to Bis-GMA that is widely used in commercial dental composites.¹¹

Reinforcing inorganic particles are essential to improve the mechanical properties of the composites. Typically, silica, quartz or ceramics are dispersed in the resin matrix as reinforcing particles in a ratio of 35% to 85% in resin-based dental composites.² The properties of composites are determined by the size, shape, and quantity of the filler particles. Different inorganic filler particles such as colloidal silica, quartz, silica glass containing strontium, barium, and zirconium are used to get the higher mechanical properties and lower polymerization shrinkage and water absorption of the composites.⁸

Inorganic nanoparticles are used as fillers in a resin matrix after surface modification. In the modification process, a silane is used as a binding agent to create a strong interface between the inorganic particle and the matrix phase, which is critical for the properties of composite materials.¹² Nanoparticles are commonly silanized with 3-methacryloxypropyltrimethoxysilane (MPTS), and also camphorquinone (CQ) and ethyl-4-(N, N-dimethylamino) benzoate (4EDMAB) are added as an initiator and accelerator in the resin based composites.³

Although resin-based dental composites are very popular due to their mechanical, optical and biocompatible properties suitable for tooth structure, they also have disadvantages such as polymerisation shrinkage. Polymerisation shrinkage is very important due to the growth of microorganisms such as *Streptococcus mutans* and *Candida albicans* in the space between the tooth enamel and the filling, leading to secondary caries.¹³ Different studies are ongoing to prevent polymerisation shrinkage and improve the mechanical properties of dental composites.

The aim of this study was to investigate the effects of barium glass and zirconia nanoparticles on the mechanical and physical properties of resin-based composites. The individual and combined effects of 20 wt.% and 30 wt.% barium glass and 1 wt.% and 2 wt.% ZrO₂ nanoparticles on the composite were investigated. The total filler content of all prepared composites was maintained at 65 wt.%. The effects of these nanoparticles on the flexural and compressive strength, depth of cure, water absorption, solubility and polymerisation shrinkage of the composite were examined. The modification of the particles was analysed by Fourier Transform Infrared Spectroscopy (FTIR) and the fracture surfaces of the specimens were examined by Scanning Electron Microscopy (SEM) and EDS Analysis.

CHAPTER 2

DENTAL COMPOSITE MATERIALS

2.1. Structure of the Human Tooth

The structure of human teeth is highly complex. Compared to restorative materials, they exhibit superior mechanical properties and biocompatibility, among other properties. The mechanical properties of human teeth depend on their composition and structure; these structures consist of enamel, dentin, cementum and pulp. Enamel, dentin and cementum are the hardest tissues in human teeth¹⁴. The schematic illustration of the structure of a human tooth is given in Figure 2.1.

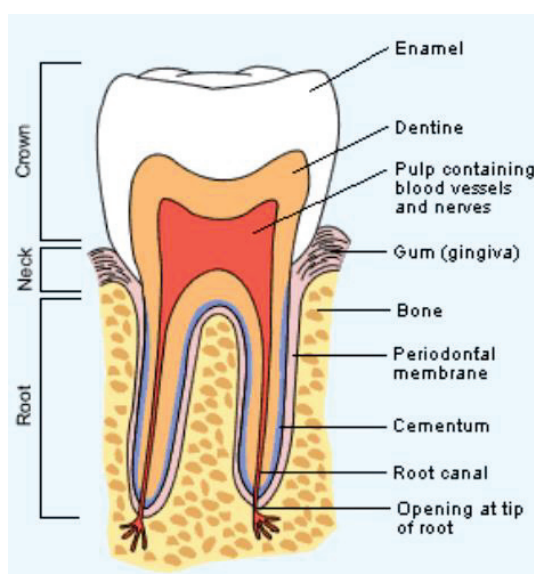


Figure 2.1. General structure of a human tooth

Enamel, the hardest and most mineralised tissue in the body, is white and transparent. Enamel is a thin layer, approximately 2 mm thick that protects the dentin by covering it. Enamel has a crystalline structure and its composition consists of 96% inorganic materials and the remaining 3% water and 1% organic materials by weight. Hydroxyapatite, a crystallised calcium phosphate, is the fundamental mineral component of enamel.¹⁵

Dentin is a tissue that surrounds the pulp and root canals just below the enamel. Dentin is approximately 70% inorganic structure by weight, with the remainder being

organic structure and water about 18% and 12% respectively. It has a partially crystalline structure. Due to its high calcium salt content, it has a structure similar to that of bone. Dentin contains dentin tubes extending from the pulp and a high proportion of collagen.¹⁶

Cementum is a special structure similar to bone tissue that covers the surface of the tooth root. It is less hard than dentin. It consists of an inorganic structure in the form of apatite containing calcium ions and an organic structure containing both collagen and non-collagen proteins.¹⁴

Pulp is a soft structure opposite to the other three structures. It is located at the bottom and centre of the human tooth. The pulp is a soft tissue containing blood vessels and nerves that help nourish the tooth, as well as lymphatic vessels that carry white blood cells to the tooth. The white blood cells help the tooth fight bacterial infections.¹⁴ The composition of enamel, dentin and cementum is shown in Table 2.1.

Table 2.1. Component of enamel, dentin and cementum of tooth structure (Source: Zhang)

Dental tissue	Composition (wt.%)		
	Inorganics	Organics	Water
Enamel	96	1	3
Dentin	70	18	12
Cementum	45-50	50-55	

Teeth are classified into two distinct groups: incisors and canines are anterior (the front teeth), premolars and molars are posterior (the back teeth) teeth. Premolars and molars are used for grinding food, while incisors and canines are used for tearing and piercing food. Therefore, the forces the teeth are exposed to are different. As incisors and canines are primarily used for cutting and biting, they require higher flexural strength. On the other hand, premolars and molars require higher compressive strength due to the pressure exerted during chewing.¹⁷

2.2. Dental Composites

Composites are materials that are a combination of two or more different types of materials and have properties that are superior to the properties of the individual materials in which they are combined.¹⁸ Composite materials consist of an organic

phase or a continuous phase, and an inorganic phase, or a discontinuous phase. The continuous phases are called the matrix, while the discontinuous phases are called the reinforcing materials or reinforcements. Reinforcements are uniformly distributed within a matrix to achieve superior properties, as they have higher mechanical properties than the matrix.¹⁹

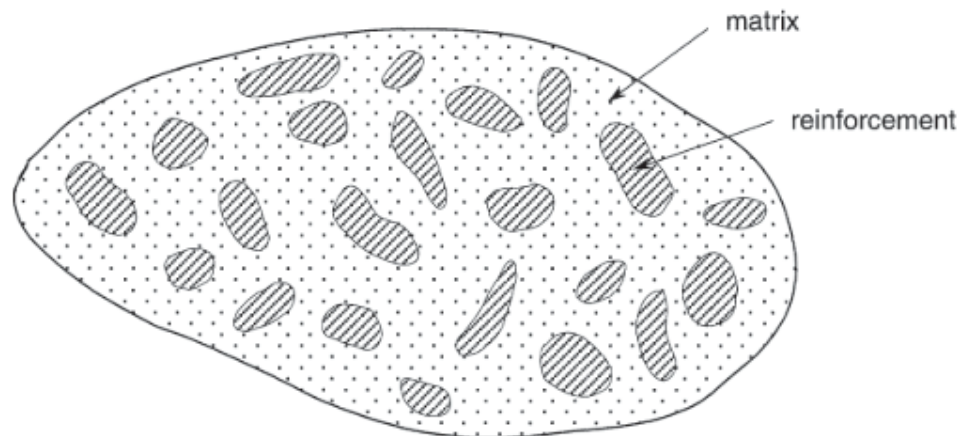


Figure 2.2. Schematic illustration of a composite

A new dental composite was developed when Bowen discovered Bis-GMA monomer. The properties of the matrix and the interfacial properties between the organic silane, coupling agent, and the surface of the modified inorganic fillers have been improved. This overcomes the problems that have been encountered with previous dental composites.¹⁶

Dental composites, which have been the subject of further research since this important invention, are an important part of dentistry. Today, they are very popular in aesthetic tooth repair because they are very close to the structure, colour and translucency of the tooth. The surfaces of the small particle size, high surface area nanoparticles are homogeneously distributed in the resin matrix after binding with silane coupling agent. This results in composites with improved physical properties, biocompatible and simultaneously highly resistant to external mechanical effects. As they can be well bonded to the surface of the tooth, they offer the possibility of repairing with a small amount of loss from the intact surface of the tooth, without the need for large cavities as with amalgam fillings.²⁰

2.3. Structure of the Resin-Based Composites

Dental composites consist of three principal parts; organic phase (matrix), inorganic phase (reinforcement or reinforcing fillers) and coupling agent. Other additives such as initiators, accelerators and pigments for colour matching are also important for dental composites.

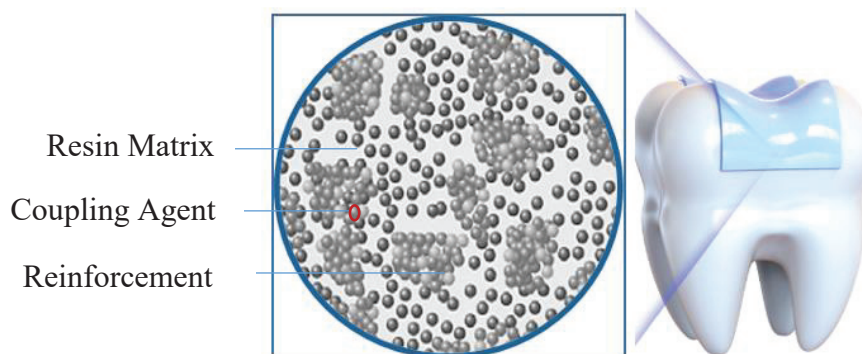


Figure 2.3. Structure of dental composite resin materials

2.3.1. Organic Phase (Resin Matrix)

Metacrylate-based resins are used as the organic phase in dental composites due to the C=C group in their structures. These C=C bonds in the structure of photo-initiated polymers give a rigid polymer. In commercial resin-based dental composites, dimethacrylate-based resins are widely preferred owing to their excellent mechanical properties, aesthetic quality, rapid polymerisation, good bonding to the enamel surface and ease of application.³

Bis-GMA (bisphenol a glycidyl dimethacrylate) is also known as Bowen materials since it was patented by Bowen in 1962. It is the most widely used monomer in resin based dental composites. Bis-GMA monomer, which forms the majority of the matrix phase, is a widely used monomer in resin based dental composites. It offers several advantages such as durable composites, fast curing and low polymerisation shrinkage during curing due to the low C=C bonds in its structure and its high molecular weight (MW=512 g/mol).²¹ The higher the molecular weight, the higher the viscosity of the monomer, therefore; Bis-GMA is an extremely high viscosity monomer ($\eta=1,200\text{Pa}\cdot\text{s}$), and this property makes it very difficult to add organic particles to the monomer, resulting in low particle composites.²² Dental composites with low inorganic

particle content have negative properties such as low mechanical properties and high polymerisation shrinkage, which can lead to the formation of secondary caries.³

Low viscosity TEGDMA (triethylene glycol dimethacrylate) monomer (MW=286 g/mol, $\eta=0.01$ Pa.s) is used to overcome the drawbacks of Bis-GMA by mixing with Bis-GMA monomer and diluting the composite. However, the addition of TEGDMA monomer is undesirable because it has some disadvantages for dental composites. The addition of TEGDMA monomer reduces mechanical properties, increases polymerisation shrinkage and water solubility. It also affects the colour stability of composites.

Another monomer commonly used in resin-based dental composites is UDMA (urethane dimethacrylate) monomer. This monomer has been used as an alternative high molecular weight monomer (MW=470 g/mol) to overcome the limitations of Bis-GMA monomers in composites. In addition, UDMA monomer is a monomer with lower viscosity ($\eta=23$ Pa.s) and higher flexibility compared to Bis-GMA.¹¹ It has excellent mechanical properties and reduced viscosity in combination with Bis-GMA.²¹ It is also preferable to use UDMA and TEGDMA together because of the negative properties of TEGDMA, such as polymerisation shrinkage and reduced mechanical strength. Therefore, UDMA is widely used in commercial composites and improves the mechanical and physical properties of the resin based dental composites.²³

Another important monomer is Bis-EMA (ethoxylated bisphenol a dimethacrylate) for resin based dental composites. Bis-EMA, similar in molecular weight (MW=540 g/mol) to Bis-GMA but lower viscosity than Bis-GMA. Due to the lack of hydroxyl groups in its structure, Bis-EMA has weak secondary intermolecular bonds. This makes it a low viscosity ($\eta=0.9$ Pa.s) monomer.¹¹ This monomer is an alternative monomer developed against the toxic properties of Bis-GMA. The synthesis of Bis-GMA uses bisphenol A with two methyl groups. This bisphenol A in the structure of Bis-GMA, which is the final product, is released as a result of hydrolysis by salivary enzymes. This situation has a negative impact on human health and causes some health problems, so the use of Bis-GMA in dental composites is controversial.²⁴ For these reasons, Bis-EMA has replaced Bis-GMA.

These monomers are of critical importance and are widely utilised in resin-based dental composites and commercial composites. The properties of these four monomers are given in Table 2.2. and their chemical structures are given in Figure 2.4.

Table 2.2. Detailed properties of the monomers (source: V. Gajewski et.al.2012)

Monomers	Chemical nomenclature	Molecular weight (g/mol)	Molecular formula	Viscosity (Pa.s)
Bis-GMA	bisphenol A glycidyl dimethacrylate	512	C ₂₉ H ₃₆ O ₈	1200
Bis-EMA	ethoxylated bisphenol A dimethacrylate	540	C ₃₉ H ₄₄ O ₈	0.9
UDMA	urethane dimethacrylate	470	C ₂₃ H ₃₈ N ₂ O ₈	23
TEGDMA	triethylene glycol dimethacrylate	286	C ₁₄ H ₂₂ O ₆	0.01

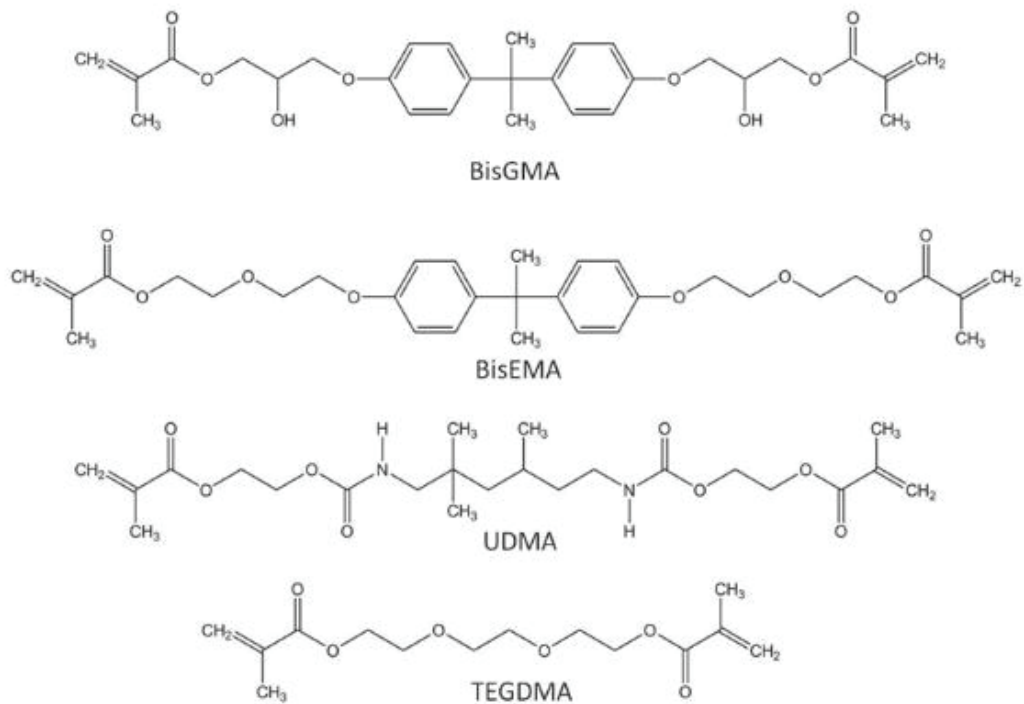


Figure 2.4. Chemical Structure of the monomers (Source: V. Gajewski et.al.2012)

2.3.2. Inorganic Phase (Reinforcement)

Inorganic nanoparticles form the reinforcement phase in composite. The addition of these fillers to the matrix phase is critical in determining the final properties of the dental composite, such as chemical, physical and mechanical properties. The particle size, quantity and distribution of filler particles in the matrix phase also significantly affect the final properties of the resin based dental composites.³ The addition of inorganic filler particles to the monomers enhances the optical properties, aesthetic appearance, fracture toughness, resistance to abrasion and elasticity modulus of the dental composites, while reducing polymerisation shrinkage, water absorption and coefficient of thermal expansion.⁸ The distribution of filler particles in the matrix phase must be homogeneous and in optimum quantities, otherwise the improved properties of the composite mentioned above will not be achieved.

There are a number of ways in which resin composites can be classified. Filler composition, filler morphology, filler size distribution and shape, surface porosity, refractive index, radiopacity and density are important for identification of inorganic particles. The distribution and average particle size of the fillers in the composite is one of the most common classifications. This classification includes macrofilled, microfilled, hybrid and nanofilled composites. Furthermore, fillers are divided into two categories: traditional fillers are macrofilled and microfilled, while modern fillers are hybrid and nanofilled. Macrofilled composites with particle size is 5-50 μm were used as the first resin based composites in 1960. They have limited and poor properties due to their large particle size. This is why they are not preferred for use in dentistry. Microfilled composites were developed to overcome the deficiencies of macrofilled composites. The particle size of the filler particles in microfilled composites is in the range 0.1-100 μm . Better polishability, improved aesthetics and excellent enamel-like translucency have been achieved with microfilled composites.³

Nanocomposites with a particle size of 0.1-100 nm play a crucial role in dentistry in the development of final product properties. Smaller filler size and surface area help to achieve good wettability and increasing the amount of filler in the matrix improves the mechanical properties, physical properties, wear resistance, aesthetic appearance and decreases polymerization shrinkage, water absorption of dental composites. There are two types of nanocomposites: nanofilled and nanohybrid.²⁵

Nanofillers allow to increase the amount of filler in the matrix phase so that the dental composite shows smoother surface and good physical properties as the gap between particles is reduced. Although it is theoretically known that 90-95 wt.% of nanofillers can be added, these amounts adversely affect the properties of the composite. The wettability of the particles is reduced and nanoparticles are easily agglomerated, so in practice lower proportion of nanofillers are added to the matrix phase.²⁵ The filler content of these existing commercial composites ranges from 70 to 80 wt.%.

Nanohybrid composites contain smaller and sub-micron particles and the hybrid composite improves dental composites by increasing the filler loading.³ The size of the nanofilled particles is between 1 and 100 nm, while the size of the nanohybrid particles is larger and in a wide range from 0.4 to 5 μm , which is why they are called nanohybrids composites.²⁵

2.3.2.1. Silica (SiO₂)

Silica (silicon dioxide), which is called quartz in crystalline form is a common filler for the resin based dental composites. Top-down approach, bottom-up solution particle synthesis and pyrogenic particle synthesis are different methods of synthesising silica particles. Irregularly shaped silica particles are obtained by the top-down process. The distribution of fillers, particle shape and particle size are critical for determining the properties of resin-based dental composites. The spherical particles showed excellent mechanical properties compared to irregularly shaped particles. For this reason, a bottom-up solution is used to obtain spherical particles in the synthesis of pyrogenic particle synthesis.

When the silica is used with Bis-GMA and TEGDMA resin mixtures, it becomes inconsiderably more opaque than some other filler particles. This is explained by the refractive indices of the silica, which at 1.46 is lower than that of conventional Bis-GMA and TEGDMA mixtures. Silica is generally preferred in dental composites due to its ease of use, low cost and its advantages such as better results after surface modification with silane coupling agents.²⁶

2.3.2.1.1. Fumed Silica

Fumed silica is a type of silicon dioxide. However, it differs from other silicon dioxides in its extremely small particle size, large surface area and amorphous structure. It, so called because silicon tetrachloride is burned in a hydrogen-oxygen furnace, is a form of colloidal silica obtained by burning silicon tetrachloride in a hydrogen-oxygen furnace.²⁷ The pyrogenic silica process (or fumed silica method) is one of the commercially developed gas synthesis processes.

Fumed silica is widely preferred as a commercial reinforcing nanoparticles in resin-based composites due to its transparency, viscosity control, polishing and adhesion properties. However, fumed silica with a particle size ranging from 7-40 nm is added to the resin at a restricted rate because of its extensive surface area. As a result, it absorbs too much resin and hold it in its structure. This prevents the composite from flowing and increases the viscosity.²⁸ Therefore, the rheological properties of the dental composite can be affected by the addition of fumed silica. The addition of fumed silica increases viscosity and improves handling properties by decreasing flow. Composite materials with excessively high or low viscosity are challenging to apply during restorative procedures. This is why the filling process does not take place as desired and the filling material cannot fully fulfil its function. It is therefore crucial to achieve the desired viscosity by adding fumed silica to the composite in specific ratio.²⁷

Fumed silica shows hydrophilic properties due to silanol groups on the surface. Silanol groups increase the viscosity by affecting the fluidity with hydrogen bonds. Fumed silica, which has shear thinning properties due to surface silanols, has a very high surface energy. Therefore, it is very difficult to disperse in the resin. This problem is overcome by modifying the surface of the silica to create hydrophobic structures with low surface energy. During the modification process, functional groups are formed on the silica surface. This makes it easier to disperse the silica particles in the resin.^{28,29}

2.3.2.1.2. Colloidal Silica

Colloidal silica particles are used as fillers in dental composites to improve the mechanical properties and polymerisation shrinkage of the composite due to their small particle size, spherical shape, high strength and low surface roughness. It is known as uniformly dispersed spherical silica particles, obtained by solution synthesis of silica

particles known as colloidal silica. The Stöber method, a sol-gel synthesis technique, is the most commonly used synthesis method. This method allows to control the shape and size of the silica particles during synthesis, resulting in spherical silica particles with diameters ranging from 5 nm to several micron size silica particles.^{26,28}

2.3.2.2. Zirconia (ZrO₂)

Zirconia, also known as zirconium dioxide (ZrO₂), is a widely used material in various application areas. Zirconia, which has been used as a biomaterial in the biomedical field since 1960, has recently become one of the most important and popular nanoparticle fillings in dentistry due to its unique properties. The mechanical properties of zirconia are similar to tooth and its colour is compatible with tooth.³⁰ It is a material with excellent resistance to corrosion and chemical reactivity, as well as being incredibly durable and strong. It has high wear resistance and high toughness, great hardness and outstanding mechanical properties. Zirconia is biocompatible, which is one of the most important features for human health, and it is also important from an aesthetic point of view because it has a natural white colour.¹

Zirconium is used as a radiopaque inorganic particle with different fillers in resin-based dental composites since zirconium is an element with a high atomic number. Radiopacity is important in restorative materials to distinguish between the natural human tooth and the restorative material. This property is achieved by adding particles containing higher atomic number elements, such as Sr (38), Zr (40) and Ba (56).³¹

Zirconia is also an opacifying metal oxide. Opacifying metal oxides have a different refractive index than the resin into which they are added. Differences in refractive index, particle size and shape will affect the transmission of light and cause the colour of the composite to be different from the desired colour. Opacifiers with irregular shapes and smaller size have higher light transmittance compared to larger spherical shaped opacifiers. Therefore, zirconia should be added to the resin in the optimum size, in the optimum shape and in limited quantities.³²

2.3.2.3. Barium Glass

Resin-based dental composites are translucent materials. The radiopaque properties of the composite allow the detection of secondary caries, worn surfaces and

cavities. This property is achieved by using fillers. However, not all fillers used in dental composites are radiopaque, for example, quartz and silica nanoparticles are not radiopaque particles. Glass and ceramic fillers containing heavy elements such as barium (Ba), zirconium (Zr), and strontium (Sr) must be added to the composite to make it radiopaque. Ba glass is a commonly used glass filler in dental composites. Glass fillers used as good radiopaque fillers are not inert like quartz and silica. Therefore, their strength is reduced by dissolution due to the conditions they are exposed to in the mouth over time. Glass-filled composites have a shorter lifetime than silica-reinforced composites because their wear resistance decreases over time.¹⁶

Refractive index is a critical factor to be considered in terms of optical properties of composites. In order to achieve the desired light transmittance, the refractive indices of fillers must be close to the resin mixture used. As the refractive indices of the silica particles containing BaO are similar to those of the resin mixture, the composites are more transparent. Borosilicate glasses, which have a higher refractive index than silica, give the composite these excellent optical properties. BaO silicates are widely preferred in commercial products.²⁶

2.4. Initiator and Accelerator System

Dimethacrylate monomers with carbon-carbon double bonds (C=C) in their structure, which are widely used in resin-based composites, are cured by chain growth polymerisation. This unsaturated double bonds allow the monomers to become polymers by polymerisation in three steps. These steps are called initiation, propagation and termination respectively.³³

Free radicals must be present in the environment to initiate the polymerisation process. Photoinitiators are used in majority of resin-based composites that contain methacrylate monomers as a source of free radicals. The weak bonds in their structure are broken in several different ways and activated to form free radicals. The initiation phase begins when the free radicals attack the double bond in the monomer, opening the pi (π) bond and converting the C=C bond into a C-C bond.³³ Molecules donate electrons. The remaining electron from the electron donor molecule goes to its end and the whole molecule becomes radical and attacks the molecule next to it. Monomers are connected to each other in this way and the polymerisation chain continues to grow. The polymerisation chain continues to grow until two radicals in the environment react and

terminate each other to finish the polymerisation. There are three different methods for the initiation of resin-based dental composites. These methods, also known as polymerisation or curing mechanisms, are light cured, chemical cured (self-cured), and dual cured.³⁴

2.4.1. Chemically cured Composites

The self-curing composites are made up of two pastes, a catalyst paste and a base paste. In these composites, the catalyst paste contains BPO (benzoyl peroxide) as initiator and the base paste contains aromatic tertiary amine (TA) as accelerator. Tertiary amine is needed to decompose BPO at room temperature.³⁵ Several tertiary amines are used as accelerators in self-cured composites, but N,N-dimethyl-p-toluidine, which is extremely reactive accelerator with BPO, is the most widely used.³⁴

2.4.2. Light-cured Composites

Light-cured composites have been used since the early 1970s. In the early days of resin-based composites, self-curing systems with two-phase components or UV initiators for photoinitiation were used for curing composites. In 1978, the discovery of camphorquinone led to its use as a visible light initiator in resin-based composites. In light-cured composites, UV initiators were initially used. However, the use of UV light sources in the 360-400 nm range for initiation of polymerisation in UV-initiated composites has been discontinued due to health concerns related to eyes and oral tissues. Therefore, super bright blue light emitting diodes (LEDs in the wavelength range 450 - 490 nm) have been proposed as an alternative light source to initiate polymerisation. In addition, visible light-cured composites were launched in 1978 with the discovery of camphorquinone. The use of camphorquinone (CQ) in combination with tertiary amine (TA) co-initiator in this new photoinitiator system resulted in greater depth of cure compared to UV-initiator systems and a higher degree of conversion than observed in chemically cured composites.³⁶

The photoinitiator system used as photoinitiator and electron donor (tertiary amine) enables photopolymerisation to take place in light-cured composites. Camphorquinone, which has a broad absorption range of 360 - 510 nm, is a yellow powder commonly used as a photoinitiator due to its peak absorption at 468 nm in the

visible light spectrum.³³ CQ interacts with TAs by absorbing light, forming short-lived excited ions in both CQ and TAs. As amines are electron donors, they transfer charge from the amine nitrogen pair to active carbonyl of CQ, resulting in the formation of two free radicals. These radicals then attack the unsaturated double bond (C=C) in the monomer, initiating the formation of new radicals in the polymer chain.³⁷ Photoinitiator mechanism of CQ with tertiary amine is given in Figure 2.5. and schematic illustration of the polymerization steps are shown in Figure 2.6.

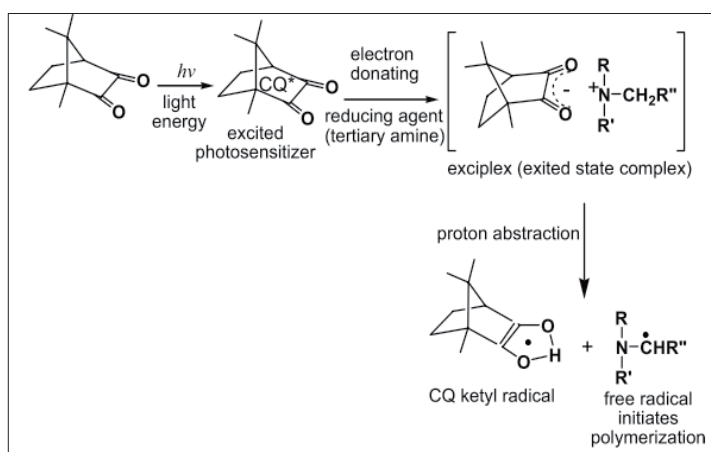


Figure 2.5. Photoinitiator mechanism of CQ in the presence of tertiary amine (Source: I.Kunio et.al.2010)

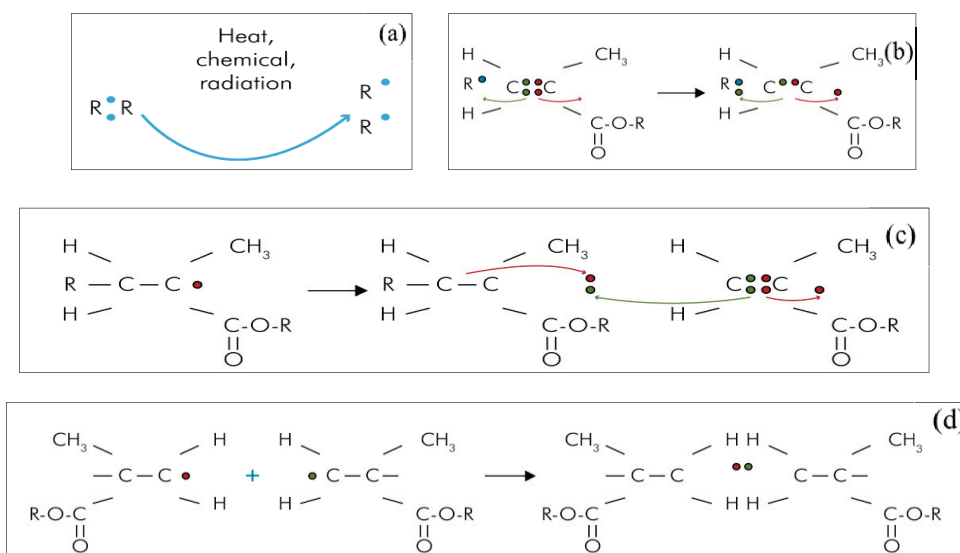


Figure 2.6. Polymerization steps (a) free radicals formation, (b) initiation step, (c) polymer chain propagation step of the polymerization by addition of the monomer units, (d) chain termination step of polymerization by monomer radical collision (Source: I. Kunio et.al.2010)

In addition to CQ, (PPD) phenylpropanedione and TPO (2,4,6-trimethyl-benzoyldiphenyl phosphine oxide) are also used as initiators in light-cured composites. Their molecular structure and detailed properties are given in Figure 2.7 and Table 2.3, respectively. PPD and TPO is white colour, unlike CQ. Therefore, while CQ may adversely affect the colour of the composite due to its yellow colour, this disadvantage is not seen with these white initiators. However, CQ is the most desirable initiator for light-cured composites due to its absorption range closely matching the emission spectrum of LEDs.³⁸

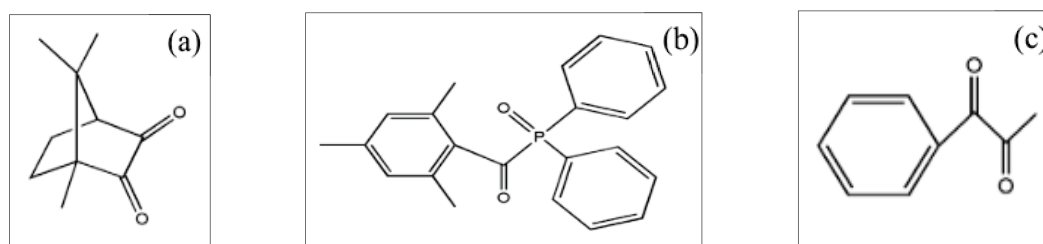


Figure 2.7. Molecular structure of widely used initiators; a)CQ, b)TPO, c)PPD
(Source: B. Pratap et.al.2019)

Table 2.3. Basic Properties of widely preferred initiators (Source:B.Pratap et.al.2019)

Name	Molecular weight	Refractive index	Density (g/cm ³)	Colour	Absorbance(nm)	
					Range	Peak
CQ	166	*	0.97	Yellow	360-510	474
TPO	348	1.48	1.12	White	230-510	385
PPD	148	1.53	1.1	White	300-480	410

Amines are used as accelerators or co-initiators to accelerate the polymerisation. Ethyl-4-(dimethylamino) benzoate (4-EDMAB), 2-(N,N-dimethylamino)ethyl methacrylate (DMAEMA) and N,N-dimethyl-p-toluidine (DMPT) are the most common accelerators used with CQ in light-cured composites. However, DMPT has been found to be toxic due to its low molecular weight.³³ Therefore, EDMAB and DMAEMA are widely preferred accelerators in light-cured composites in combination with CQ.³⁹ Their molecular structure and detailed properties are given in Figure 2.8 and Table 2.4, respectively.

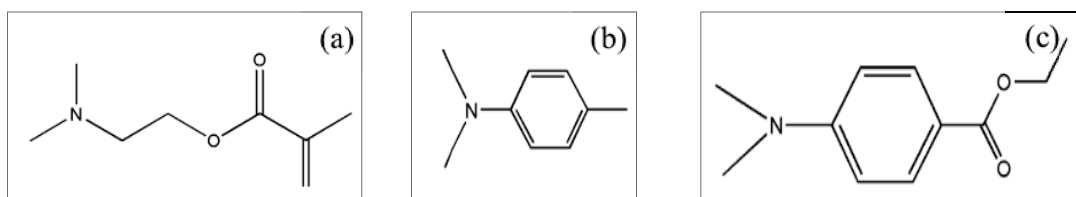


Figure 2.8. Molecular structure of widely used co-initiators; (a) DMAEMA, (b) DMPT, (c) EDAB (Source : B.Pratap et.al.2019)

Table 2.4. Basic properties of widely preferred coinitiators (Source: B.Pratap.al.2019)

Name	Molecular weight	Refractive index	Density (g/cm ³)	Colour	Absorbance (nm) (Range)
DMAEMA	157	1.44	0.93	Transparent	NA
DMPT	135	1.54	0.94	White	NA
EDAB	193	1.53	1.06	Transparent	NA

NA: Not Applicable

2.4.3. Dual cured Composites

Dual cured composites are a combination of self-cured and light cured composites. Two pastes, catalyst phase as an initiator and base phase as an accelerator are used as in chemically cured composites. However, visible light-activated photoinitiators such as CQ/amine are present in the base paste. The amine exists in the base phase to enable chemical polymerisation. Chemical cured polymerisation begins immediately at a slow rate when the two pastes are mixed. Light curing can be used to accelerate the curing process at any stage of the reaction.³⁴

2.5. Coupling Agent

The improvement of the properties of the dental composite depends significantly on the interphase formed between the matrix and the inorganic particles. The strong interphase or bond formed between them means that the inorganic particles are strongly bound to the matrix phase and have a positive effect on the mechanical and physical properties of the composite. Surface modification is applied to the inorganic particles to obtain this strong interphase. Surface modification creates a functional interphase

between the polymer matrix and the reinforcing filler, allowing covalent bonding. It also reduces the surface energy of the filler, thus increasing the amount of filler in the resin and achieving a homogeneous filler distribution.³⁷

Silane coupling agents are commonly used for surface modification of dental composites. X-Si-(OR)₃ is chemical formulation of the organofunctional silane. This organofunctional silane, which has an organofunctional (methoxy) (X) at one end and a hydrolyzable alkyl group (R) at the other, can form covalent bonds with both the silicon-oxygen groups of silica-based fillers and the methacrylate groups in the resin matrix.

The thickness of the silane film on the filler particles has an important in surface modification as it affects the efficiency of the silanization process. During silanization, the single layer closest to the particle surface is chemically bonded to the surface and ensure that a critical silane thickness is reached on the surface of the particles. Otherwise, the excess silane layer binds to the silane film covalently attached to the silica surface, forming a second organosilane layer. This has a negative effect on the ability of silane molecules to bind fillers to the matrix. Depending on the type of silane, the thickness of this critical silane layer is determined.³⁵

Silane coupling agents have shown favourable results in the inorganic phase, especially in silica particles, so silica-containing inorganic fillers have been used in the majority of composite resins. Silane coupling agents containing trialkoxysilane are commercially used in dentistry. Among these trialkoxysilane silane types, 3-methacryloxypropyltrimethoxysilane (γ -MPS) is widely used.⁴⁰ Figure 2.9. illustrate the structure of γ -MPS and the surface modification of filler particles with γ -MPS silane respectively.

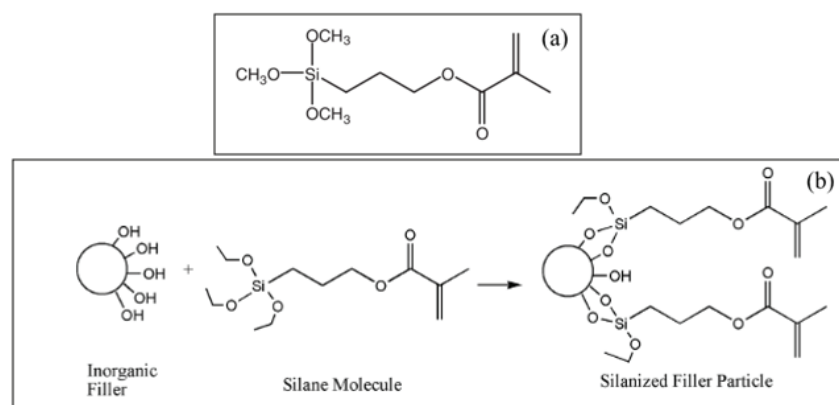


Figure 2.9. (a) structure of γ -MPS, (b) process of surface threaded fillers with γ -MPS (source: N.B. Cramer et.al.2011, ICC.de M. Porto et.al.2010)

2.6. Properties of Resin Based Composites

Restorative composites are used to repair any problem that occurs in the tooth. These composite materials are expected to be compatible with the natural tissue, to have the same properties and to maintain these properties for as long as possible. The restorative material used must be able to withstand chewing forces, different pH and temperature values in the mouth. In addition, water absorption and solubility properties of restorative composite materials are expected to be at minimum value. In terms of aesthetic appearance, it is expected to be close to the natural colour of the tooth and to restore the aesthetic appearance. The properties of the dental material also determine these properties.

2.6.1. Degree of conversion

The degree of conversion (DC), also known as the polymerisation degree of a monomer, is the proportion of C=C double bonds that are converted to C-C single bonds during polymerisation to form a polymer from a monomer. High DC values in resin-based composites are desirable to improve the mechanical and physical properties of the composites as well as their biocompatibility. It is important to note that DC is below the 100%, and for dimethacrylate polymers DC is typically ranges between 43% and 75%.³⁵

The properties of the composite material, such as strength, colour stability, water absorption and solubility, hardness and dimensional stability, are significantly affected by DC. As a result of these properties, it has a significant effect on secondary caries, microleakage and possible pulpal reactions. Several factors influence the DC in resin-based composites, including the quantity and size of inorganic fillers, the amount, ratio, and types of monomers, and the amount and type of initiators and accelerators. Additionally, factors such as composite translucency, light source colour and wavelength, and curing time can also affect the DC of the composites.⁴¹ The thickness of the composite is also a factor that affects the DC. The intensity of light reaching the underside of the composite is less than that reaching the surface. As the thickness of the composite increases, light absorption decreases due to scattering and as a result DC decreases.³⁵ The degree of conversion of the composite is characterised using Raman spectroscopy or infrared characterisation methods.⁴²

2.6.2. Polymerization Shrinkage

One of the major disadvantages of dental composites is the shrinkage that occurs during polymerisation. This property is directly related to the amount of filler in the composite and the resin used. The van der Waals bonds of the matrix phase prior to polymerisation are transformed into tighter covalent bonds as a result of the polymerisation reaction. During this transformation, a decrease in voids and volumetric shrinkage is observed, which is called polymerisation shrinkage. As a result of polymerisation shrinkage, shrinkage stresses occur in the composite. Internal stresses and deformations occur in the adjacent tooth, resulting in adverse symptoms such as poor bonding of the composite to the tooth, secondary caries and pain. The polymerisation shrinkage is affected by the filler content, molecular weight of the monomer, and DC. Additionally, the elastic modulus of the composite has a significant impact on the shrinkage.^{43,44}

The conversion of the monomers into a densely packed polymer network during the polymerisation process, which results in a volumetric shrinkage, occurs at a rate of approximately 2 to 6% in resin-based composites. The prevention of polymerisation shrinkage, which is one of the most important problems in dental composites, is an important issue and various measurements can be taken for this. These measurements include preferring high molecular weight resin matrix, increasing the amount of inorganic filler particles and changing the light source used for curing. The use of low molecular weight TEGDMA as a diluent to reduce viscosity increases the amount of polymerisable carbon-carbon double bonds, resulting in greater shrinkage. In order to avoid this problem, it is preferable to use high molecular weight monomers such as Bis-GMA. As the molecular weight of the resin matrix decreases, the polymerisation shrinkage increases.³⁵

It is known that the thickness of the composite affects polymerisation and consequently polymerisation shrinkage. Increasing the thickness has a disadvantage on curing. The curing depth of the light source used for light-cured composites is 2 mm. In order to avoid this problem, dental composites are placed and cured in layers. This technique decreases the effect of shrinkage stresses and improves bond quality. This decreases interfacial microleakage and prevents secondary caries. It is important to avoid gaps between the layers.³⁵

2.6.3. Mechanical Properties

The mechanical properties of dental composites must be able to withstand the conditions in which the tooth is placed in the mouth. For this reason, it is a critical property that needs to be emphasised. There are several criteria that impact the mechanical characteristics of dental composites. As inorganic particles form the inorganic phase that provides strength to the composite, the type of filler, the size, geometry, and amount of these particles, as well as their uniform distribution in the resin and whether they are agglomerated or not are among the most critical factors affecting the mechanical properties of dental composites. In addition, spherical filler particles enhance the mechanical properties of the dental composite.²⁶

Polymerisation and resin is another criterion affecting the mechanical behaviour of the resin-based composite. Higher molecular weight resins such as Bis-GMA and UDMA have a good cross-linked bond after polymerisation, resulting in low water sorption and solubility, which provides better mechanical strength. The mechanical property increases with cross-linked bond density. In this case, curing conditions are also important as they affect the cross-linked bond of the resin after polymerisation.⁴¹

Another very critical factor is the bond between the reinforcements and the matrix phase. The modification of the particle surfaces with the silane coupling agent is a well done method to create a strong bond between the resin and the filler. The coupling agent does not hydrolyse in a liquid or saliva environment, preventing the particles from separating from the matrix and thus improving the mechanical properties of the composite.⁴⁵ Increasing the amount of inorganic filler, cross-linking bond density, effective particle surface modification using a silane coupling agent, and using spherical particles enhance the mechanical properties of dental composite materials.

2.6.4. Colour stability & Aesthetic Properties

Aesthetic appearance is an important factor in matching the natural appearance of the tooth. One of the most common problems affecting the aesthetic appearance of composites is discolouration of the composite. The colour pigments, the type of resin, the good salinization of the filler particles, the shape and size of the filler particles used, the refractive index between the resin and the particles have a significant effect on the colour of the composite. The colour change of the composite is also related to the

hydrophilic properties of the resin and the type of silane used for the surface modification. In composites with poor hydrophilic properties and poor silanation process, water absorption and solubility increases, which causes the colour of the composite to change in an undesirable direction.⁴⁶

2.6.5. Water Sorption and Solubility

Although resin-based dental composites offer several advantages in terms of adhesion to the tooth surface and aesthetics, as well as superior mechanical properties, they also have the disadvantage of monomer release due to water absorption in liquid environment. Water ingress into the dental composite causes hydrolytic degradation of the bond formed between the inorganic particles and the silane coupling agent, resulting in debonding of the matrix and filler. This hydrolytic degradation due to water ingress into the composite over time has a negative effect on the physical and mechanical properties of the composite. Water absorption and solubility reduce wear resistance, modulus and surface hardness of the composite, change colour stability, reduce fracture strength, fracture toughness and flexural strength.⁴⁷

Filler particles do not absorb water, so water absorption and solubility decrease as the filler content increases. The size and distribution of particles in the resin matrix are important. As the particle size decreases, the increased surface area in contact with water increases, which subsequently results in increased absorption.⁴⁸

In composites where the amount of inorganic particle is low, the amount of resin is high. Accordingly, water absorption and solubility increase in composites with high resin content. The type of resin used is also important for good bonding and affects this property. The use of high molecular weight monomers such as Bis-GMA (bisphenol A glycidyl dimethacrylate) and UDMA (urethane dimethacrylate) leads to a decrease in water absorption and solubility, while the use of hydrophilic monomers such as HEMA (hydroxyethyl methacrylate) and TEGDMA (triethyl- eneglycol dimethacrylate) monomers leads to an increase. These high molecular weight resins provide very good binding in the presence of coupling agents and reduce water absorption and solubility.⁴⁹ In light polymerised composite resins, complete polymerisation must be correct and sufficient, otherwise water absorption and solubility of the composite resin will increase.

2.6.6. Optical Properties

The optical properties of dental composites are of great interest in order to obtain composites that aesthetically match the natural appearance of the tooth. The light transmittance of the composite should be similar to that of the enamel and dentin layers in order to achieve an aesthetically natural appearance. The translucent enamel layer and the opaque dentin layer have a light transmittance of 70% and 52% respectively. The shape, size and amount of the filler particles added into the resin, colourants, opacifiers, refractive index between the filler particles, quality of curing and the resin, as well as the type of resin a used directly affect the translucency of the composite.³⁵

Light transmission has important role in optical properties of resin-based composites and particles added to the resin affect this property by interfacing with the matrix phase. As light moves deeper into the composite, some of it is lost. According to the law of refraction, this is related to the amount by which light deviates from its original direction when it encounters an interface. The difference in refractive index between the two phases is responsible for this deviation. In order to increase the translucency of the composites, the refractive indices of the resin mixtures and the filler particles added to the resin should be close to each other. The refractive index of the polymer is also directly related to the crosslink density of the resin. As the crosslink density increases, the refractive index increases.⁴¹ The refractive indices of fillers and resin are presented in Table 2.5. The shape, quantity and size of the added particles also affect the translucency of the composite by scattering the incident light. Consequently, the light transmittance is augmented by incorporating nanoparticles that are smaller than the wavelength of visible light, which ranges from 400 to 800 nm. Thus, the curing depth and translucency of the composite are also increased.³⁵ Considering all these properties and criteria, composites with high quality optical properties are obtained.

Table 2.5. Refractive indices of resin monomers and fillers (Source: Habib et al.2016)

Resin Monomers	Refractive Index
Bis-GMA	1.55
Bis-EMA	1.49
UDMA	1.49
TEGDMA	1.46
Inorganic Fillers	Refractive Index
Silica	1.46
Zirconia	2.16
Barium borosilicate glass	1.55

2.6.7. Radiopacity

Radiopacity or opacity to high energy photons (X-Rays), is an essential property that is required to detect problems caused by the formation of cavities or secondary caries from tooth. The radiopacity properties of dental composites depend on how much x-ray energy the material absorbs. Atoms with higher atomic numbers absorb more X-ray energy. Since resins are radiolucent, high atomic number components are used to make the composite radiopaque.¹⁶ High radiopacity inorganic particles are added to give the composite radiopacity. Barium ($Z = 56$) is the most commonly used heavy element as a radiopaque filler in resin based composite. In addition, other heavy elements like strontium ($Z = 38$), zirconium ($Z = 40$), bismuth ($Z = 83$), ytterbium ($Z = 70$) and lanthanum ($Z = 57$) are used as radiopaque fillers. According to ISO 4049, the minimum radiopacity of resin-based composites is determined by absorbing a 1 mm layer of pure aluminum ($Z = 13$).⁴¹ Dental composites with high radiopacity block the details of the neighbouring atom, while those with low radiopacity are invisible in X-rays. It is therefore important that the composite has a certain radiopacity.¹⁶

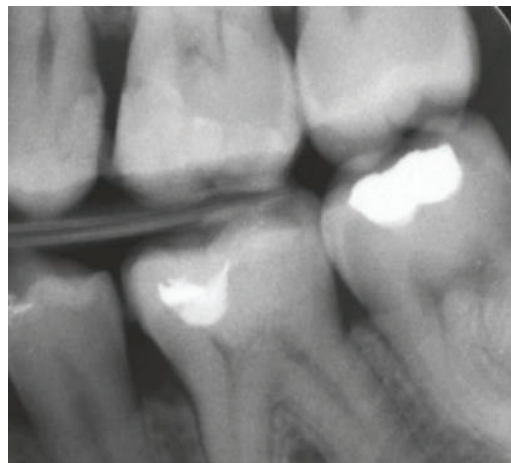


Figure 2.10. Radio-opacity image of dental composite (Source: V.Miletic 2018)

CHAPTER 3

LITERATURE REVIEW

Resin-based composites are becoming more commonly used in dentistry to replace amalgam for restoring damaged tooth tissue. Research on the enhancement of resin-based dental composites is continuously increasing. These improvements have contributed to a significant improvement in the physical and mechanical properties of the composite.⁵⁰ Resin-based dental composites are highly preferred due to their excellent mechanical and physical properties, as well as their high level of aesthetics thanks to nanoparticles and hybrid filling techniques.⁵¹ Nowadays, studies have been used to improved dental composites using different reinforcing inorganic fillers in various forms. In recent years, numerous studies have focused on the ability of ceramic nanoparticles to improve the properties of resin-based composites, specifically the mechanical properties, due to their unique characteristics. Therefore, many studies in the literature have focused on the effect of inorganic filler type, filler size, morphology and formulation variations on the mechanical properties of dental composites.

Khaje et al. (2015), investigated the effect of surface modification and different mass fractions of fumed silica filler on the mechanical properties of resin-based dental composites. It was reported that the maximum addition of unmodified fumed silica to the matrix was limited to 12 wt.%. However, the addition in the matrix increased from 12 wt.% to 20 wt.% due to surface modification. In addition, different concentrations (12 wt.%, 16 wt.% and 20 wt.%) of salinized fumed silica were added and their effect on mechanical properties was investigated. An increase in flexural strength was observed when fumed silica content was increased from 12 wt.% to 16 wt.%, with flexural strengths of 25.95 MPa and 33.35 MPa, respectively. However, there was no significant change in flexural strength when the amount of fumed silica was increased from 16 wt.% to 20 wt.%. Additionally, it was reported that adding more than 20 wt.% fumed silica to the resin mixture is challenging.⁵²

Hosseinalipour et al. (2010), examined the effect of filler content on mechanical properties. Surface modified silica particles (average particle size from 20 nm to 50 nm) with different mass fractions of 20 wt.%, 30 wt.%, 40 wt.% and 50 wt.% were added to the Bis-GMA and TEGDMA resin mixture. The flexural strength of the composites

increased from 103.4 ± 7.62 MPa to 149.74 ± 8.14 MPa as the mass ratio increased from 20 wt.% to 40 wt.%. However, the flexural strength decreased to 122.83 ± 6.13 MPa when the mass ratio continued to increase up to 50 wt.%. In this paper, it was reported that filler content is important for flexural strength. However, above a certain mass fraction, silica particles reduce the mechanical properties as a result of agglomeration.⁵³

Fumed silica has a significant effect on the rheological properties of the composite. The handling properties of the composite can be enhanced by increasing the viscosity of the composite up to a certain level with fumed silica.²⁷ However, it is not possible to incorporate large amounts of fumed silica into the resin mixture. Colloidal silica is the preferred filler particle in dental composites to increase the filler content of the composite due to its spherical structure. In addition to this advantage, colloidal silica also has a positive effect on some of the properties of the composite, such as its mechanical properties.⁵⁴

Satterthwaite et al. (2009), examined the effects of spherical and irregular shape fillers of different sizes on the composite. The shape and size of the fillers were found to have a significant effect on the viscosity of the composite. In addition, it was reported that composite materials containing spherical fillers exhibit a higher maximum tensile strength compared to those containing irregular shape fillers. It was also observed that the maximum tensile strength of composites containing both spherical and irregular shape fillers decreased with increasing filler size.⁵⁵ Kim et al. (2002), studied the flexural properties of composites containing prepolymerised filler particles, round shape filler particles and irregularly shaped filler particles. The highest flexural strengths were recorded for round shape particle composites, followed by prepolymerised composites and the lowest for regularly shaped composites.⁵⁶

Badr (2018) investigated the effect of zirconia nanoparticles on the physical and mechanical properties of the composite. The addition of zirconia nanoparticles at different weight fractions (1wt.%, 3wt.%, 5wt.%, 7wt.%, and 10wt.%) results in a decrease in the depth of cure and an increase in water sorption and solubility. The composite that contains 10wt.% ZrO_2 exhibits the highest water absorption and the lowest curing depth. The composite with 1wt.% zirconia has the highest flexural strength (118.98 ± 6.90 MPa). However, the flexural strength of the composite decreases with the addition of zirconia nanoparticles. The author reported that a 1wt%

concentration of zirconia has a positive effect on both the physical and mechanical properties of the composite.⁵⁷

Haas et al. (2017), aimed to investigate the impact of different opacifiers on the translucency and colour change of the composite. Three opacifiers, Al₂O₃, TiO₂, and ZrO₂, were added to the resin mixture at varying concentrations (0.25 wt.%, 0.5 wt.%, 0.75 wt.%, and 1 wt.%). TiO₂ has the greatest negative effect on opacity and colour change, followed by ZrO₂ and Al₂O₃. It was found that the opacity and colour change of the composite regularly decrease as the concentration of ZrO₂ increases.³²

Chan et al. (2009), found that the addition of zirconia nanoparticles increased the fracture toughness of composites compared to silica-filled composites. In zirconia filled composites, cracks are deflected by the particles and fracture occurs along the matrix/particle interface. ZrO₂ nanoparticles have a higher fracture toughness than silica nanoparticles. As a result, these composites are more resistant to fracture.⁵⁸

Wang et al. (2020) reported that zirconia particles, modified with γ -MPS, increased the light transmission of the composite by decreasing the refractive index compared to the control group.³¹

A different study by Zidan et al. (2021) studied the 3 wt.% concentration of zirconia nanoparticles with and without surface treatment. Silanized zirconia fillers with γ -MPS increased the flexural strength but unsilanized zirconia nanoparticles decreased the flexural strength compared to the control group. They found that the surface modified zirconia nanoparticles significantly increased the flexural strength.⁵⁹

Tarumi et al. (1995), investigated the flexural strength and water sorption properties of barium glass and silica-filled composites with different particle sizes. They found that the flexural strength of the barium glass filled composites was higher than that of the silica filled composites. The flexural strength of the composites increased as the size of both barium glass and silica fillers decreased. However, the water sorption properties of the composites were negatively affected by the barium glass compared to the silica-filled composites. Smaller particle sizes increased the water sorption of the composite.⁶⁰

Marovic et al. (2014), examined the effect of barium glass and strontium glass fillers on the flexural strength of the composite. In this study, the researchers added 10 wt.% of barium glass and 10 wt.% of strontium glass. They reported that the barium glass filler exhibited the highest flexural strength. Flexural strength was improved by

barium glass compared to the control group. In addition, barium glass had a more significant effect on flexural strength.⁶¹

CHAPTER 4

EXPERIMENTAL

4.1. Materials

In this research, the polymeric matrix phase was formed using Bis-EMA (ethoxylated bisphenol A dimethacrylate), UDMA (urethane dimethacrylate), and TEGDMA (triethylene glycol dimethacrylate) monomers. The high molecular weight monomers Bis-EMA, UDMA and the diluent monomer TEGDMA were used in a ratio of 40%, 30%, 30% by weight.

The photopolymerisation initiator used was camphorquinone (CQ), which has the widest absorption range close to the emission spectrum of light emitting diodes (LEDs), and the accelerator was ethyl 4-(dimethylamino) benzoate (EDMAB). The molecular weight of the chemicals used and the suppliers of these chemicals are given in Table 4.1.

Table 4.1. The molecular weight and supplier of the chemicals used for resin matrix

Chemicals	Bis-EMA	UDMA	TEGDMA	CQ	EDMAB
Properties					
Molecular Weight (g/mol)	376.4	470.56	286.32	166.22	193.24
Supplier	Sigma-Aldrich, Germany	Sigma-Aldrich, Germany	Sigma-Aldrich, Germany	Sigma-Aldrich, Germany	Sigma-Aldrich, Germany

Hydrophilic fumed silica nanoparticles CAB-O-SIL® M-5, colloidal silica MP 1040, zirconia nanoparticles and barium glass nanoparticles were used to form the inorganic phase of the dental composite. The properties of these nanoparticles used as reinforcement, such as average particle size, density, purity and BET surface area are given in Table 4.2. The suppliers of these nanoparticles particles are also given in Table 4.2.

Table 4.2. Detailed properties of the fillers used in resin-based dental composites

Particles Properties	CAB-O-SIL® M-5	MP 1040	Zirconia	Barium Glass
Average Particle Size (nm)	200	100	20-30	700
BET Surface Area (m² /g)	200	31	35	
Density (g/cm³)	2.2	1.298		
Purity	> 99.8 wt.%SiO ₂	40.7wt.%SiO ₂		
Supplier	Cabot Corporation, USA	Nissan Chemicals, Japan	Skyspring Nanomaterials, Inc., USA	Schott Ag Landshut, Germany

The surface of the inorganic nanofillers was modified with γ -MPS silane to create a good interface between the matrix phase and the inorganic phase. As the barium glass particle was supplied silanized with γ -MPS silane, all other particles used were modified. A chemical solution was prepared for the silanization process using γ -MPS, n-propylamine and cyclohexane. Table 4.3 provides detailed information regarding the chemicals and their suppliers.

Table 4.3. Details of the chemicals used for surface modification

Chemicals Properties	γ-MPS	Cyclohexane	n-propylamine
Molecular Weight (g/mol)	248.35	84.16	59.11
Density (g/cm³)	1.045	0.779	0.719
Supplier	Sigma-Aldrich, Germany	Sigma-Aldrich, Germany	Sigma-Aldrich, Germany

4.2. Surface Modification of Inorganic Particles

In contrast to other nanoparticles, colloidal silica is in a liquid form. The colloidal silica (MP 1040) is composed of 60 wt.% water and 40 wt.% silica. Therefore, colloidal silica was pre-dried in the oven at 100°C to remove the liquid and obtain dried powdered colloidal silica particles. Colloidal silica before and after pre-drying is shown in Figure 4.1.

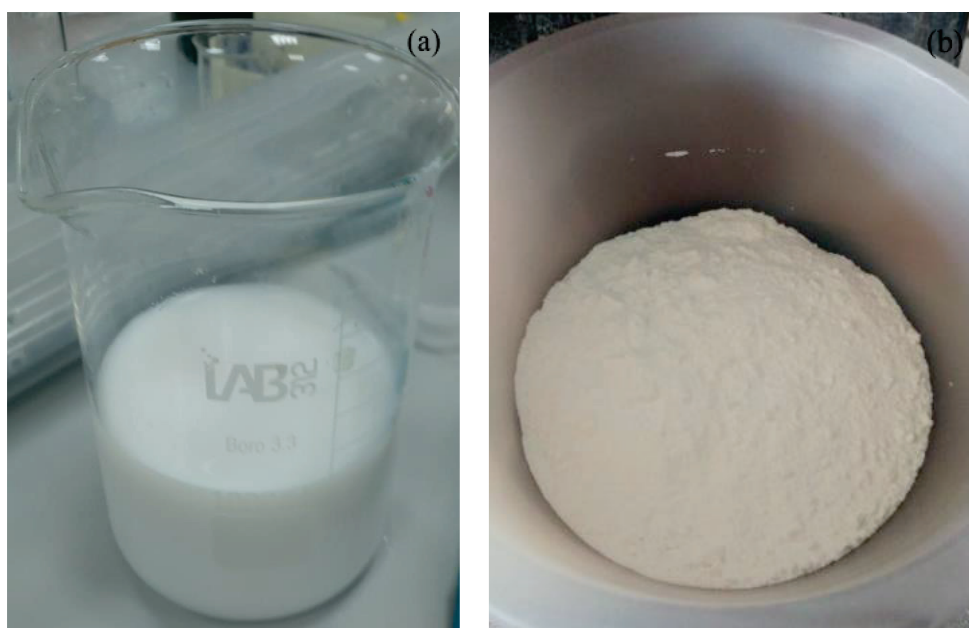


Figure 4.1. (a) Colloidal silica 40 wt.% SiO₂-60 wt.% water, (b) colloidal silica after pre-drying

In the first step of the surface modification procedure, a chemical solution was prepared by adding 100 ml of cyclohexane, 0.1 g of n-propylamine, and 0.5 g of γ -MPS silane to a glass beaker. In order to accelerate the reaction n-propylamine was used. They were stirred on a magnetic stirrer for 1 minute to obtain a homogeneous mixture. The solution was prepared separately for each type of particle, and 5.0 g of particles were added to each of the solutions. They were then stirred using a magnetic stirrer at 400 rpm for 1 hour, the first 30 minutes at room temperature and the following 30 minutes at 60°C. The mixtures were kept in the oven at 80°C for 24 hours to remove volatile chemicals at the end of the one-hour period. The process of surface modification of the particles is shown in Figure 4.2.



Figure 4.2. Surface modification process of the nanoparticles; (a) chemical mixture, (b) particle addition to chemical mixture, (c) remove the volatile chemicals at 80°C for 24 hours, (d) surface modified particles

4.3. Preparation of Dental Composites

Resin-based dental restorations were prepared using different particle ratios with a total particle content of 65 wt.%. The inorganic filler contents used in each composites are given in the Table 4.4. Bis-EMA, UDMA and TEGDMA monomers were used for the matrix phase of the resin-based composites. Bis-EMA, UDMA, and TEGDMA monomers were mixed in a beaker at a ratio of 40:30:30 wt.%, respectively, using a glass rod. The beaker was covered with aluminum foil to prevent curing caused by ambient light. In order to obtain a homogeneous resin mixture, this resin mixture was first mixed with a hand spatula at room temperature and then kept in an ultrasonic bath at room temperature for 15 minutes. At the end of these 15 minutes, 0.7 wt.% CQ as an initiator and 0.3 wt.% EDMAB as an accelerator were added to the resin mixtures. In order to obtain homogenous of distribution of accelerator and initiator in the resin for a further 15 minutes it was kept in the ultrasonic bath at room temperature.

The inorganic particles listed in the Table 4.4 were added to the prepared resin mixture in the following order ZrO₂, Ba glass, colloidal silica and finally fumed silica.

Table 4.4. Inorganic nanoparticles concentration of the composite groups produced

Sample	Inorganic nanoparticles (wt.%)				
	CAB-O-SIL® M-5	MP 1040	Ba Glass	ZrO ₂	Total
RER	20	45	0	0	65
Ba20	20	25	20	0	65
Ba30	20	15	30	0	65
Z1	20	44	0	1	65
Z2	20	43	0	2	65
Ba20Z1	20	24	20	1	65
Ba20Z2	20	23	20	2	65
Ba30Z1	20	14	30	1	65
Ba30Z2	20	13	30	2	65

The inorganic particles listed in the Table 4.4 were added to the prepared resin mixture in the following order ZrO₂, Ba glass, colloidal silica and finally fumed silica. After the addition of each type of particle, except fumed silica, according to the contents given in the Table 4.4, they were homogeneously distributed in the resin using a spatula, as shown in Figure 4.3(a-d). Due to its large surface area, adding fumed silica to the resin manually with a spatula is more challenging than adding other particles. Therefore, fumed silica was added to the composite at the final stage using a mortar mill. The fumed silica was gradually added to the mortar mill chamber, which was preheated at 80°C for 30 minutes before use, and homogeneously dispersed into the composite using a RETSCH RM 200 mortar mill. RETSCH RM 200 mortar mill is shown in Figure 4.4. The composite was stirred in the mortar mill for a total of 30 minutes. Figure 4.3. (e-f) shows the appearance of the composite during the mixing process in the mortar mill.

A total of 9 different groups of composites were produced, including the reference composite, by trying different ratios of ZrO₂ and Ba glass particles in composites with a total particle ratio of 65 wt.%. Samples were prepared to test the properties of all these composites after they had been produced. The state of each stage of preparation of composite is given in Figure 4.3. After the paste mixture preparation stage, the test specimens were prepared by placing the composites into the specimen moulds.

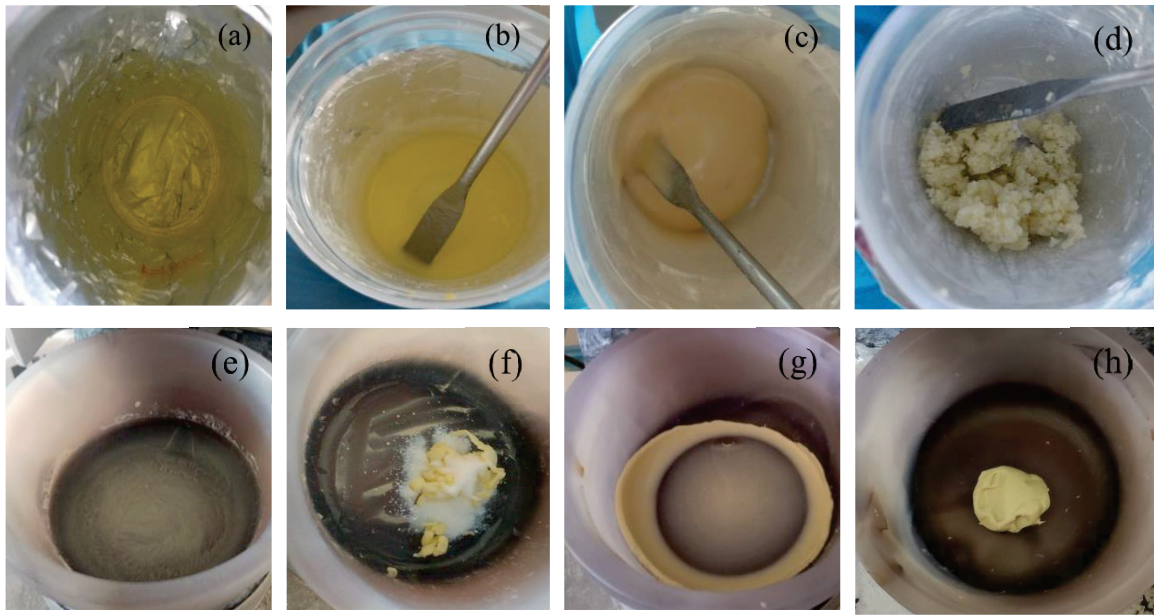


Figure 4.3. (a) Resin mixture with CQ&EDMA,(b) ZrO_2 ,Ba glass particles addition,(c) colloidal SiO_2 addition,(d) fumed SiO_2 by hand mixing,(e) after mixing in mortar mill,(f) fumed SiO_2 addition in the mortar mill,(g) composite mixing in mortar mill, (h) final state



Figure 4.4. Automatic mortar mill for homogeneous dispersion of the particles

Test specimens were prepared by placing the composites into specimen moulds. Frekote release agent was applied to the mould in which the sample was to be placed, to help remove the samples from the mould easily, and the mould was then placed on transparent film. The composite was then placed in the mould. The composite was

carefully placed in the mould by applying pressure with a spatula to minimise the formation of voids within the specimen. The composite was filled to the top of the mould and then covered with transparent film when the process was complete. The mould was pressed with a flat object to remove air bubbles. The specimens were prepared and subsequently cured using a LITE-Q Auto Ramp-Up LD-107 light curing source, which emitted light at a wavelength of 450-470 nm and a brightness of up to 1000 mW/cm². The light curing unit used is shown in the Figure 4.5. The samples were cured for 30 seconds on each side (front and back side of the mould). The samples were kept in a desiccator at room temperature for 24 hours after curing.



Figure 4.5. Light curing unit used in the curing process

4.4. Characterization of Particles and Dental Composites

The inorganic nanoparticles dispersed in the resin were characterised by Scanning Electron Microscopy (SEM), Fourier Transform Infrared Spectroscopy (FTIR) and Dynamic Light Scattering (DLS). The fracture surfaces of the composites were characterised by Scanning Electron Microscopy (SEM).

4.4.1. Scanning Electron Microscopy (SEM) and EDS Analysis

The surface morphology of the inorganic fillers dispersed in the organic phase was analysed by scanning electron microscopy (SEM) (FEI QUANTA 250 FEG), (ZEISS EVO10). Before SEM analysis, the nanoparticles were kept in the oven at

100°C for 1 hour to remove any moisture. In order to avoid the problem of charge during analysis, nanoparticles were placed on conductive carbon tape and the charges were transferred along the tape.

The fracture surfaces of the three point bending test specimens were also examined by SEM. The fracture surfaces were examined in order to obtain information about the composites by examining the elements that would reduce the strength of the composite, such as porosity, and the distribution of particles in the composite. Before SEM analysis, the fracture surfaces were coated with gold using a sputtering apparatus and placed on conductive carbon tapes. Elemental analysis of the samples was carried out by EDS analysis to determine the elemental distribution within the structure.

4.4.2. Dynamic Light Scattering (DLS) Analysis of Nanoparticles

The size distribution and average particle size of inorganic nanoparticles were analysed as a function of volume % by Dynamic Light Scattering (DLS) technique using Particulate Systems NanoPlus Particle Size Analyser. A laser light with a wavelength of 660 nm was used during the analysis. Before analysis, a suspension was prepared in which the particles were dispersed in the solvent. 1.0 g of nanoparticles were dispersed individually in 10 ml ethanol and left in the ultrasonic bath for a period of 30 min.

Malvern Zetasizer Nano ZS was used as an alternative device in order to perform a more sensitive analysis of the same analysis technique on zirconia nanoparticles. The suspension was prepared by adding 0.01 g of ZrO₂ nanoparticles to 10 ml of water with the addition of Tween 80 as a surfactant. In order to attain an acceptable results suspension concentration were adjusted in the range of 0.01 to 5 wt.% followed by dispersing nanoparticles individually in the solvent.

4.4.3. Fourier Transform Infrared Spectroscopy (FT-IR)

Fourier Transform Infrared (FTIR) analysis (PERKIN ELMER Spectrum Two) was carried out to confirm the successful surface modification of γ -MPS silanized nanoparticles. The functional groups in both silanized and non-silanized nanoparticles for all inorganic nanoparticles were analysed by FTIR spectrometer and the results compared. ATR-FTIR spectra were recorded in the transmission mode in the 4000-400

cm⁻¹ wavelength range with 20 scans per spectrum and a resolution of 4 cm⁻¹. Before analysis, the samples were dried and placed in a desiccator to remove any moisture.

4.5. Mechanical Tests of Dental Composites

Mechanical properties are of great importance in dental composites. The flexural and compressive strengths of composites are reported to be in the range of 60 to 130 MPa and 150 to 250 MPa, respectively, for hybrid-filled resin-based resins.

4.5.1. Three Point Bending Test

Three point bending test was used to determine the flexural strength of the composites. At least 5 samples with dimensions of (25±2) mm × (2.0±0.1) mm × (2.0±0.1) mm from each dental composite group were prepared in accordance with ISO 4049 standard for three-point bending test. The specimens were prepared using a metal mould according to the ISO 4049 standard dimensions. The mould was designed in two parts for easy removal without damaging test specimens. The mould used for the flexural strength test specimen is shown in the Figure 4.6. All composite pastes placed in the mould were cured from both sides for 30 seconds at 9 different points in accordance with the ISO 4049 standard as illustrated in Figure 4.7.

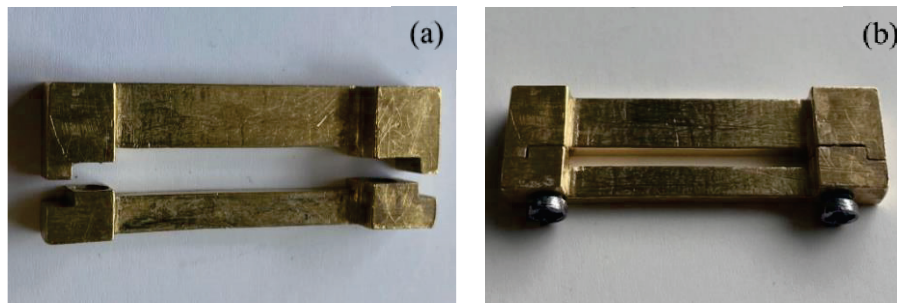


Figure 4.6. Mould used in the preparation of bending specimens: (a) open,(b) close

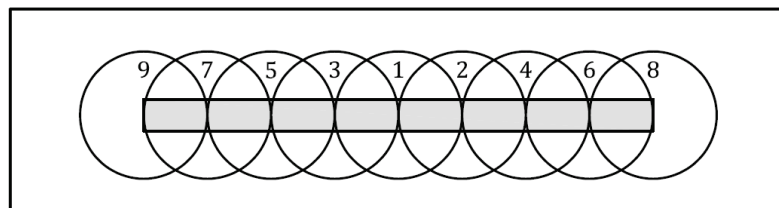


Figure 4.7. The top view of the curing zones of flexural strength test specimen

The flexural strength of the specimens was tested in a Shimadzu Autograph AGJ-S universal testing machine. The distance between the two supports (span length) was set at 20 mm for the three-point bending test. In accordance with the standard, cylindrical rods with a diameter of 2 mm were utilised as supports. During the test, a load was applied to the specimens at a crosshead speed of 0.75 mm/min, and the maximum load applied to the specimens at fracture was reported. The three-point bending test setup for flexural strength of the specimens and the specimens after the three-point bending test are illustrated in Figure 4.8 and Figure 4.9, respectively.



Figure 4.8. The test setup for three-point bending test

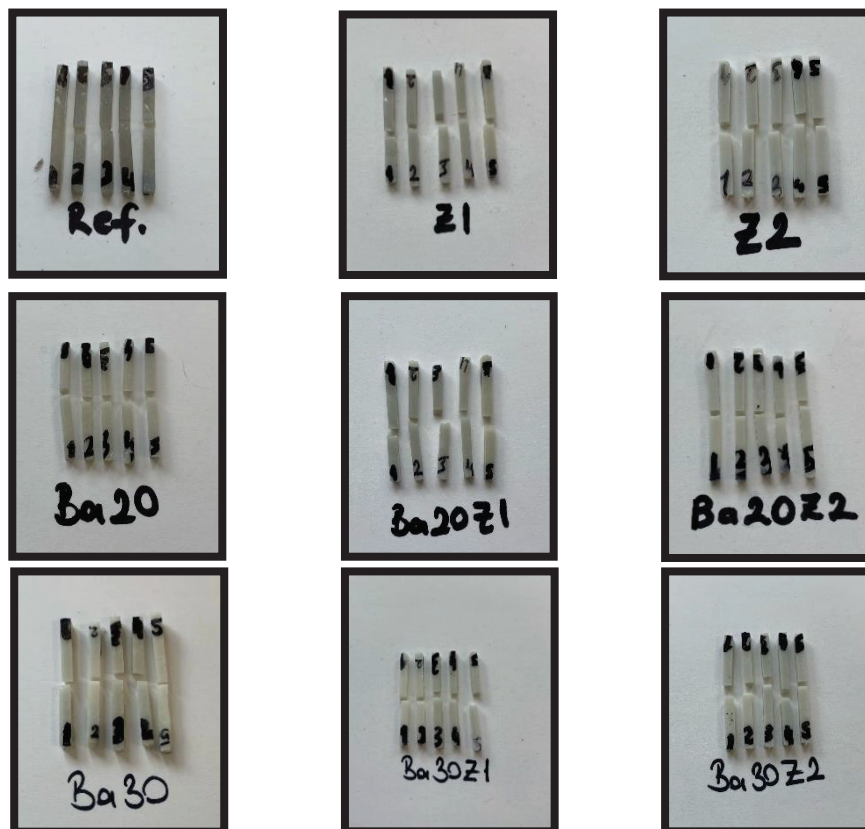


Figure 4.9. The specimens were tested using a three-point bending method

The equations below were used to calculate the flexural strength (σ_f) and modulus (E_f) of the composites.

$$\sigma_f = \frac{3FL}{2bh^2} \quad (4.1)$$

$$E_f = \frac{F_1L^3}{4bh^3d} \quad (4.2)$$

In these equations, F is the maximum applied load in Newton, L is the distance between supports in mm, b is the specimen width in mm, h is the height of the specimen in mm, d is the displacement of the sample in mm at load F_1 during the test.

4.5.2. Compression Test

A minimum of 5 specimens were prepared for each composite group to determine the compressive strength of the composites. The samples were prepared using a stainless steel mould with a diameter of 4 mm and a height of 6 mm. In order to easily remove the specimens without damaging them, this mould was designed in two pieces. All composite pastes placed in the mould were cured from both sides for 30 seconds. The mould used to prepare the specimens is shown in Figure 4.10. Compression test samples removed from the mould are illustrated in Figure 4.12.

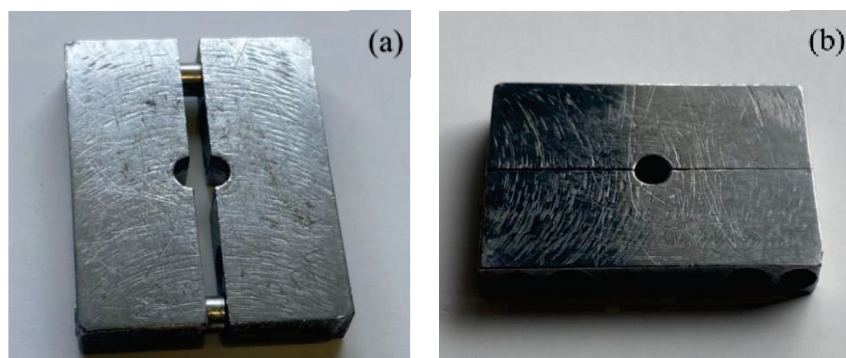


Figure 4.10. Mould used in the preparation of compression specimens: (a) open, (b) close

The compressive strength of the specimens was tested using the Shimadzu Autograph AGJ-S universal testing machine. The test was performed at a crosshead

speed of 0.75mm/min and the maximum load applied to the sample at the point of fracture was reported. The compression test setup for the compressive strength of the specimens is shown in Figure 4.11.



Figure 4.11. Compression test setup

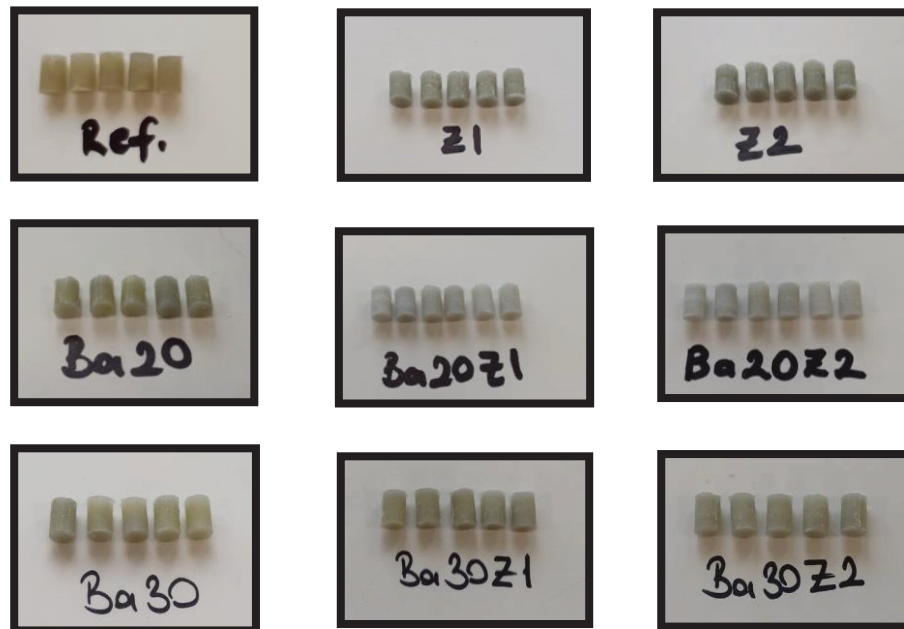


Figure 4.12. Compression test specimens

The compressive strength (F) was determined by dividing the maximum load at the point of fracture by the cross-sectional area (A) of the sample. The diameter of the sample (R) was measured in millimetres.

$$CS = \frac{F}{A} = \frac{F}{\frac{\pi r R^2}{4}} \quad (4.3)$$

4.6. Depth of Cure Determination of Dental Composite

Specimens were prepared according to the ISO 4049 standard to determine the curing depth of the composites. For each type of composite, 3 specimens were prepared. The specimens were 4 mm in diameter and 6 mm in height, in the same manner as the compressive strength specimens. The curing process was carried out for 30 seconds from one surface of the specimens. After removing the specimen from the mould, the uncured composite was removed from the uncured surface using a metal spatula. The remaining specimen was measured for height with a caliper, and the value obtained was divided by 2 in accordance with the standard procedure. For opacified restorative materials, all three values must be at least 1.0 mm, while for all other materials, they must be at least 1.5 mm.

4.7. Water Sorption and Solubility Test of Dental Composites

In order to determine the water absorption and solubility values of resin-based composites 3 samples with a thickness of 1 mm and a diameter of 15 mm were prepared. The mould for the preparation of specimens and the top view of the curing zones of the specimens in this test performed according to ISO 4049 standard are given in the Figure 4.13 and each zone was cured for 30 seconds. Water absorption and solubility samples removed from the mould are illustrated Figure 4.14.

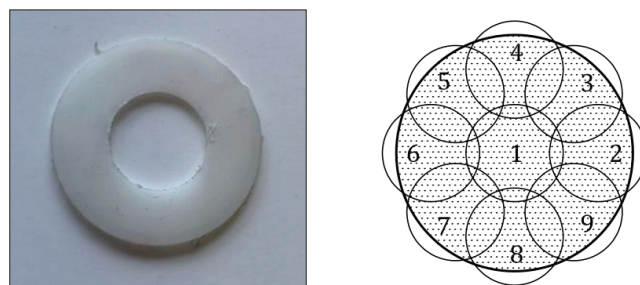


Figure 4.13. View of the mould and curing zones used for water absorption and solubility samples

The samples prepared for water absorption and solubility tests were placed in the oven at 37°C and dried for 24 hours. Then the samples were taken to the desiccator and kept for 2 hours and weighed until the weight change was ± 0.1 mg. This mass was accepted as the initial weight m_1 . The samples with initial weights were placed in small beakers with 10 ml of distilled water in an oven at 37°C and kept in distilled water for

one week. The samples were removed after 1 week and washed with distilled water and wiped until the water on the surface was free of observable moisture. The samples were shaken in air for 15 seconds and then the samples weighed at 15, 30 and 60 minutes were weighed at 1 hour intervals until the 9th hour. After the 24th hour of weighing, weighing continued at 24 hour intervals until a constant weight m_2 was obtained. After obtaining the m_2 value, the samples were returned to the oven at 37 °C. The measurement continued at 24 hour intervals until the mass reached a constant value. This constant value was recorded as m_3 .

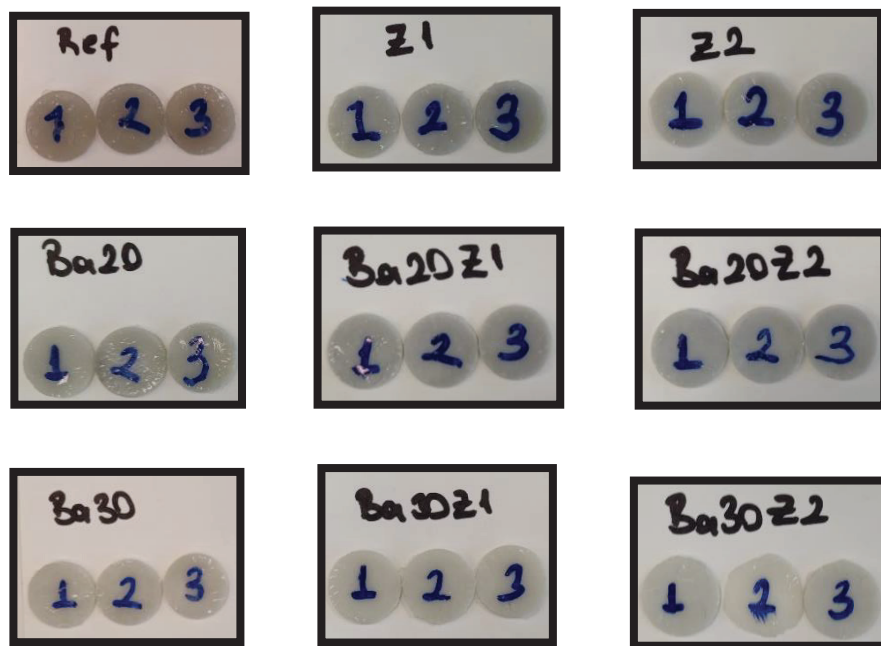


Figure 4.14. Water sorption and solubility test specimens

The water absorption and solubility values of dental composites were calculated by the equations given below, respectively. According to the ISO 4049 standard, the maximum water sorption and solubility values are 40 $\mu\text{g}/\text{mm}^3$ and 7.5 $\mu\text{g}/\text{mm}^3$, respectively.

$$W_{sp} = \frac{m_2 - m_3}{V} \quad (4.4)$$

$$W_{sl} = \frac{m_1 - m_3}{V} \quad (4.5)$$

Where V is the initial volume of the specimens.

4.8. Polymerization Shrinkage Measurement of Dental Composites

Polymerisation shrinkage of the dental composites is related to density of the specimens before and after the curing process. This test was carried out according to the ISO 17304 standard. Archimedes' principle was used in order to examine the density of the specimens for polymerisation shrinkage. Uncured and the cured specimens were prepared in different mass and numbers according to the standard. Six different specimens (1.0 ± 0.1) g mass for uncured composites and 12 different specimens (0.50 ± 0.05) g mass for cured composites were measured and pressed with a spatula into large sterile cups and flattened. They were preheated in the oven at 37°C for 24 hours. The specimens were removed from the oven and given a spherical shape. The specimens were spherically shaped by applying pressure with the fingers after wearing gloves to prevent the formation of air bubbles inside the specimens. The curing process for the cured specimens was from the top and bottom of the specimens for 30 seconds each.

The beaker was filled with distilled water so that the depth of immersion of the samples was at least 20 mm. The masses of each uncured and cured specimens were measured first in air and then in water. The mass measurement of a sample in both air and water in its setup for the Archimedes' principle setup is shown in the Figure 4.15.

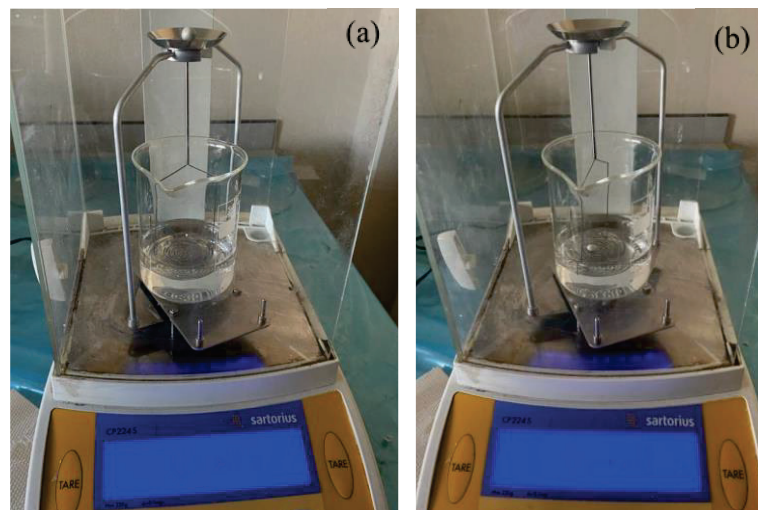


Figure 4.15. Measuring the mass of a sample in (a) air, (b) water.

In this equation, D is the density of the specimen, m_1 is the mass in air and m_2 is the mass in water of the sample. D_0 is the density of water at the exact measured

temperature in °C according to the density table of distilled water, and D_L was the air density (0.0012 g/ cm³) The polymerization shrinkage was calculated for sample using the following formula.

$$\Delta V = \frac{(D_{cured} - D_{uncured})}{D_{cured}} * (100) \quad (4.6)$$

CHAPTER 5

RESULTS AND DISCUSSION

5.1. Characterization Results

In this section, FTIR analysis, particle size distribution and microstructural properties of inorganic nanoparticles (fumed silica, colloidal silica, zirconia and barium glass) used as fillers in this study are presented. The microstructural properties of the composites are given in this section by examining the fracture surface using SEM microscopy and EDS analysis. In addition, the mechanical and physical properties of the composites were also analysed by performing tests on the composites and the results are presented in this section.

5.1.1. Scanning Electron Microscopy (SEM) and EDS Analysis

SEM images of fumed silica and colloidal silica nanoparticles without surface modification are illustrated in the Figure 5.1 and Figure 5.2, respectively. Fumed silica nanoparticles were observed to exhibit an irregular shape and to be agglomerated while colloidal silica nanoparticles were observed to have a regular spherical shape from the SEM images. The size distribution of colloidal silica and the average particle size of about 100 nm were measured as shown in the Figure 5.2(b).

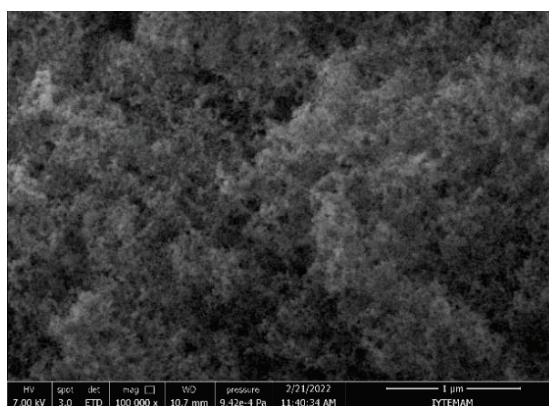


Figure 5.1. SEM image of untreated fumed silica nanoparticles at 100000X magnification

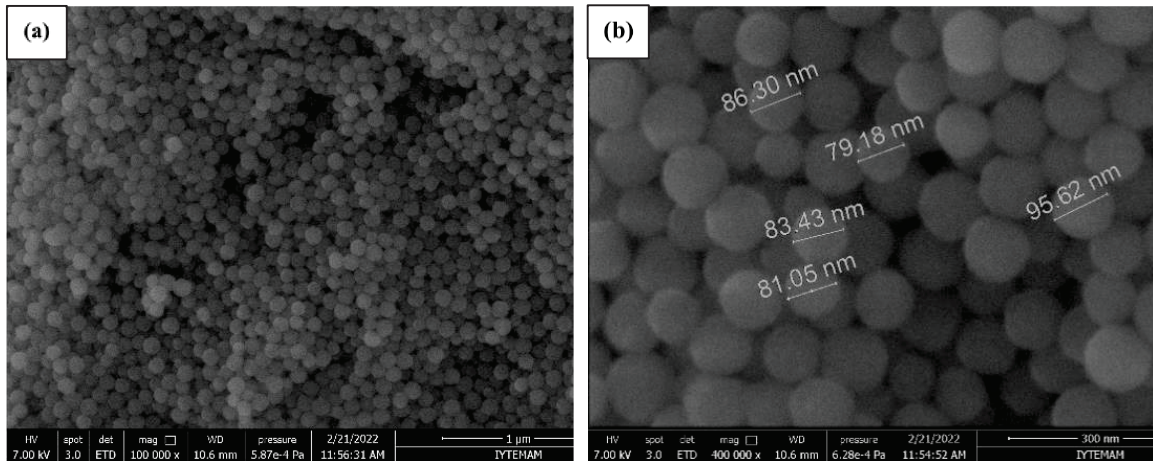


Figure 5.2. SEM image of untreated colloidal silica nanoparticles: (a) at 100000X magnification, (b) average particle size at 400000X magnification

SEM images of untreated zirconia nanoparticles at different magnifications are illustrated in Figure 5.3. Zirconia nanoparticles were observed to have a spherical shape and to agglomerate into clusters. The size distribution of zirconia nanoparticles and the average particle size of 30 nm were measured as shown in the Figure 5.3(b).

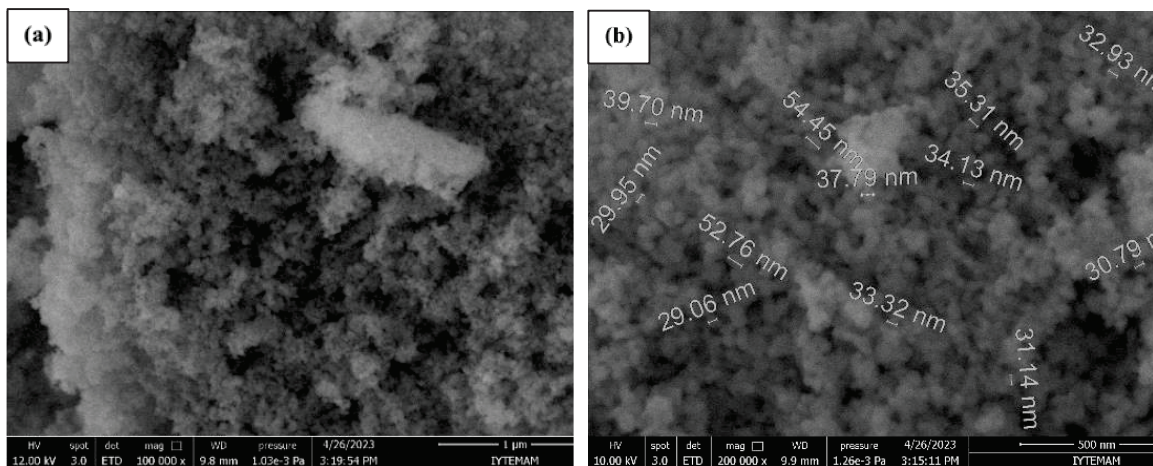


Figure 5.3. SEM image of untreated zirconia nanoparticles: (a) at 100000X magnification, (b) average particle size at 200000X magnification

SEM images of the modified barium glass particles at different magnifications are shown in the Figure 5.4. It was observed from the SEM images that the barium glass particles have a characteristic irregular shape. In addition, as can be seen from the SEM image in Figure 5.4(b), the average particle size distribution of the barium glass particles was measured to be 0.7 μm.

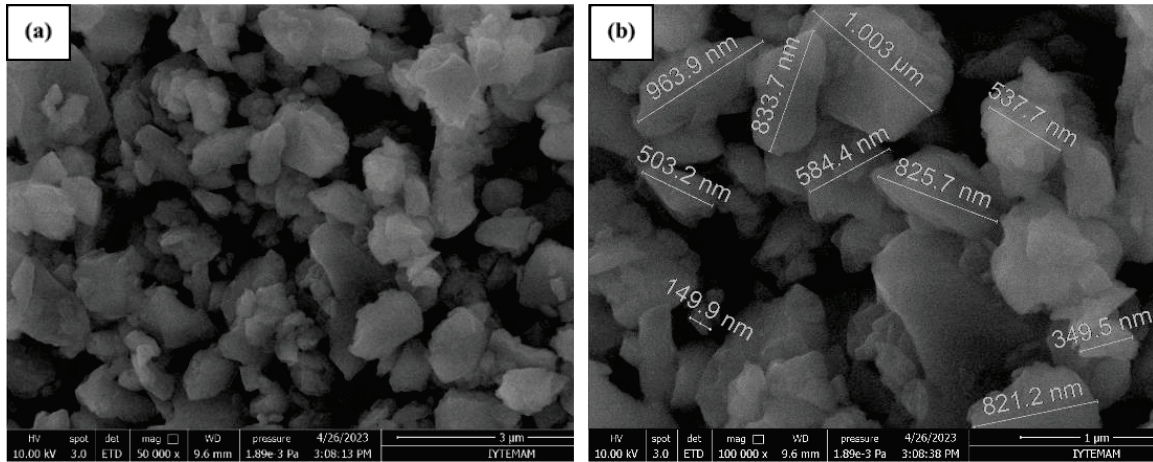
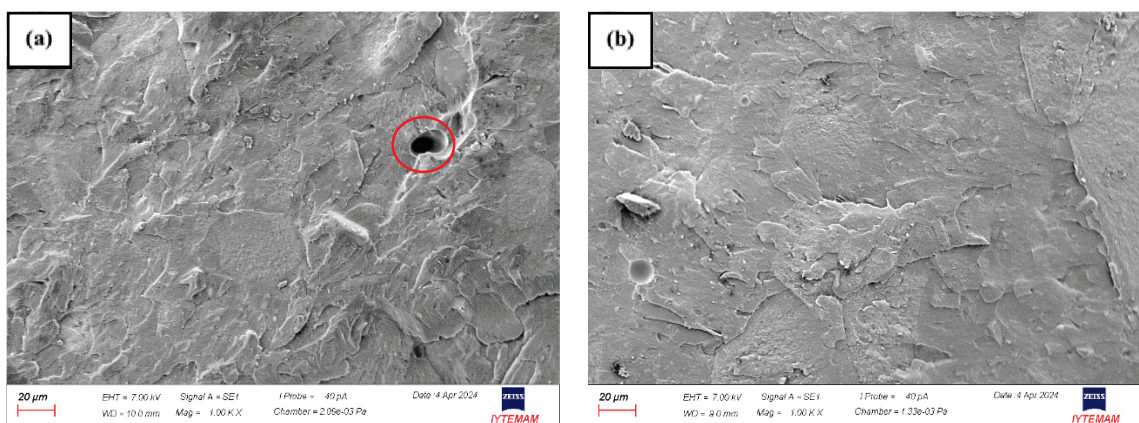


Figure 5.4. SEM image of modified barium glass particles: (a) at 50000X magnification, (b) average particle size at 100000X magnification

SEM images of the fracture surfaces of all composites at 1000x magnification in the secondary electron mode are shown in Figure 5.5 and at 25000x magnification in the backscattered electron mode are shown in Figure 5.6. The SEM images clearly show the distribution of irregularly shaped and spherical filler particles in the resin and their effective interaction with the monomer matrix. It is seen in Figure 5.5 that the Ref. sample, which only contains silica, has a flat fracture surface in comparison to the other composites. The SEM images evidence that the addition of barium glass and zirconia significantly increases the roughness of the fracture surface. Largest porosity sizes in the fracture surfaces of Ref., Ba30 and Ba30Z2 samples are obtained in Figure 5.5.



(cont. on next page)

Figure 5.5. SEM images in the secondary electron mode of the fracture surface of composites: (a) Ref., (b) Z1, (c) Z2, (d) Ba20, (e) Ba20Z1, (f) Ba20Z2, (g) Ba30, (h) Ba30Z1, (i) Ba30Z2

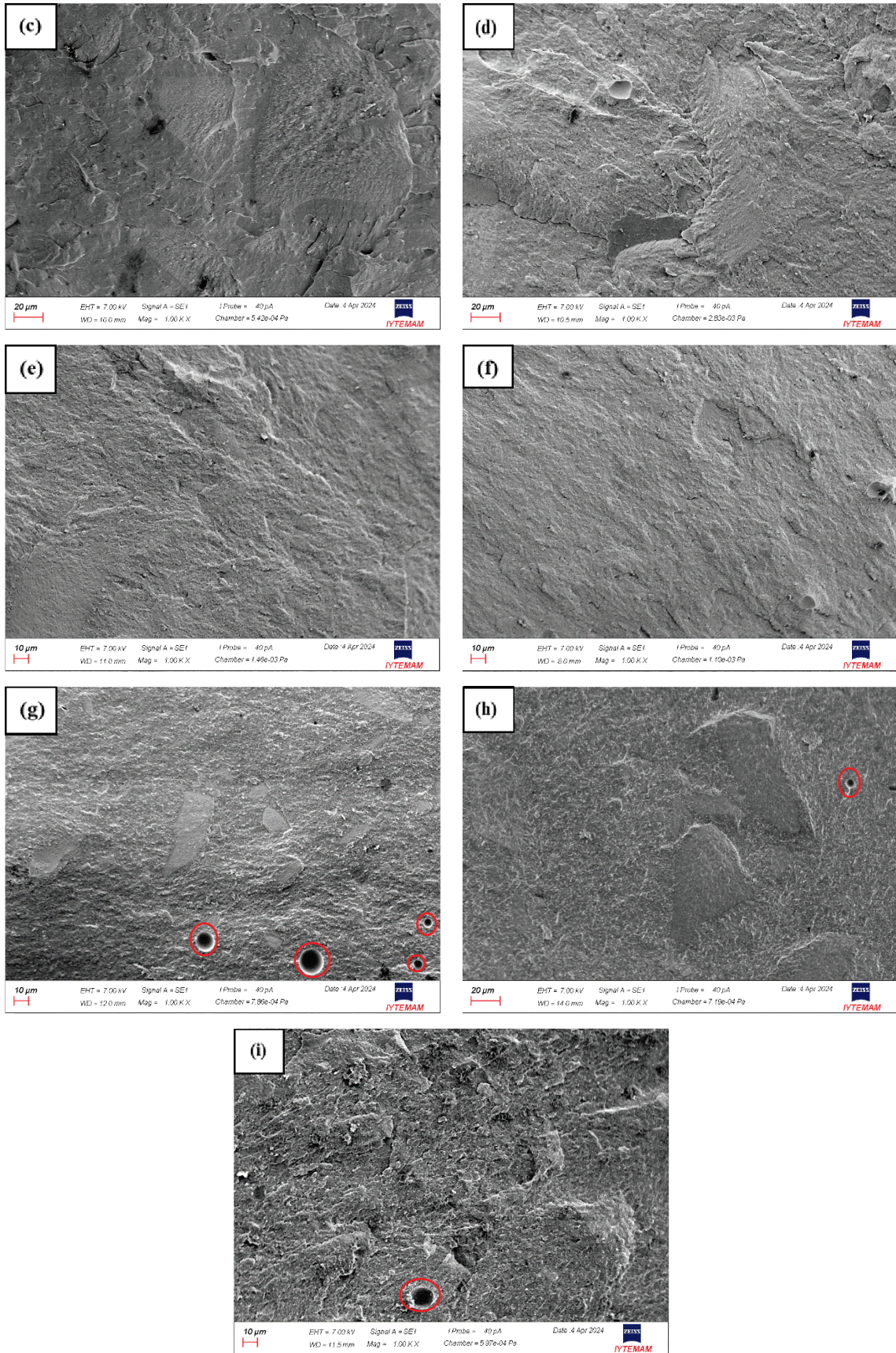
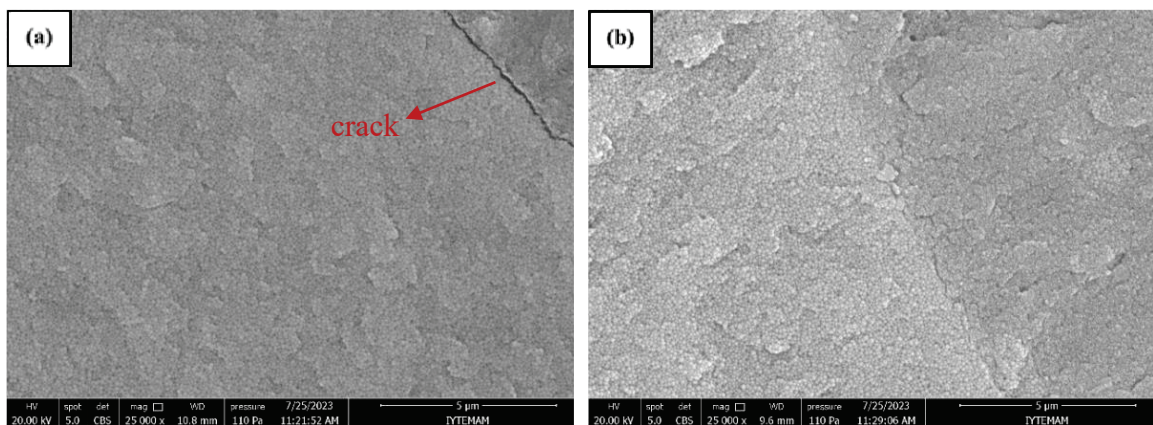


Figure 5.5. (cont.)

It can be seen from Figure 5.6(a-c) that the resin contains more densely impregnated filler nanoparticles. However, as the barium glass was increased, it was observed that the fillers were more sparsely distributed in the resin at the fracture surfaces in Figure 5.6(d-i). The distance between the filler particles increases as the barium glass content increases, which is supported by the SEM images. This is due to the irregular shape and larger particle size of barium glass compared to silica and zirconia (see Figure 5.4).

Although most part of the fillers were successfully integrated into the resin without agglomeration, some particles did come together to form agglomerates. It was proved from Figure 5.6(c, f) when zirconia was increased from 1 to 2 wt.%, zirconia nanoparticles agglomerate. The agglomeration of spherical colloidal silica is also evident from Figure 5.6(d, f, i). As the amount of barium glass was increased to 20wt.% and 30wt.%, it was obtained from SEM images that fillers were more homogeneously dispersed in the resin, resulting in less agglomeration.

The amount of filler per unit area in the matrix decreases as the barium glass content increases, resulting in homogeneous distribution of fillers in the resin. However, this also reduces the viscosity of the composite and affects its handling properties. Therefore, it can be said that microvoids can form when the composite is placed in the mould. This is also supported by the SEM images in Figure 5.6(d-i).



(cont. on next page)

Figure 5.6. SEM images in the backscattered electron mode of the fracture surface of composites: (a) Ref., (b) Z1, (c) Z2, (d) Ba20, (e) Ba20Z1, (f) Ba20Z2, (g) Ba30, (h) Ba30Z1, (i) Ba30Z2

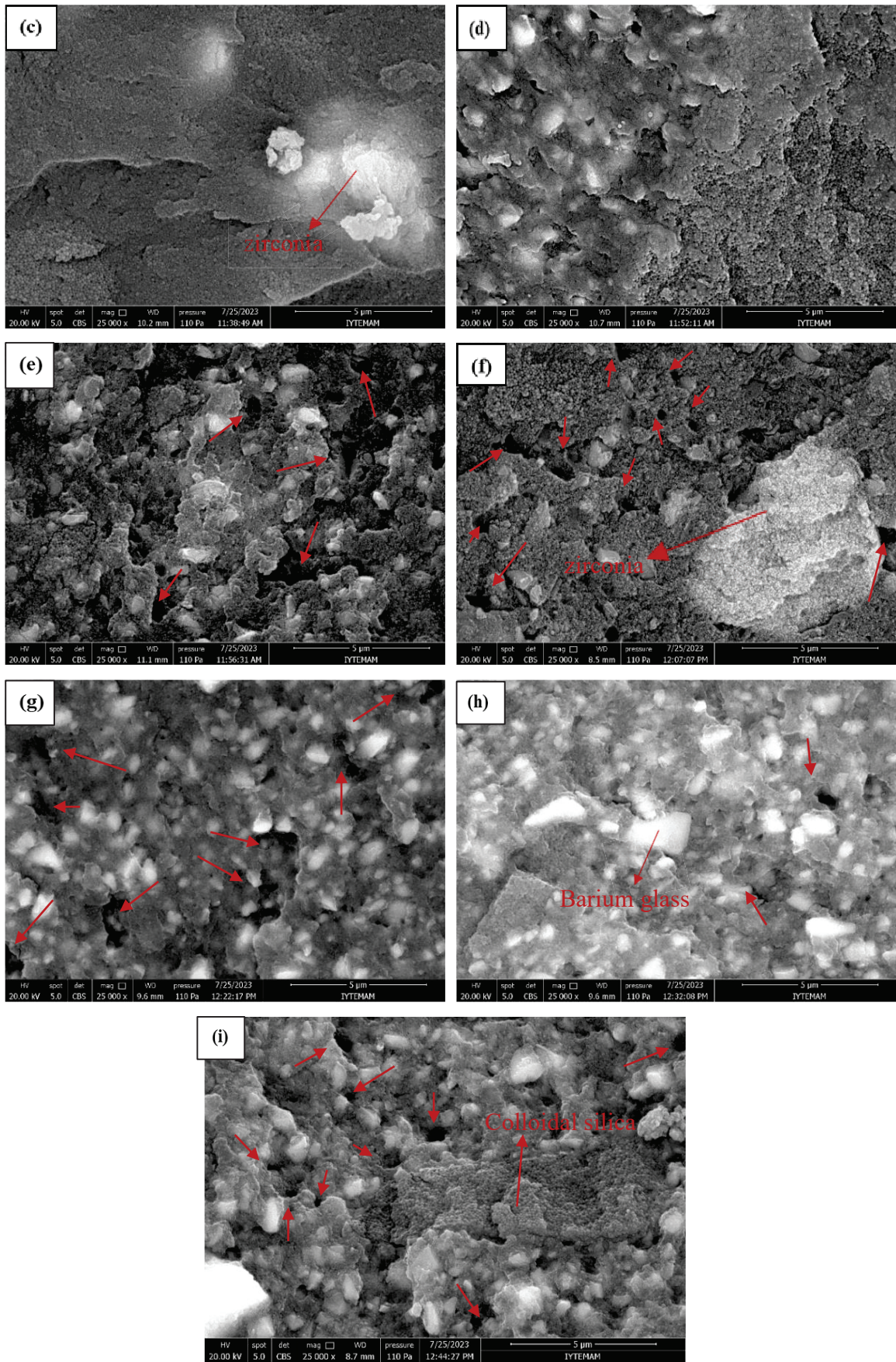


Figure 5.6. (cont.)

The EDS data obtained from the SEM device of the Z2 composite sample shown in Figure 5.7 and Figure 5.9 from two different regions, Spectrum1 and Spectrum2, are shown in Figure 5.8 and Figure 5.10, respectively.

The EDS result for spectrum 1 in Figure 5.8 demonstrates that the chemical composition of the Z2 composite contains 28.37 wt.% oxygen (O), 18.73 wt.% carbon (C), 4.95 wt.% silicon (Si), and 47.95 wt.% zirconium (Zr). This evidence suggests that zirconia nanoparticles agglomerate together.

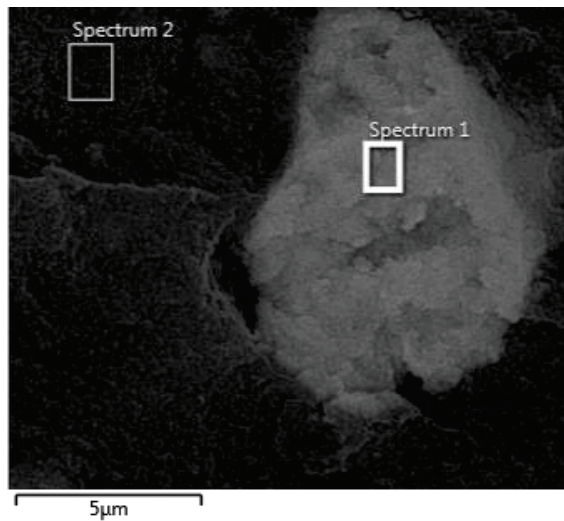


Figure 5.7. Morphological structure image shows spectrum 1 of Z2 composite

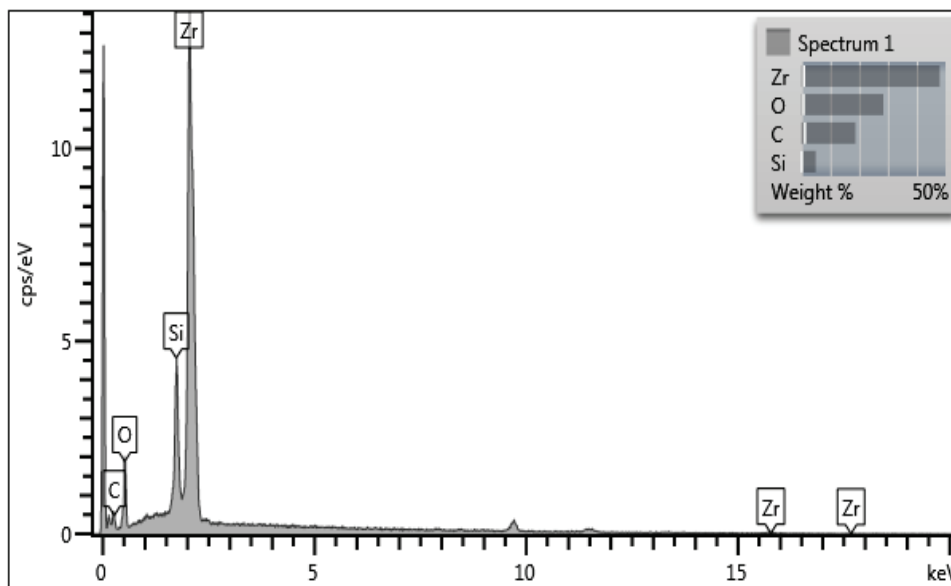


Figure 5.8. Elemental analysis of Z2 composite results for spectrum 1

The EDS result for Figure 5.10 spectrum 2 indicates that the Z2 composite contains 42.55 wt.% oxygen (O), 30.35 wt.% carbon (C), and 27.1 wt.% silicon (Si) in its chemical composition.

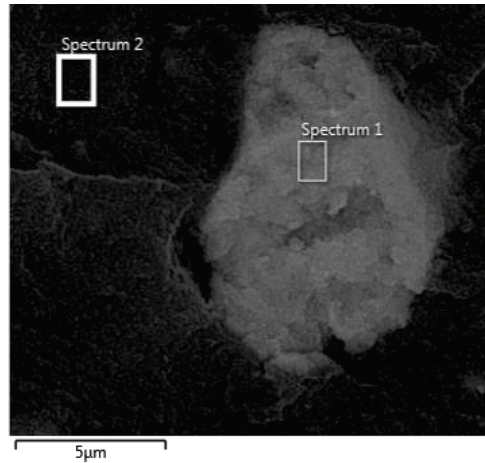


Figure 5.9. Morphological structure image shows spectrum 2 of Z2 composite

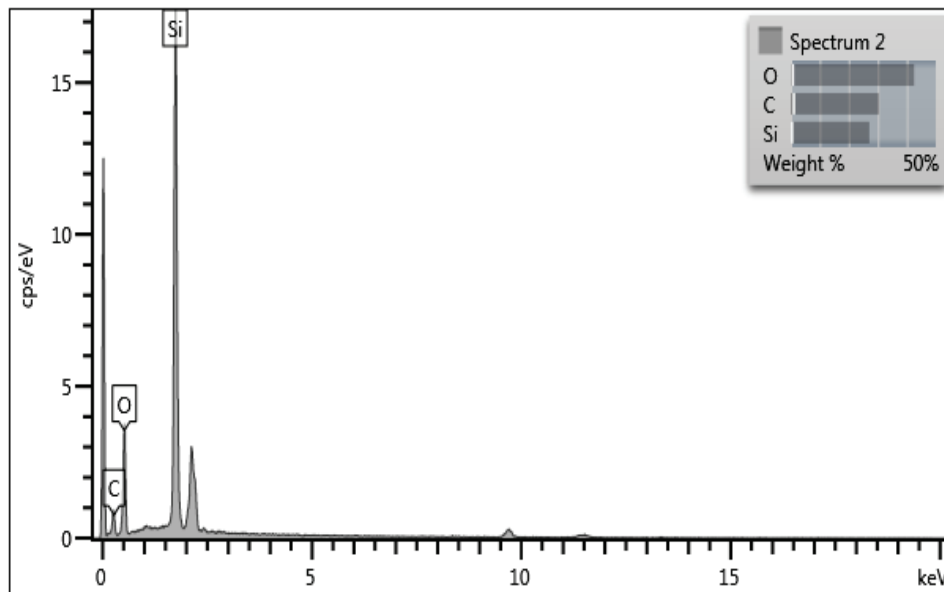


Figure 5.10. Elemental analysis of Z2 composite results for spectrum 2

In addition, EDS mapping analysis of Z2 composite is given in Figure 5.11. The elemental distribution within the structure was determined according to the SEM images in Figure 5.11. When analysed, it was found that carbon, oxygen and silicon in the structure exhibited a homogeneous distribution in general, but zirconium showed clustering in some regions.

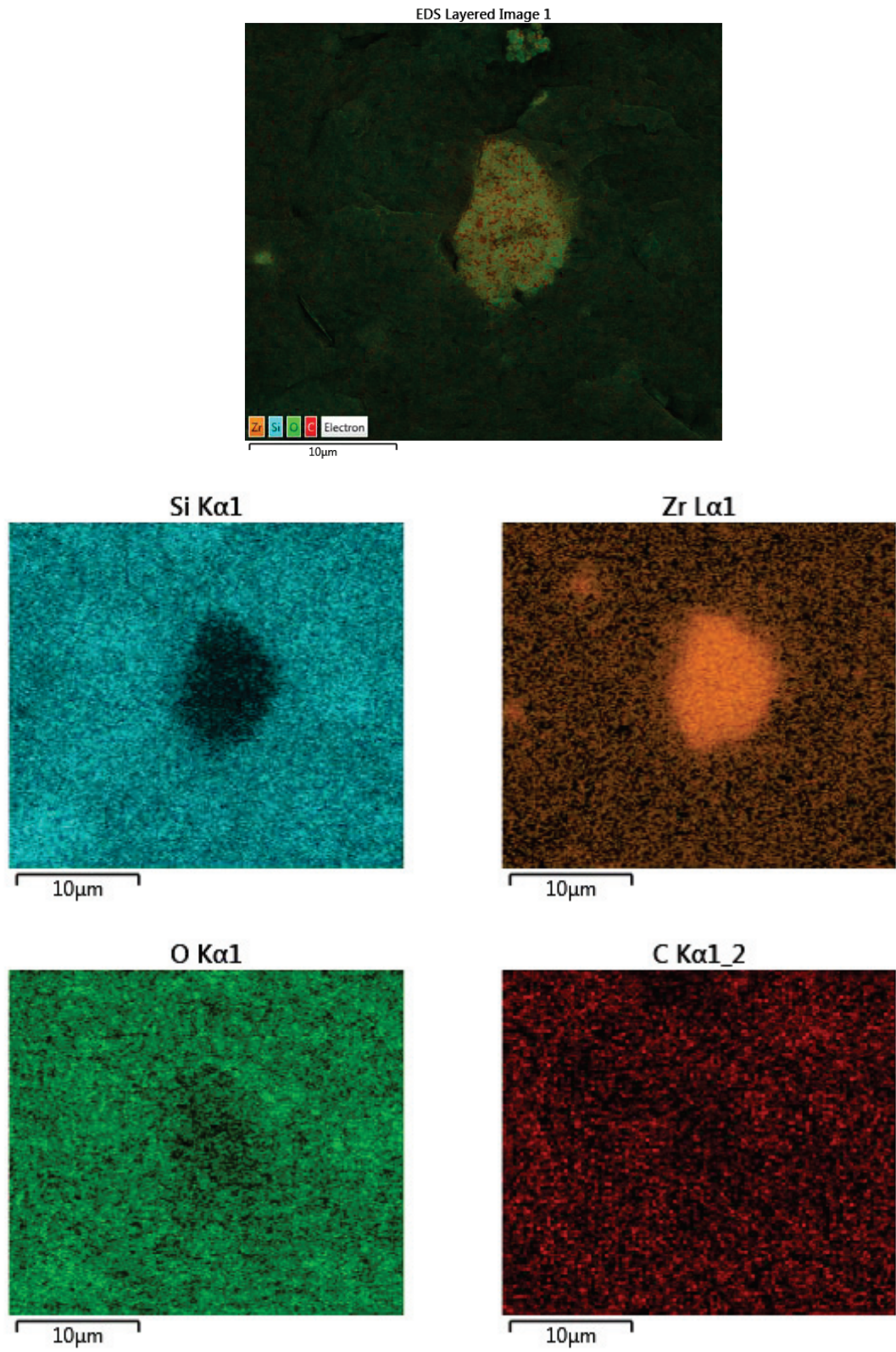


Figure 5.11. EDS mapping analysis of Z2 composite

The EDS data of the Ba2OZ2 composite sample obtained from the SEM instrument was obtained from spectrum 10 in Figure 5.12. The EDS result for spectrum 10 in Figure 5.13 indicates that the Ba2OZ2 composite contains 34.77 wt.% oxygen (O), 55.98 wt.% zirconium (Zr) and 9.24 wt.% silicon (Si) in its chemical composition.

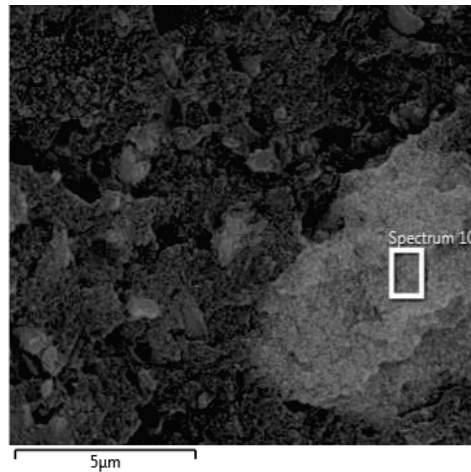


Figure 5.12. morphological structure image of Ba2OZ2 composite

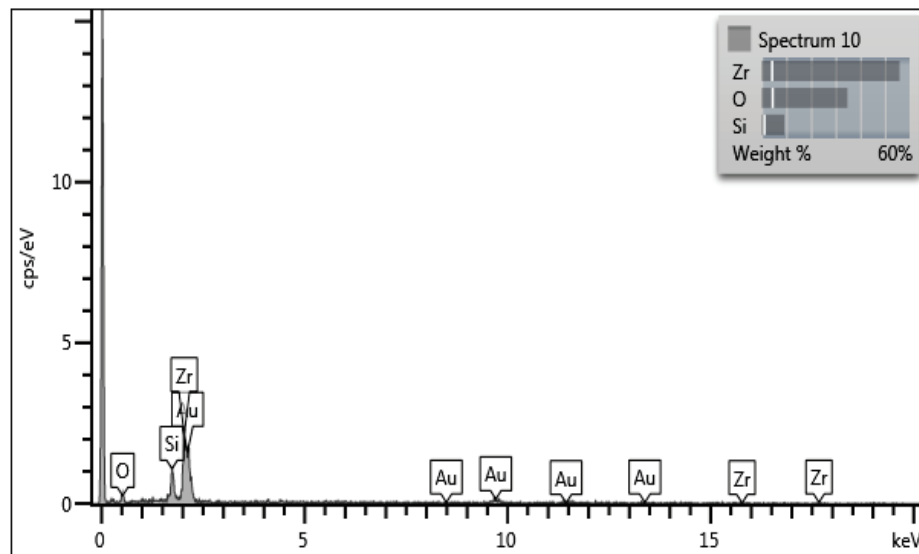


Figure 5.13. Elemental analysis of Ba2OZ2 composite results for spectrum 10

5.1.2. Dynamic Light Scattering (DLS) Analysis of Nanoparticles

The volume % and particle size distributions of fumed silica, colloidal silica, zirconia and barium glass nanoparticles are shown in Figure 5.14, Figure 5.15, Figure 5.16 and Figure 5.17, respectively. The particle sizes of colloidal silica, zirconia

and barium glass were observed to be 60-300 nm, 7-40 and 560-770 nm respectively, while the particle size of fumed silica was found to be in the wide range of 70-600 nm.

Fumed silica nanoparticles agglomerate due to the hydrogen bonds of the silanol groups ($\equiv\text{Si-OH}$) in their structure. Clusters formed by agglomeration are measured as large particles in particle size distribution analysis. This explains the wide range of particle size distributions of fumed silica.

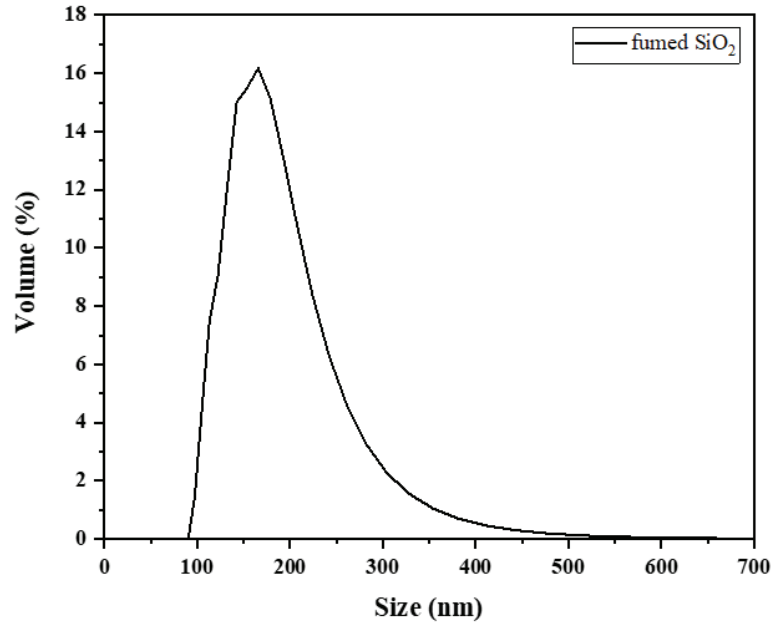


Figure 5.14. Particle size distribution of fumed silica

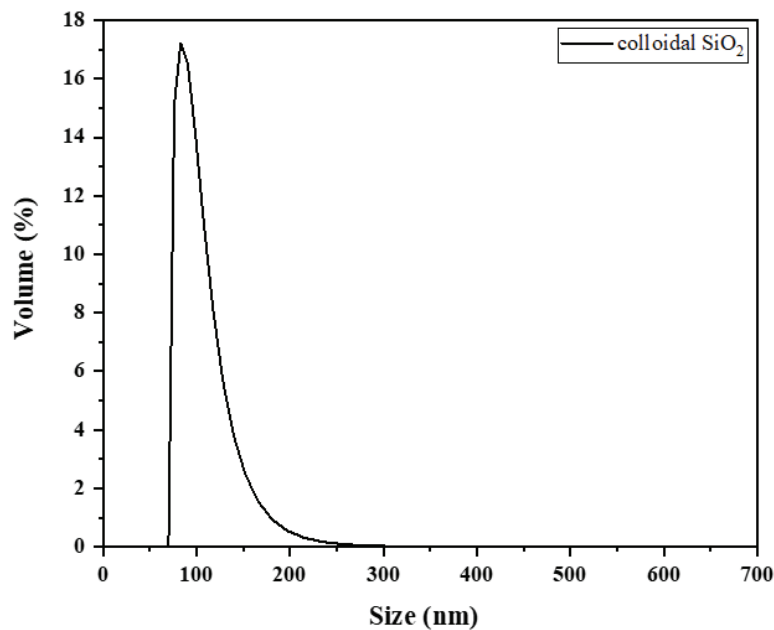


Figure 5.15. Particle size distribution of colloidal silica

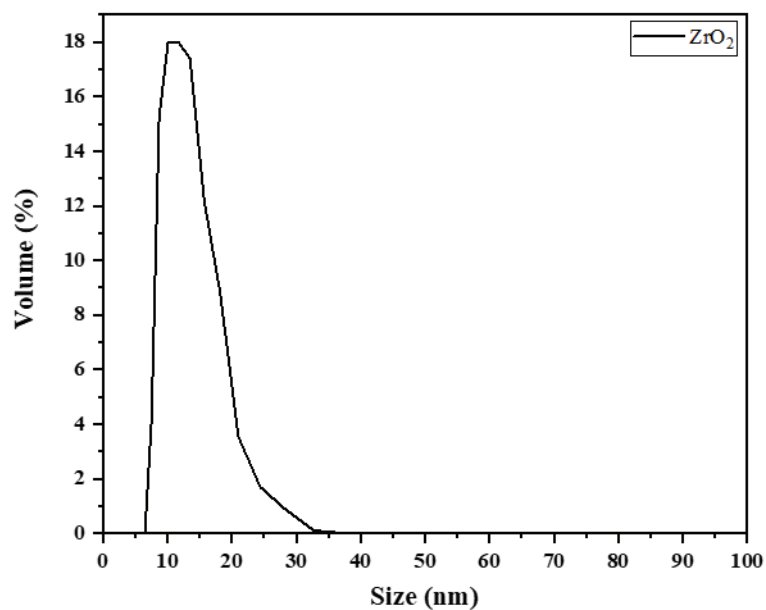


Figure 5.16. Particle size distribution of zirconia

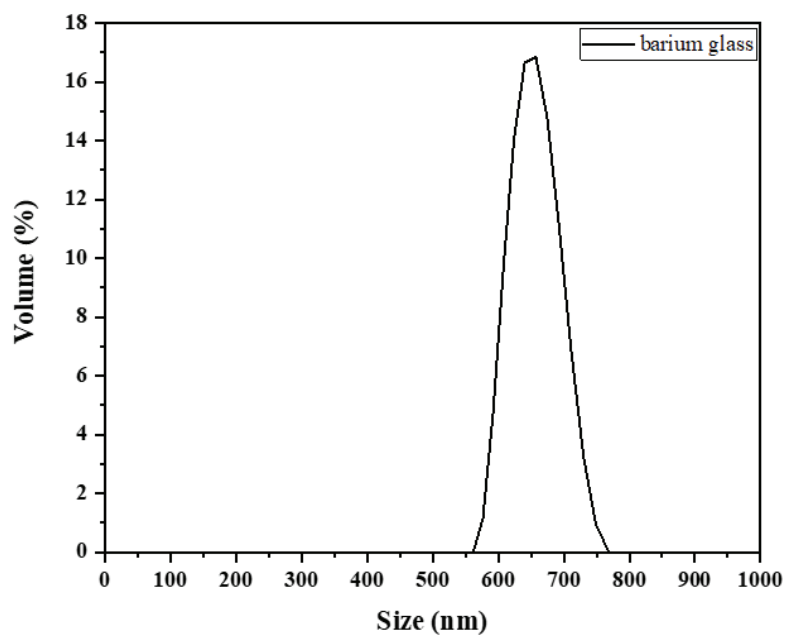


Figure 5.17. Particle size distribution of barium glass

The mean particle sizes of fumed silica, colloidal silica, zirconia and barium glass nanoparticles were obtained as 212.0 nm, 134.3 nm, 12.99 nm and 654.4 nm, from the data presented in Figure 5.14, Figure 5.15, Figure 5.16 and Figure 5.17, respectively.

5.1.3. Fourier Transform Infrared Spectroscopy (FT-IR)

The FTIR spectra of fumed silica, colloidal silica, zirconia and barium glass particles with untreated surface and surface treated with γ -MPS silane are shown in Figure 5.18, Figure 5.19, Figure 5.20 and Figure 5.21, respectively.

As shown in Figure 5.18 and Figure 5.19 strong bending vibrations of Si-OH and stretching vibration of Si-O-Si (siloxane) bonds are observed at around 811 cm^{-1} and around 1110 cm^{-1} respectively. These bonds are indicative of the presence of silica in the environment because they are present in the silica structure and are also formed after surface treatment with γ -MPS.²³ Peaks are observed at 1720 cm^{-1} and $2890\text{-}2980\text{ cm}^{-1}$. These peaks are referred to as the stretching vibrations of the C=O and C-H bonds that are observed in the silica particles treated with γ -MPS. These peaks are an indication of successful surface modification between the silica hydroxyl of pure SiO₂ and the methoxyl of γ -MPS.^{62,54}

As seen in Figure 5.20 peaks are obtained at $450\text{ to }850\text{ cm}^{-1}$ which are related to the bending vibration of the Zr-O bond in the zirconia structure. The formation of peaks at 1150 cm^{-1} is related to the stretching vibration of the Zr-O-Zr bond^{63,64}. The new peaks at 1720 cm^{-1} and 2980 cm^{-1} correspond to the stretching vibration of the C=O bond and the C-H bond in the γ -MPS structure, respectively.⁶⁵

In Figure 5.21, the peak at around 450 cm^{-1} represents the bending vibration of the Si-O-Si existence in the glass structure. The peak at 692 cm^{-1} , indicating the presence of barium ions in the structure, is the bending vibration of Ba-O bond formation of glass network. The peaks at 795 cm^{-1} is a symmetric stretching vibration of the O-Si-O bond.^{66,67} The peak around at 980 cm^{-1} is presumably the vibration of the B-O bonds of the BO₄ units and also the stretching frequency of the Si-O-B bond.⁶⁸ The peaks at 1320 cm^{-1} and 1402 cm^{-1} are assigned to the symmetric stretching relaxation of the B-O bond of the BO₃ units.⁶⁷ The peak at 1720 cm^{-1} is attributed to the stretching vibration of the C=O bond present in the γ -MPS structure.

The bonds in the FTIR spectra of the modified and unmodified nanoparticles given in Figure 5.18, Figure 5.19, Figure 5.20 and Figure 5.21 were analysed. The peaks consisting of the stretching vibration of the C-O (carbonyl group) at 1720 cm^{-1} and the stretching vibration of the C-H bond at 2890 cm^{-1} and 2970 cm^{-1} are present in the γ -MPS functionalised group. These bonds were observed in the FTIR spectrum of the

modified nanoparticles. The results showed that the nanoparticles had been modified successfully.⁶⁵

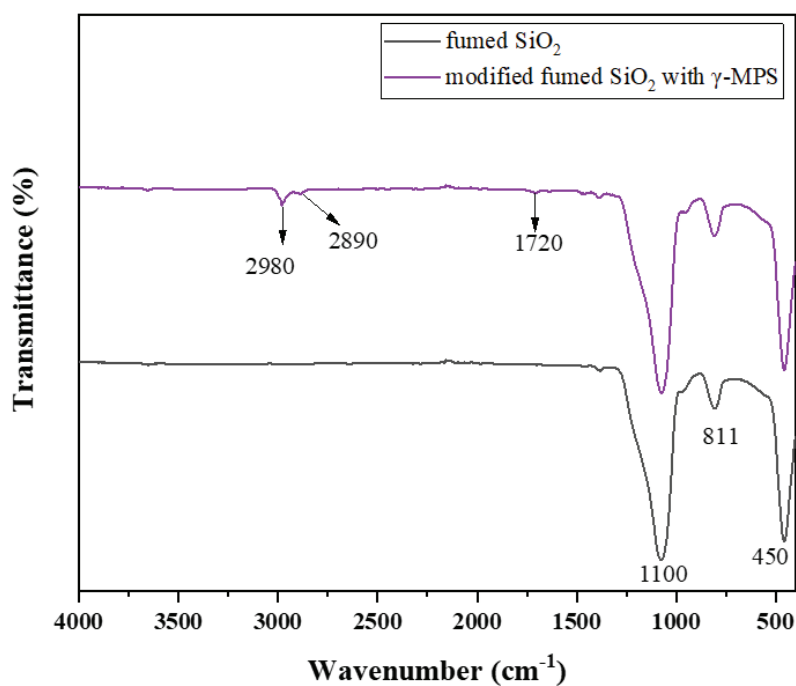


Figure 5.18. FTIR spectra of fumed silica particles with and without surface modification

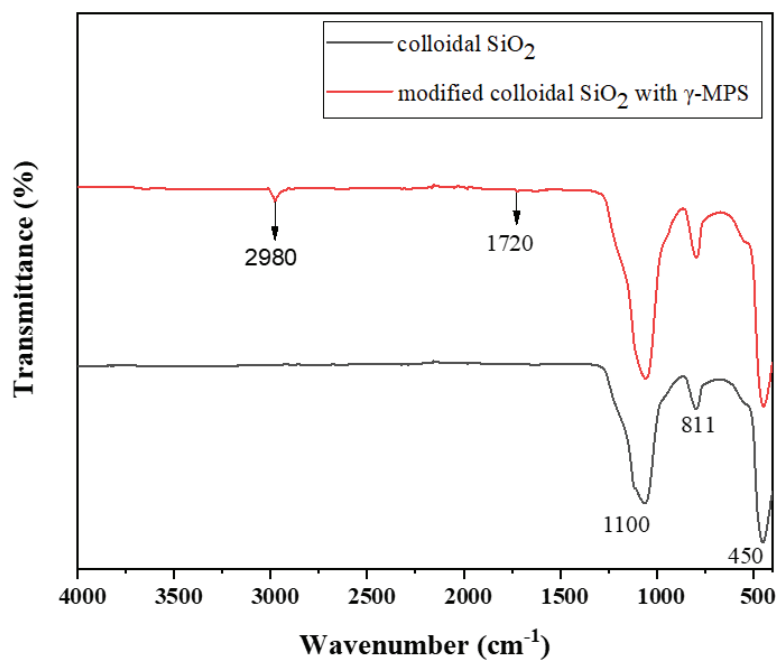


Figure 5.19. FTIR spectra of colloidal silica particles with and without surface modification

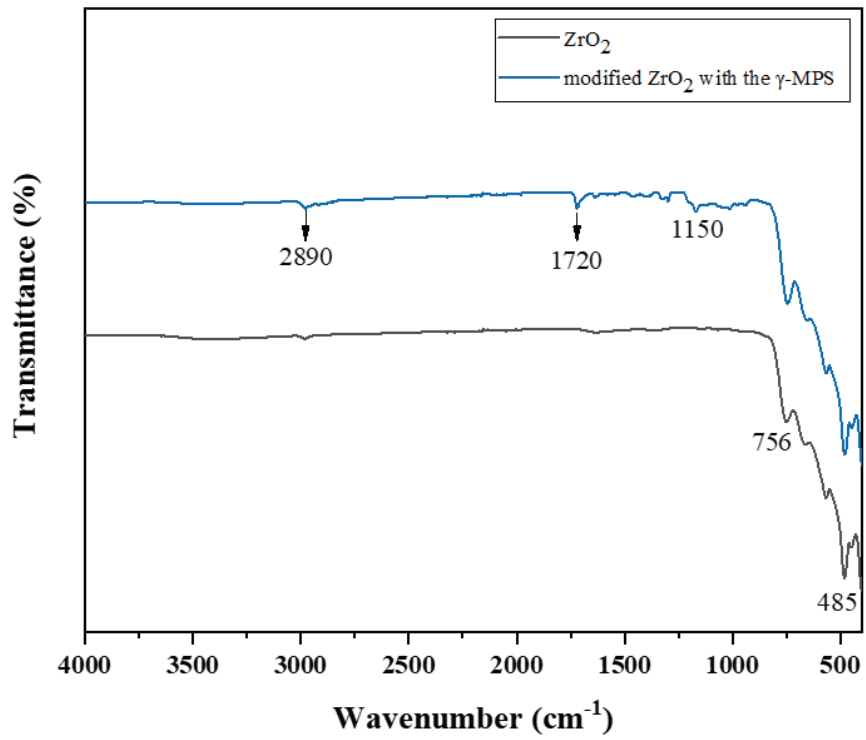


Figure 5.20. FTIR spectra of zirconia particles with and without surface modification

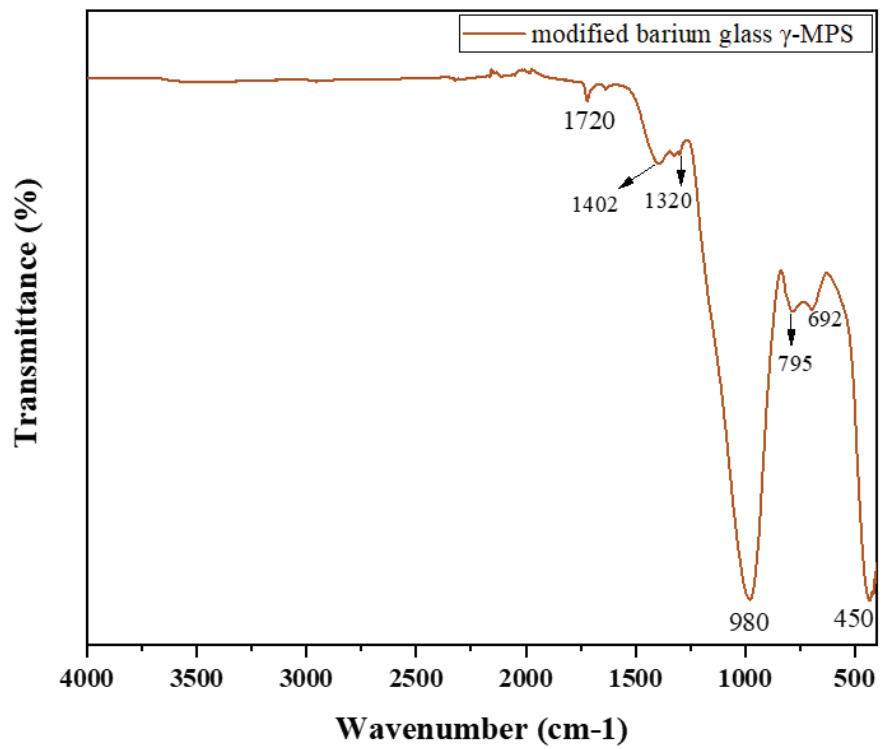


Figure 5.21. FTIR spectra of barium glass particles with and without surface modification

5.2. Mechanical Test Results

Teeth are subjected to forces during chewing. Therefore, resin-based dental composites that replace teeth must be able to withstand these forces. Flexural and compressive strength are therefore critical for resin-based dental composites.

5.2.1. Three-Point Bending Test Results

Flexural strength and flexural modulus are given in Table 5.1, Figure 5.22 and Figure 5.23 for all composites. The ISO 4049 standard specifies flexural strength in two different ways. For Type 1 dental materials and Type 2 all other polymer-based restorative materials. Type 1, materials should have a minimum of 80 MPa, while the other group Type 2, should have a minimum of 50 MPa flexural strength. Therefore, it can be said that the flexural strength of all composites is above the value for Type 2 specified by the standard and flexural strength of sample Ba30Z1 in Type 1 materials.

Table 5.1. Flexural strength and modulus of dental composites

Sample	Flexural Strength (MPa)	Flexural Modulus (GPa)
REF	57.77 ± 5.0	3.73 ± 0.3
Z1	60.54 ± 4.8	4.11 ± 0.44
Z2	63.75 ± 2.5	3.98 ± 0.4
Ba20	68.82 ± 4.8	4.38 ± 0.29
Ba30	67.81 ± 1.16	4.29 ± 0.35
Ba20Z1	71.03 ± 0.6	4.52 ± 0.23
Ba20Z2	72.88 ± 2.0	3.75 ± 0.36
Ba30Z1	79.09 ± 3.32	4.92 ± 0.24
Ba30Z2	74.09 ± 1.67	4.63 ± 0.23

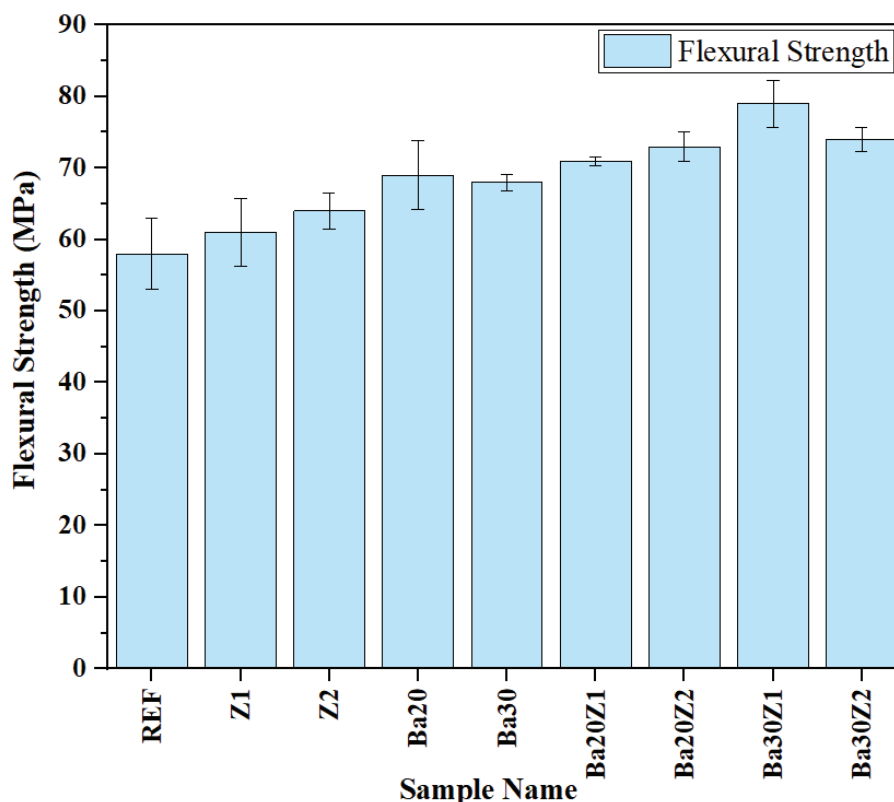


Figure 5.22. Flexural strength results of dental composites with their standard deviation

The lowest flexural strength 57.77 ± 5.0 MPa was obtained from the reference sample containing only the silica fillers. The addition of zirconia and barium glass nanoparticles increased the flexural strength of the composites. The low flexural strength of the reference specimen can be explained by the fact that the flat surface of the specimen shows less resistance to crack propagation and requires less energy. This is supported by the SEM image in Figure 5.6(a) shows a flat surface and a crack.

It was found that the addition of barium glass and zirconia enhance the flexural strength of the composites compared to the Ref. The addition of 20 wt.% Ba glass to the composites resulted in a 19% increase in flexural strength compared to the reference. No significant differences in flexural strength was observed in specimens Ba20 and Ba30. The addition of 1 wt.% and 2 wt.% zirconia increased flexural strength by 5% and 10%, respectively. Agglomeration of zirconia nanoparticles of Z2 sample was found in Figure 5.6(f). This can have a negative effect on flexural strength.

Increasing the zirconia content from 1 wt.% to 2 wt.% resulted in a 5% increase in flexural strength, whereas increasing the barium glass content from 20 wt.% to 30 wt.% led to around 2% decrease in flexural strength. Figure 5.6(d-i) SEM, it is clearly seen that the distance between the fillers increases as the amount of barium increases. It

can be said that the increase in the space between the fillers affects the handling properties by reducing the viscosity of the paste. This can lead to microvoids and porosity formation when the sample is placed in the mould. This is supported by the SEM image of the Ba30 sample in Figure 5.5(g) and Figure 5.6(g). Microvoids are seen in Figure 5.6(g) and large porosities on the of fracture surface of the 30 wt.% sample are also noticed in Figure 5.5(g). Voids have a negative effect on the flexural strength of the sample. Therefore, microvoids and large porosities on the fracture surfaces can be attributed to the no change in flexural strength between Ba20 and Ba30 sample.

There was no difference between the flexural strengths of the Ba20Z1 and Ba20Z2 specimens. This can be attributed to the agglomeration of zirconia nanoparticles and the agglomeration of some spherical silica in Ba20Z2 from the SEM image in Figure 5.6(f).

The interaction between zirconia and barium glass is crucial. The highest flexural strength of 79.09 ± 3.32 MPa was observed in Ba30Z1 specimen. Increasing the barium glass content from 20 wt.% to 30 wt.% while keeping the zirconia content constant at 1 wt.% resulted in a significant 12% increase in flexural strength. The SEM image of fracture surfaces of the composites in Figure 5.6(h) illustrates that the fillers were homogeneously distributed throughout the matrix and well bonded to the matrix phase.

A 7% decrease in flexural strength was reported in the Ba30Z2 specimen compared to the Ba30Z1 specimen. This decrease may be due to agglomeration of the colloidal silica nanoparticles or microvoids caused by poor handling properties when replacing the sample in the mould. Colloidal silica nanoparticles agglomeration and microvoids on the fractured surface of the specimen were seen when examining the SEM image in Figure 5.6(i) and also porosity on the fracture surface of the Ba30Z2 sample is shown in Figure 5.5(i)

The flexural modulus of the composites is also shown in Figure 5.23. The flexural modulus of the composites is in the range of 3.73 - 4.92 GPa. In the literature for hybrid filled resin based composites the flexural modulus is between 3 and 10 GPa, therefore it can be said that the flexural modulus of the composites is comparable with the literature. Adding particles to the resin increases the modulus by limiting the movement of the resin. The addition of zirconia and barium glass nanoparticles increased the flexural modulus of the composites compared to the reference.

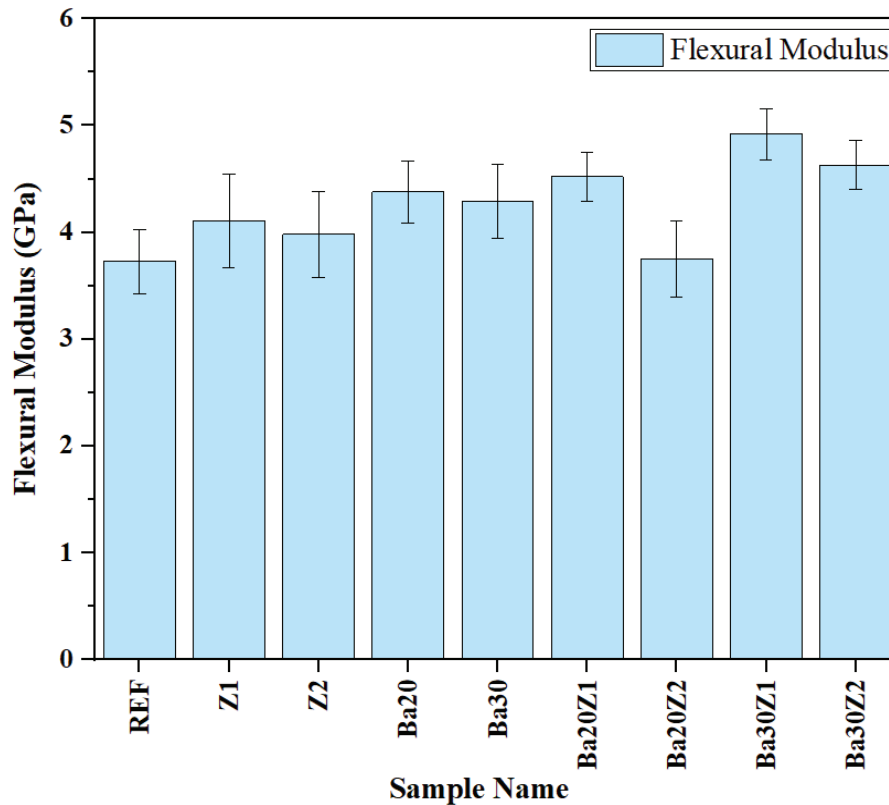


Figure 5.23. Flexural modulus results of dental composites with their standard deviation

5.2.2. Compression Test Results

Table 5.2 and Figure 5.24 show the compressive strength of the composite that contained different concentration of the silanized zirconia, barium glass and silica fillers and their cross effect. According to the literature compressive strength of the resin based dental composite filled with hybrid inorganic filler from 150 to 250 MPa. All results of the compressive strength in that range.

The result shows lowest compressive strength of 177.31 ± 8.3 MPa was observed REF sample which only silica particles were present. All samples have higher compressive strength compare to the REF. Therefore, addition of zirconia and barium glass filler enhanced the compressive strength of the composites.

It was found that the addition of barium glass offered a significant increase in compressive strength compared to zirconia. The compressive strengths of specimens containing both barium and zirconia particles were higher than those containing only barium or only zirconia particles. Therefore, barium glass and zirconia nanoparticles have the synergetic effect together. The highest compressive strength value of 250.05 ± 8.01 MPa was achieved by sample Ba20Z2.

Table 5.2. Compressive strength of dental composites

Sample	Compressive Strength (MPa)
REF	177.31 ± 8.3
Z1	182.15 ± 8.2
Z2	194.99 ± 8.1
Ba20	220.08 ± 8.8
Ba30	213.254 ± 9.8
Ba20Z1	223.23 ± 6.5
Ba20Z2	250.05 ± 8.01
Ba30Z1	243.08 ± 11.4
Ba30Z2	232.51 ± 8.7

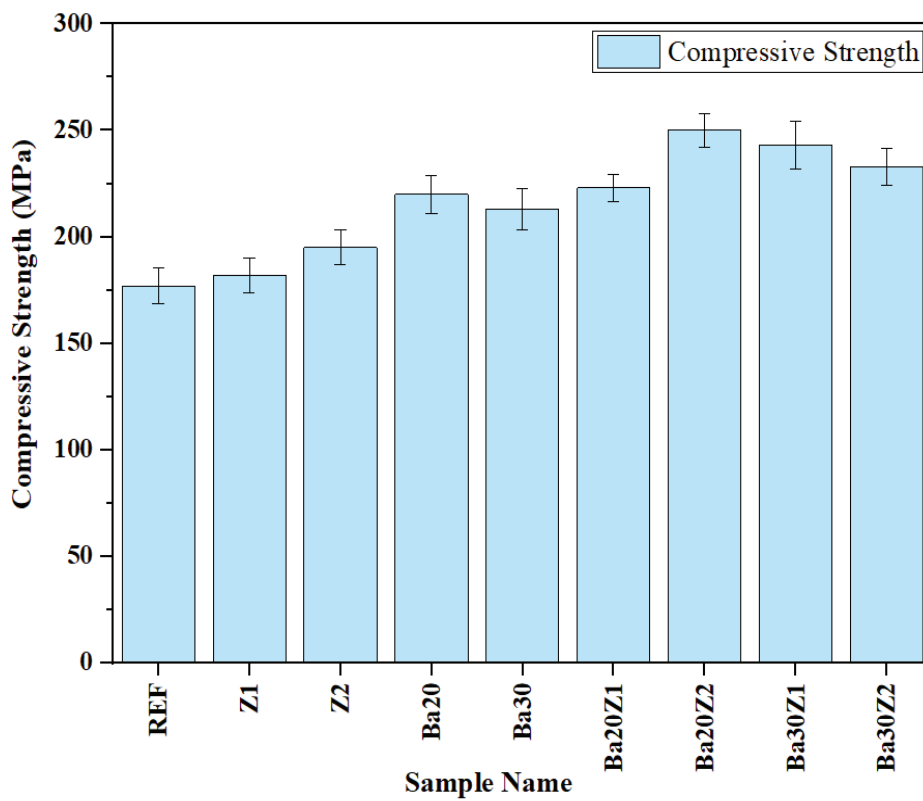


Figure 5.24. Compressive strength results of dental composites with their standard deviation

The compression values of the 30 wt.% barium specimens were lower than the Ba20 specimen. As the viscosity of the paste decreases with the addition of barium glass, voids may form when the paste is placed in the mould. This decrease in

compressive strength can be explained by voids formed in the specimen or non-uniform distribution of fillers in the matrix. From the SEM images in Figure 5.6, it was seen that the composites containing 30 wt.% Ba glass had spaces between the fillers. There is enough space to add more nanoparticles to these composites. Based on these SEM images, it can also be said that the decrease in compressive strength of composites containing 30 wt.% Ba glass is due to the porosity and microvoids formed during transfer into the composite mould.

As the addition of zirconia increased, the compressive strength of the composites increased. However, the compressive strength of the Ba30Z2 sample decreased by 4% compared to the Ba30Z1 sample. This may be related to the depth of cure or agglomeration of the zirconia nanoparticles. The refractive index of zirconia is much higher than that of resin and the curing depth of the composites decreased as the addition of zirconia increased. Therefore, the composite may not cure properly, leading to a reduction in compressive strength.

5.3. Depth of Cure Determination Results of Dental Composites

The depths of cure of the dental composites with standard deviations were measured as shown in the Table 5.3 and Figure 5.25.

Table 5.3. Curing depth of the composites

Sample	Depth of Cure (mm)
REF	3.09 ± 0.052
Z1	2.39 ± 0.05
Z2	2.28± 0.063
Ba20	2.7 ± 0.065
Ba30	2.59 ± 0.04
Ba20Z1	2.36 ± 0.05
Ba20Z2	2.23 ± 0.04
Ba30Z1	2.34 ± 0.034
Ba30Z2	2.11 ± 0.047

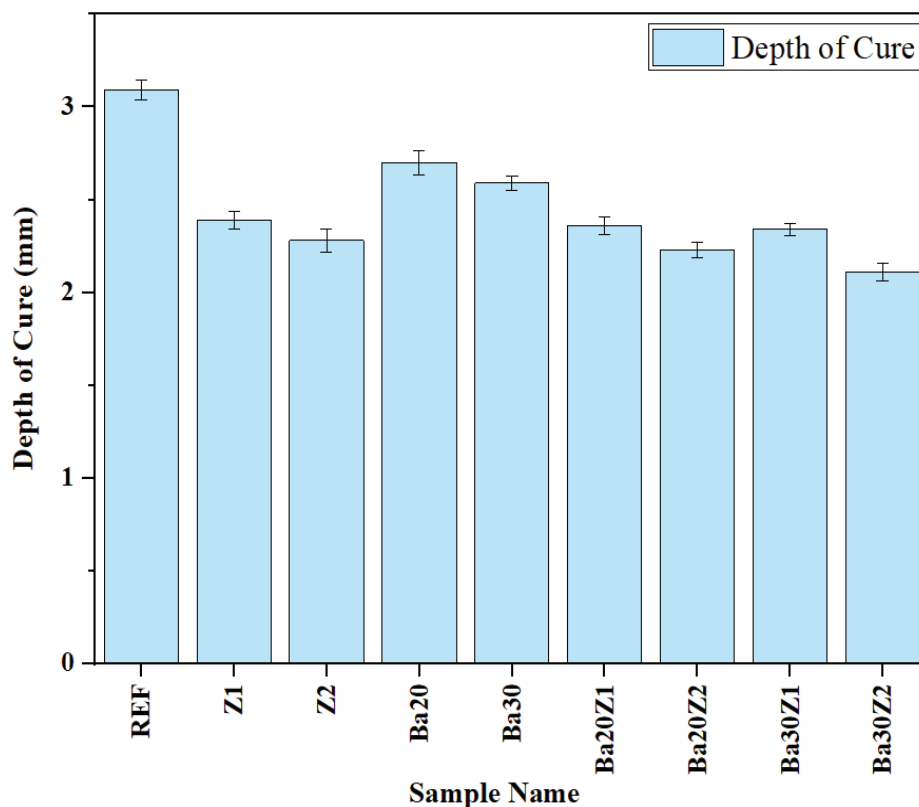


Figure 5.25. Curing depth of dental composites with their standard deviation

The highest curing depth was achieved with the reference composite, and a decrease in composite curing depth was observed when barium glass and zirconia inorganic nanoparticles were added to the composite.

It was observed that zirconia had a greater effect on curing depth than barium glass when considering the effect of zirconia and barium glass particles. The reason for this is directly related to the refractive index. As shown in the Table 2.5 the refractive index of zirconia is higher than the refractive index of barium glass. Inorganic particles added to the resin cause light scattering and adversely affect light transmission. This has a direct effect on the depth of cure. The refractive indices of the inorganic particles added to the resin should be very close to the resin to reduce light scattering. The Table 2.5 shows that the refractive index of the silica nanoparticles is very close to that of the monomers used. Therefore, the curing depth was highest in the reference where there is less light scattering compared to other composites. The addition of inorganic particles, such as zirconia and barium glass, to the resin increases light scattering and decreases curing depth due to their higher refractive indices. Composites containing zirconia have a lower depth of cure compared to those containing barium glass due to

higher refractive index of zirconia than barium glass. Thus, high light scattering in composites containing zirconia reduces the depth of cure.

The highest curing depth of 3.09 ± 0.052 mm was measured in REF, while the lowest curing depth of 2.11 ± 0.047 mm was measured in Ba30Z2. The curing depth of all composites is above the minimum of 1.5 mm specified in ISO 4049 standard.

5.4. Water Sorption and Solubility Test Results of Dental Composites

Water sorption causes disadvantages such as swelling and discolouration of the composite over time, so it is an important property of composites. It is important to keep water sorption in composites as low as possible in order to minimise these negative effects⁵⁷. Water sorption and solubility values were determined on the basis of ISO 4049 and the results are given in Table 5.4, Figure 5.26 and Figure 5.27. According to ISO 4049, the maximum acceptable values for water sorption and solubility are $40 \mu\text{g}/\text{mm}^3$ and $7.5 \mu\text{g}/\text{mm}^3$, respectively.

All composites have high water absorption and solubility values, but these values are below the maximum limit value according to ISO 4049. The composite with only 65 wt.% silica exhibits the lowest water sorption with a value of $26.19 \pm 2.02 \mu\text{g}/\text{mm}^3$. The water sorption is increased by the addition of barium glass and zirconia.

Table 5.4. Water sorption and water solubility of the dental composites

Sample	Water Sorption ($\mu\text{g}/\text{mm}^3$)	Solubility ($\mu\text{g}/\text{mm}^3$)
REF	26.19 ± 2.02	4.30 ± 1.97
Z1	27.09 ± 6.72	4.65 ± 0.47
Z2	28.06 ± 3.58	4.92 ± 1.28
Ba20	31.69 ± 2.75	5.04 ± 1.68
Ba30	35.02 ± 2.93	5.44 ± 1.77
Ba20Z1	32.24 ± 2.08	5.25 ± 1.47
Ba20Z2	33.65 ± 4.4	6.61 ± 1.15
Ba30Z1	36.12 ± 3.99	6.44 ± 1.81
Ba30Z2	37.43 ± 7.19	6.68 ± 1.55

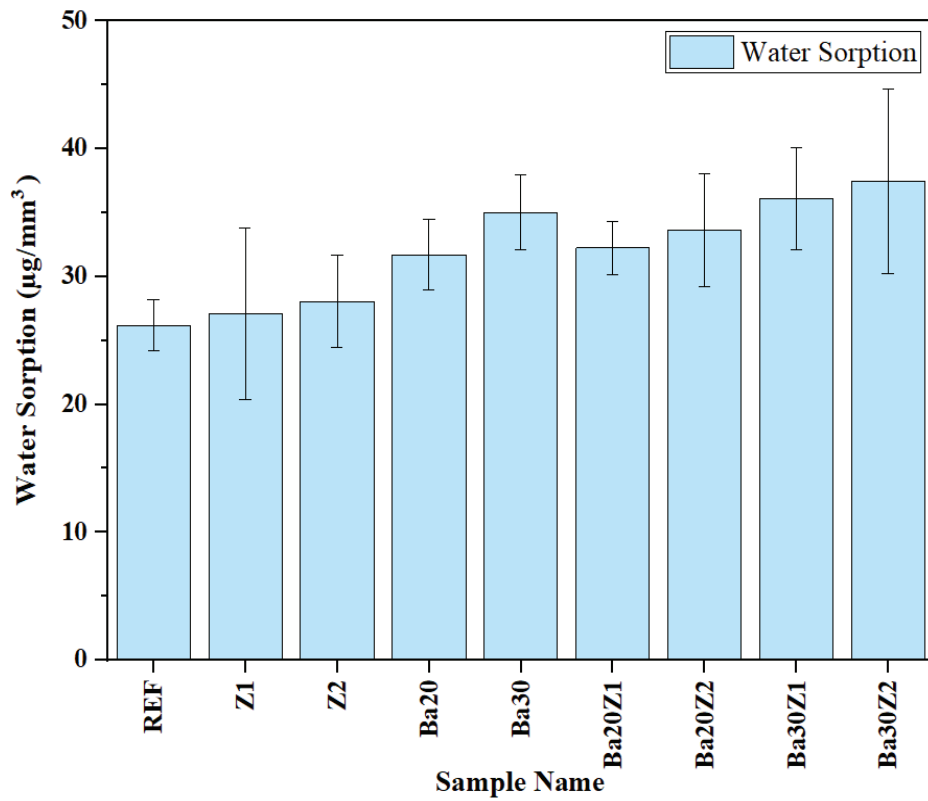


Figure 5.26. Water sorption results of dental composites with their standard deviation

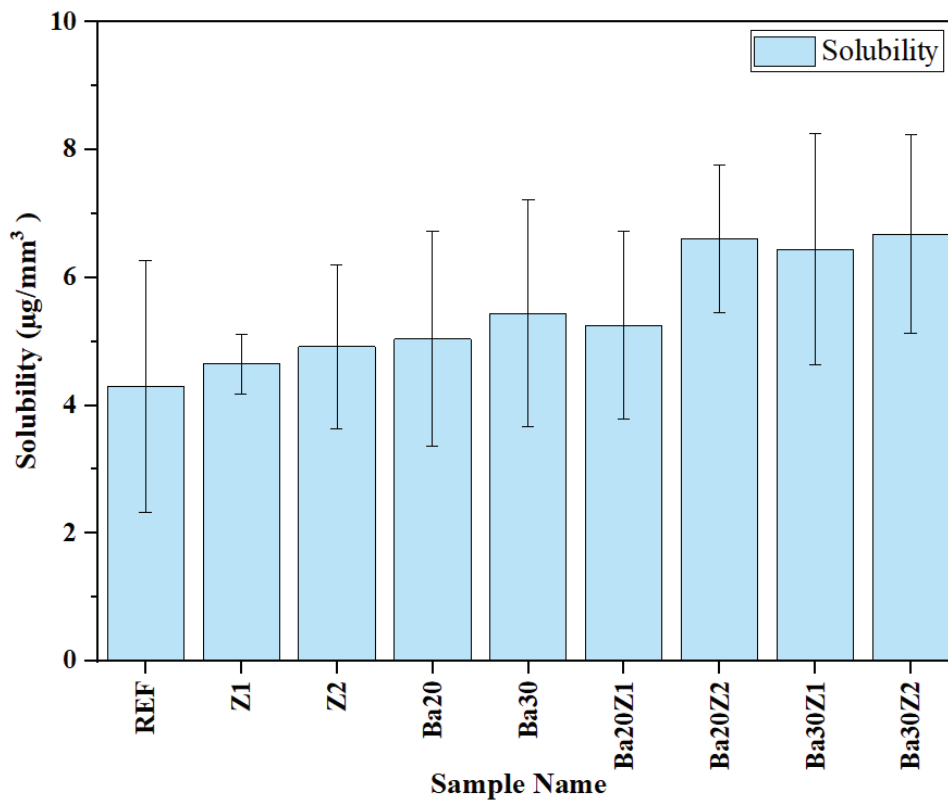


Figure 5.27. Water solubility results of dental composites with their standard deviation

The barium replaces the hydrogen ion in the water when composites containing barium glass come into contact with water. This results in an increase in the pH of the water and the hydrolysis of the silanol bond occurred between the filler and of γ -MPS silane. Therefore, interface between the matrix and filler is destroyed. As a result, water sorption is high due to the low water resistance of barium glass-filled composites.⁶⁰

The results in Figure 5.26 show an increase in water sorption between the control group and increasing zirconia nanoparticles. This is attributed to the high surface area of the zirconia nanoparticles. As the amount of zirconia increases, the surface area of the fillers in the composite increases. Thus increasing the diffusion of water molecules through the gaps between the matrix chains.⁵⁷

Furthermore, as the barium glass increases, the amount of resin in the composites increases and the amount of filler per unit area decreases. This means that sparse fillers are present in the matrix instead of compact tight fillers. Moreover, this situation allows water molecules to move more easily through the matrix chains due to the presence of more matrix phases in the environment. It can be said that the increase in water absorption of composites as barium glass increases is directly related to this situation. In addition, this may also lead to a decrease in viscosity, resulting in the formation of voids during the moulding of the composite. The presence of micro voids and porosity in the samples of barium glass, as shown in Figure 5.5 and Figure 5.6, may also increase to water sorption. The water solubility of the composites increased with increasing barium and zirconia concentration.

5.5. Polymerization Shrinkage Test Results of Dental Composites

The polymerization shrinkage of the composites was calculated in accordance with ISO 17304, using Archimedes' principle and the results are given in Table 5.5 and Figure 5.28. The Ref sample exhibits the lowest polymerization shrinkage. An increase in polymerization shrinkage was observed with increasing concentrations of zirconia and barium glass in the composites. The polymerization shrinkage values obtained vary between 3.45% and 7.9%, depending on the fillers and their contents in the composite. The highest polymerisation shrinkage value, 7.9%, was measured in the Ba30Z2 sample, while the lowest polymerisation shrinkage value, 3.45%, was measured in the reference sample.

Table 5.5. Polymerization shrinkage of dental composites

Sample	Pol. Shrinkage (%vol.)
REF	3.45
Z1	3.99
Z2	4.25
Ba20	4.49
Ba30	5.46
Ba20Z1	4.58
Ba20Z2	4.73
Ba30Z1	5.85
Ba30Z2	7.9

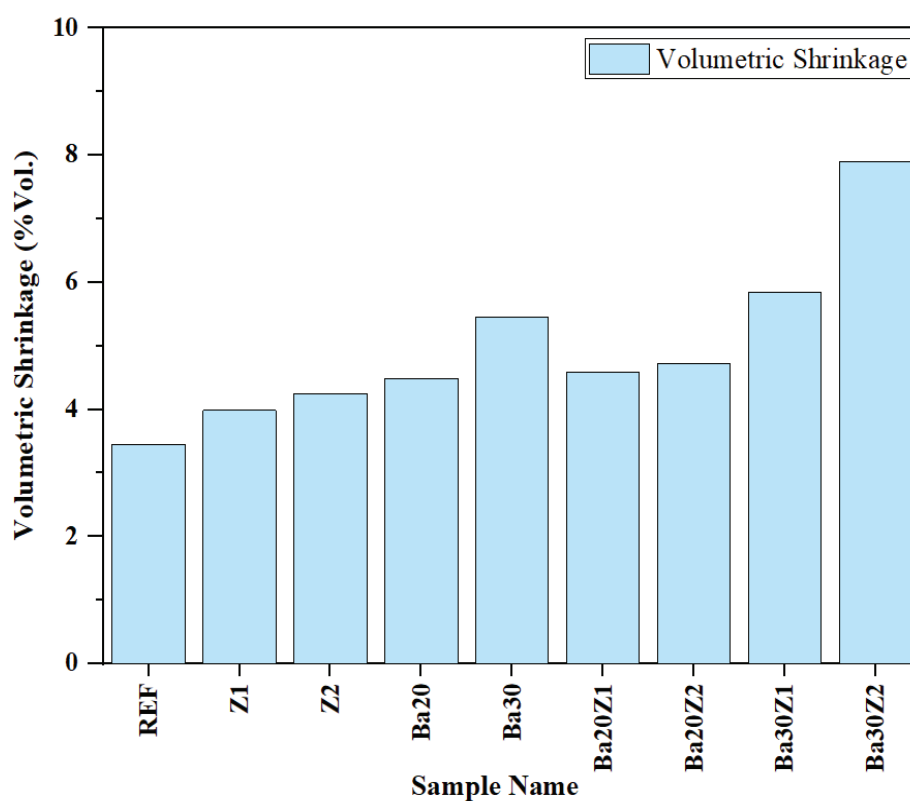


Figure 5.28. Polymerization shrinkage results of dental composites

Also, the polymerization shrinkage values of composites containing two inorganic phases were higher than those of composites containing a single type of inorganic phase.

The polymerisation shrinkage of the composites increased with the concentration of zirconia and barium glass. However, the addition of the 30 wt.% barium glass had a significant negative impact on the polymerization shrinkage of the composites. An increase in the amount of monomer per unit area was observed in barium-glass composites due to the increase barium glass filler particles. This was also evident from the SEM images in Figure 5.6. During polymerisation, the resin turns into a solid form. This causes shrinkage and volume reduction in the resin. There is no volume change in solid filler particles. Therefore, as the amount of resin in the composite increases, an increase in polymerisation shrinkage is expected. Consequently, the composite undergoes volumetric shrinkage.

CHAPTER 6

CONCLUSION

In recent years, resin-based dental composites have become a widely used material in dentistry. Amalgam, which is used as a traditional filling material, presents a significant risk to human health due to the mercury it contains. Amalgam fillings also cause aesthetic concerns due to their dark colour. The development of resin-based composites to overcome these negative properties has achieved a significant scientific breakthrough in dentistry. Today, there is an increasing demand for dental composites. Therefore, studies have focused on improving the mechanical and physical properties of currently used dental composites in various ways. Nanoparticles used as reinforcements have a critical effect on the mechanical and physical properties of the composite. Different filler particles can be used at different filler contents to improve the mechanical and physical properties of composites.

In this thesis, the aim was to improve the mechanical and physical properties of composites using barium glass and zirconia nanoparticles. Due to its large particle size, barium glass allows the amount of filler incorporated into the resin to be increased, allowing the composite to achieve high filler ratios. High filler content improves the mechanical properties of composites. It was known from the literature that zirconia nanoparticles are used because of their positive effect on the mechanical and aesthetic properties of composites. From the literature, 20 wt.% and 30 wt.% for barium glass, 1 wt.% and 2 wt.% for zirconia nanoparticles were determined to be added to the composite. Flexural strength, compressive strength, depth of cure, water absorption and solubility, and polymerisation shrinkage of the composites were examined. Fourier Transform Infrared Spectroscopy (FTIR) was used to determine whether the surface modification of the nanoparticles added to the resin was successful and Scanning Electron Microscopy (SEM) was used to examine the fracture surfaces of composite samples to determine the appropriate filler content (homogeneous and void-free surface) and filler distribution. The results of the FTIR analysis indicated that the surface modification of the nanoparticles was successful. The SEM images showed that the particles were well connected to the matrix, and the composites were successfully produced.

The incorporation of barium glass and zirconia particles into the composite materials resulted in a notable enhancement in the flexural and compressive strength of the materials. The highest flexural strength was observed in the Ba30Z1 sample at 79.09 ± 3.32 MPa and the highest compressive strength was observed in the Ba20Z2 sample at 250.05 ± 8.01 MPa. A 37% increase in flexural strength and a 41% increase in compressive strength were observed in the test sample compared to the reference sample.

The highest cure depth was achieved in the reference sample and a decrease in the composite cure depth was obtained with the addition of zirconia and barium glass. The refractive indices of barium glass and zirconia nanoparticles are higher than the refractive index of the resins used. When the refractive indices are significantly different from those of the resins, light scattering occurs, which results in a reduction in the curing depth. As the refractive index of zirconia is quite high, this has a greater effect on the depth of cure. The lowest cure depth was observed in the Ba30Z2 sample with a decrease of 32%.

All composites provide the water absorption and solubility values specified in the ISO 4049 standard. While the reference sample had the lowest water absorption and solubility values, the addition of zirconia and barium glass particles showed an undesirable increase in the water absorption and solubility values of the composites. Ba30Z2 sample exhibited the highest water absorption with a high increase of 43%. The zirconia nanoparticles, with their high surface area, enable water diffusion between the matrix. As the amount of barium glass increases, the distance between the fillers in the composites increases and the amount of matrix per unit area increases. This implies that there are fewer fillers in the matrix rather than compact, dense fillers. This allows water molecules to move more easily along the matrix chains.

The lowest polymerisation shrinkage was obtained for the reference sample containing only silica. As the concentration of zirconia and barium glass increased, the polymerisation shrinkage of the composites was negatively affected. The highest polymerisation shrinkage was obtained in sample Ba30Z2. The reason for this is that the increased amount of resin leads to more deformation during curing due to the increased distance between the particles and the matrix. In other words, as the amount of barium glass increases, the amount of matrix per unit area in the composite increases and the matrix will shrink more volumetrically during curing.

6.1. Future Works

- The degree of transformation in composites is important in terms of mechanical and physical properties. Therefore, the degree of transformation will be quantified by FT-IR analysis of the composites before and after curing.
- It has been observed that colloidal silica and zirconia nanoparticles tend to agglomerate in the composites. The formation of agglomerates can be prevented by the application of more effective mixing techniques.
- It was demonstrated that as the quantity of barium glass was increased, the distance between the fillers of the composites increased. Consequently, the amount of resin per unit area increased. As this situation affects the handling properties of the composite, it is important to measure the viscosity of the composites with a rheometer.
- While the mechanical properties of the composites were enhanced by the addition of zirconia and barium glass nanoparticles, an undesirable increase in polymerisation shrinkage, water absorption and solubility was observed. Further studies could be carried out to improve the polymerisation, water absorption and solubility of composites by increasing the filler content or by investigating and adding different nanoparticles.
- The addition of barium glass resulted in an increase in the amount of resin per unit area in composites. Consequently, there is an advantage of increasing barium glass on increasing the filler content. The mechanical and physical properties of composites can be investigated by increasing the filler content.
- Barium glass was used in different concentrations, so the radiopacity of the composites should be analysed.

REFERENCES

1. Hu, C.; Sun, J.; Long, C.; Wu, L.; Zhou, C.; Zhang, X. Synthesis of Nano Zirconium Oxide and Its Application in Dentistry. *Nanotechnol. Rev.* 2019, 8 (1), 396–404. <https://doi.org/10.1515/ntrev-2019-0035>.
2. Rangreez, T. A.; Mobin, R. *Polymer Composites for Dental Fillings*; Elsevier Inc., 2019. <https://doi.org/10.1016/B978-0-12-813742-0.00013-4>.
3. Chaughule, R. S. *Dental Applications of Nanotechnology*; 2018. <https://doi.org/10.1007/978-3-319-97634-1>.
4. Yadav, R.; Kumar, M. Dental Restorative Composite Materials: A Review. *J. Oral Biosci.* 2019, 61 (2), 78–83. <https://doi.org/10.1016/j.job.2019.04.001>.
5. Chan, K. H. S.; Mai, Y.; Kim, H.; Tong, K. C. T.; Ng, D.; Hsiao, J. C. M. Review: Resin Composite Filling. *Materials (Basel)*. 2010, 3 (2), 1228–1243. <https://doi.org/10.3390/ma3021228>.
6. Gallusi, G.; Libonati, A.; Piro, M.; Di Taranto, V.; Montemurro, E.; Campanella, V. Is Dental Amalgam a Higher Risk Factor Rather than Resin-based Restorations for Systemic Conditions? A Systematic Review. *Materials (Basel)*. 2021, 14 (8), 1–17. <https://doi.org/10.3390/ma14081980>.
7. Mulligan, S.; Kakonyi, G.; Moharamzadeh, K.; Thornton, S. F.; Martin, N. The Environmental Impact of Dental Amalgam and Resin-Based Composite Materials. *Br. Dent. J.* 2018, 224 (7), 542–548. <https://doi.org/10.1038/sj.bdj.2018.229>.
8. Chen, M. H. Critical Reviews in Oral Biology & Medicine: Update on Dental Nanocomposites. *J. Dent. Res.* 2010, 89 (6), 549–560. <https://doi.org/10.1177/0022034510363765>.

9. Guo, G.; Fan, Y.; Zhang, J. F.; Hagan, J. L.; Xu, X. Novel Dental Composites Reinforced with Zirconia-Silica Ceramic Nanofibers. *Dent. Mater.* 2012, 28 (4), 360–368. <https://doi.org/10.1016/j.dental.2011.11.006>.
10. Santulli, C. *Nanostructured Polymer Composites for Dental Fillings*; Elsevier Inc., 2019. <https://doi.org/10.1016/b978-0-12-816771-7.00014-4>.
11. Gajewski, V. E. S.; Pfeifer, C. S.; Fróes-Salgado, N. R. G.; Boaro, L. C. C.; Braga, R. R. Monomers Used in Resin Composites: Degree of Conversion, Mechanical Properties and Water Sorption/Solubility. *Braz. Dent. J.* 2012, 23 (5), 508–514. <https://doi.org/10.1590/S0103-64402012000500007>.
12. Kango, S.; Kalia, S.; Celli, A.; Njuguna, J.; Habibi, Y.; Kumar, R. Surface Modification of Inorganic Nanoparticles for Development of Organic-Inorganic Nanocomposites - A Review. *Prog. Polym. Sci.* 2013, 38 (8), 1232–1261. <https://doi.org/10.1016/j.progpolymsci.2013.02.003>.
13. Makvandi, P.; Gu, J. T.; Zare, E. N.; Ashtari, B.; Moeini, A.; Tay, F. R.; Niu, L. na. Polymeric and Inorganic Nanoscopical Antimicrobial Fillers in Dentistry. *Acta Biomater.* 2020, 101 (xxx), 69–101. <https://doi.org/10.1016/j.actbio.2019.09.025>.
14. Zhang, Y. R.; Du, W.; Zhou, X. D.; Yu, H. Y. Review of Research on the Mechanical Properties of the Human Tooth. *Int. J. Oral Sci.* 2014, 6 (2), 61–69. <https://doi.org/10.1038/ijos.2014.21>.
15. Jones, F. H. Teeth and Bones: Applications of Surface Science to Dental Materials and Related Biomaterials. *Surf. Sci. Rep.* 2001, 42 (3–5), 75–205. [https://doi.org/10.1016/S0167-5729\(00\)00011-X](https://doi.org/10.1016/S0167-5729(00)00011-X).
16. Anusavice KJ. Phillips' Science of Dental Materials. 11th ed. St. Louis (Missouri): Elsevier; 2003. p.675.

17. Jin Chun, K.; Yeon Kim, C.; Yeop Lee, J. Mechanical Behaviors of Enamel, Dentin, and Dental Restorative Materials by Three-Point Bending Test. *Dent. Oral Craniofacial Res.* 2016, 2 (4), 309–312. <https://doi.org/10.15761/docr.1000167>.
18. McCabe, J. F. Resin-Modified Glass-Ionomers. *Biomaterials* 1998, 19 (6), 521–527. [https://doi.org/10.1016/S0142-9612\(98\)00132-X](https://doi.org/10.1016/S0142-9612(98)00132-X).
19. Berthelot, J. *Composite Material Mechanical Behavior and Structural Analysis*. New York: Springer-Verlag; 1999.
20. Nicholson, J. W. Adhesive Dental Materials - A Review. *Int. J. Adhes. Adhes.* 1998, 18 (4), 229–236. [https://doi.org/10.1016/S0143-7496\(98\)00027-X](https://doi.org/10.1016/S0143-7496(98)00027-X).
21. Barszczewska-rybarek, I. M. A Guide through the Dental Dimethacrylate Polymer Network Structural Characterization and Interpretation of Physico-Mechanical Properties. 2019.
22. Moszner, N.; Salz, U. New Developments of Polymeric Dental Composites. *Prog. Polym. Sci.* 2001, 26 (4), 535–576. [https://doi.org/10.1016/S0079-6700\(01\)00005-3](https://doi.org/10.1016/S0079-6700(01)00005-3).
23. Najafi, H.; Akbari, B.; Najafi, F.; Abrishamkar, A.; Ramedani, A.; Yazdanpanah, A. Evaluation of Relationship among Filler Amount, Degree of Conversion, and Cytotoxicity: Approaching Performance Enhancement Novel Design for Dental Bis-GMA/UDMA/TEGDMA Composite. *Int. J. Polym. Mater. Polym. Biomater.* 2017, 66 (16), 844–852. <https://doi.org/10.1080/00914037.2016.1277223>.
24. Söderholm, K. J.; Mariotti, A. BIS-GMA-Based Resins in Dentistry: Are They Safe? *J. Am. Dent. Assoc.* 1999, 130 (2), 201–209. <https://doi.org/10.14219/jada.archive.1999.0169>.
25. Khurshid, Z.; Zafar, M.; Qasim, S.; Shahab, S.; Naseem, M.; AbuReqaiba, A. Advances in Nanotechnology for Restorative Dentistry. *Materials (Basel)*. 2015, 8 (2), 717–731. <https://doi.org/10.3390/ma8020717>.

26. Habib, E.; Wang, R.; Wang, Y.; Zhu, M.; Zhu, X. X. Inorganic Fillers for Dental Resin Composites: Present and Future. *ACS Biomater. Sci. Eng.* 2016, 2 (1), 1–11. <https://doi.org/10.1021/acsbiomaterials.5b00401>.
27. Byrne, G. S. Adhesive Formulations Manipulated by the Addition of Fumed Colloidal Silica. *Stud. Conserv.* 1984, 29 (April), 78–80. <https://doi.org/10.1179/sic.1984.29.Supplement-1.78>.
28. Hyde, E. D. E. R.; Seyfaee, A.; Neville, F.; Moreno-Atanasio, R. Colloidal Silica Particle Synthesis and Future Industrial Manufacturing Pathways: A Review. *Ind. Eng. Chem. Res.* 2016, 55 (33), 8891–8913. <https://doi.org/10.1021/acs.iecr.6b01839>.
29. Miao, X.; Li, Y.; Zhang, Q.; Zhu, M.; Wang, H. Low Shrinkage Light Curable Dental Nanocomposites Using SiO₂ Microspheres as Fillers. 2012, 32, 2115–2121. <https://doi.org/10.1016/j.msec.2012.05.053>.
30. Bapat, R. A.; Yang, H. J.; Chaubal, T. V.; Dharmadhikari, S.; Abdulla, A. M.; Arora, S.; Rawal, S.; Kesharwani, P. Review on Synthesis, Properties and Multifarious Therapeutic Applications of Nanostructured Zirconia in Dentistry. *RSC Adv.* 2022, 12 (20), 12773–12793. <https://doi.org/10.1039/d2ra00006g>.
31. Wang, Y.; Hua, H.; Liu, H.; Zhu, M.; Zhu, X. X. Surface Modification of ZrO₂ Nanoparticles and Its Effects on the Properties of Dental Resin Composites. *ACS Appl. Bio Mater.* 2020, 3 (8), 5300–5309. <https://doi.org/10.1021/acsabm.0c00648>.
32. Haas, K.; Azhar, G.; Wood, D. J.; Moharamzadeh, K.; van Noort, R. The Effects of Different Opacifiers on the Translucency of Experimental Dental Composite Resins. *Dent. Mater.* 2017, 33 (8), e310–e316. <https://doi.org/10.1016/j.dental.2017.04.026>.

33. Pratap, B.; Gupta, R. K.; Bhardwaj, B.; Nag, M. Resin Based Restorative Dental Materials: Characteristics and Future Perspectives. *Jpn. Dent. Sci. Rev.* 2019, 55 (1), 126–138. <https://doi.org/10.1016/j.jdsr.2019.09.004>.
34. Kwon, T. Y.; Bagheri, R.; Kim, Y. K.; Kim, K. H.; Burrow, M. F. Cure Mechanisms in Materials for Use in Esthetic Dentistry. *J. Investig. Clin. Dent.* 2012, 3 (1), 3–16. <https://doi.org/10.1111/j.2041-1626.2012.00114.x>.
35. El-Banna, A.; Sherief, D.; Fawzy, A. S. *Resin-Based Dental Composites for Tooth Filling*; Elsevier Ltd, 2019. <https://doi.org/10.1016/B978-0-08-102476-8.00007-4>.
36. Santini, A. Current Status of Visible Light Activation Units and the Curing of Light-Activated Resin-Based Composite Materials. *Dent. Update* 2010, 37 (4). <https://doi.org/10.12968/denu.2010.37.4.214>.
37. Cramer, N. B.; Stansbury, J. W.; Bowman, C. N. Recent Advances and Developments in Composite Dental Restorative Materials. *J. Dent. Res.* 2011, 90 (4), 402–416. <https://doi.org/10.1177/0022034510381263>.
38. Porto, I. C. C. de M.; Soares, L. E. S.; Martin, A. A.; Cavalli, V.; Liporoni, P. C. S. Influence of the Photoinitiator System and Light Photoactivation Units on the Degree of Conversion of Dental Composites. *Braz. Oral Res.* 2010, 24 (4), 475–481. <https://doi.org/10.1590/S1806-83242010000400017>.
39. Cosola, A.; Chiappone, A.; Martinengo, C.; Grützmacher, H.; Sangermano, M. Gelatin Type A from Porcine Skin Used as Co-Initiator in a Radical Photo-Initiating System. *Polymers (Basel)*. 2019, 11 (11), 1–9. <https://doi.org/10.3390/polym11111901>.
40. Matinlinna, J. P.; Lung, C. Y. K.; Tsoi, J. K. H. Silane Adhesion Mechanism in Dental Applications and Surface Treatments: A Review. *Dent. Mater.* 2018, 34 (1), 13–28. <https://doi.org/10.1016/j.dental.2017.09.002>.
41. Miletic, V. *Dental Composite Materials for Direct Restorations*; 2018.

42. Ferracane, J. L.; Hilton, T. J.; Stansbury, J. W.; Watts, D. C.; Silikas, N.; Ilie, N.; Heintze, S.; Cadenaro, M.; Hickel, R. Academy of Dental Materials Guidance—Resin Composites: Part II—Technique Sensitivity (Handling, Polymerization, Dimensional Changes). *Dent. Mater.* 2017, 33 (11), 1171–1191. <https://doi.org/10.1016/j.dental.2017.08.188>.
43. Klapdohr, S.; Moszner, N. New Inorganic Components for Dental Filling Composites. *Monatshefte fur Chemie* 2005, 136 (1), 21–45. <https://doi.org/10.1007/s00706-004-0254-y>.
44. Kleverlaan, C. J.; Feilzer, A. J. Polymerization Shrinkage and Contraction Stress of Dental Resin Composites. 2005, 1150–1157. <https://doi.org/10.1016/j.dental.2005.02.004>.
45. Liu, Y.; Tan, Y.; Lei, T.; Xiang, Q.; Han, Y.; Huang, B. Effect of Porous Glass-Ceramic Fillers on Mechanical Properties of Light-Cured Dental Resin Composites. *Dent. Mater.* 2009, 25 (6), 709–715. <https://doi.org/10.1016/j.dental.2008.10.013>.
46. Karadaş, M.; Demirbuğa, S. Evaluation of Color Stability and Surface Roughness of Bulk-Fill Resin Composites and Nanocomposites. *Meandros Med. Dent. J.* 2017, 18 (3), 199–205. <https://doi.org/10.4274/meandros.36855>.
47. Sideridou, I.; Tserki, V.; Papanastasiou, G. Study of Water Sorption, Solubility and Modulus of Elasticity of Light-Cured Dimethacrylate-Based Dental Resins. *Biomaterials* 2003, 24 (4), 655–665. [https://doi.org/10.1016/S0142-9612\(02\)00380-0](https://doi.org/10.1016/S0142-9612(02)00380-0).
48. Nayif, an M.; Suliman, A.-H. A.; Nikaido, T.; Ikeda, M.; Foxton, R. M.; Tagami, J. Long-Term Water Sorption of Three Resin-Based Restorative Materials. *Int Chin J Dent* 2005, 5 (January 2015), 1–6.

49. Domingo, C.; Arcs, R. W.; Lopez-Macipe, A.; Osorio, R.; Rodriguez-Clemente, R.; Murtra, J.; Fanovich, M. A.; Toledano, M. Dental Composites Reinforced with Hydroxyapatite: Mechanical Behavior and Absorption/Elution Characteristics. *J. Biomed. Mater. Res.* 2001, 56 (2), 297–305. [https://doi.org/10.1002/1097-4636\(200108\)56:2<297::AID-JBM1098>3.0.CO;2-S](https://doi.org/10.1002/1097-4636(200108)56:2<297::AID-JBM1098>3.0.CO;2-S).
50. Panchbhai, A. *Nanocomposites: Past, Present, and Future of Dentistry*; Elsevier Inc., 2019. <https://doi.org/10.1016/B978-0-12-813742-0.00011-0>.
51. Liu, F.; Jiang, X.; Zhang, Q.; Zhu, M. Strong and Bioactive Dental Resin Composite Containing Poly(Bis-GMA) Grafted Hydroxyapatite Whiskers and Silica Nanoparticles. *Compos. Sci. Technol.* 2014, 101, 86–93. <https://doi.org/10.1016/j.compscitech.2014.07.001>.
52. Khaje, S.; Jamshidi, M. The Effect of Aging and Silanization on the Mechanical Properties of Fumed Silica-Based Dental Composite. *J. Dent. Biomater.* 2015, 2 (4), 124–132.
53. Hosseinalipour, M.; Javadpour, J.; Rezaie, H.; Dadras, T.; Hayati, A. N. Investigation of Mechanical Properties of Experimental Bis-GMA/TEGDMA Dental Composite Resins Containing Various Mass Fractions of Silica Nanoparticles. *J. Prosthodont.* 2010, 19 (2), 112–117. <https://doi.org/10.1111/j.1532-849X.2009.00530.x>.
54. Rodríguez, H. A.; Casanova, H. Effects of Silica Nanoparticles and Silica-Zirconia Nanoclusters on Tribological Properties of Dental Resin Composites. *J. Nanotechnol.* 2018, 2018. <https://doi.org/10.1155/2018/7589051>.
55. Kaleem, M.; Satterthwaite, J. D.; Watts, D. C. Effect of Filler Particle Size and Morphology on Force/Work Parameters for Stickiness of Unset Resin-Composites. *Dent. Mater.* 2009, 25 (12), 1585–1592. <https://doi.org/10.1016/j.dental.2009.08.002>.

56. Kyo-Han Kim, MS, PhD, a Joo L. Ong, MS, PhD, b and Osamu Okuno, MS, P. 1-S2.0-S0022391302000264-Main.Pdf. *J. Prosthet. Dent.* 2002, 87 (6), 642–649.
57. Badr, Rafid M Al. 2018. “Effect of Addition ZrO₂ Nanoparticles to Dental Composites on the Physical and Mechanical Properties.” *International Journal of Scientific & Engineering Research* 9 (6). <http://www.ijser.org>.
58. Chan, K. S.; Nicolella, D. P.; Furman, B. R.; Wellinghoff, S. T.; Rawls, H. R.; Pratsinis, S. E. Fracture Toughness of Zirconia Nanoparticle-Filled Dental Composites. *J. Mater. Sci.* 2009, 44 (22), 6117–6124. <https://doi.org/10.1007/s10853-009-3846-4>.
59. Zidan, S.; Silikas, N.; Al-Nasrawi, S.; Haider, J.; Alshabib, A.; Alshame, A.; Yates, J. Chemical Characterisation of Silanised Zirconia Nanoparticles and Their Effects on the Properties of Pmma-Zirconia Nanocomposites. *Materials (Basel)*. 2021, 14 (12), 1–16. <https://doi.org/10.3390/ma14123212>.
60. Tarumi, H.; Torii, M.; Tsuchitani, Y. Relationship between Particle Size of Barium Glass Filler and Water Sorption of Light-Cured Composite Resin. *Dent. Mater. J.* 1995, 14 (1), 37–44. <https://doi.org/10.4012/dmj.14.37>.
61. Marovic, D.; Tarle, Z.; Hiller, K. A.; Müller, R.; Rosentritt, M.; Skrtic, D.; Schmalz, G. Reinforcement of Experimental Composite Materials Based on Amorphous Calcium Phosphate with Inert Fillers. *Dent. Mater.* 2014, 30 (9), 1052–1060. <https://doi.org/10.1016/j.dental.2014.06.001>.
62. Wang, H.; Zhu, M.; Li, Y.; Zhang, Q.; Wang, H. Mechanical Properties of Dental Resin Composites by Co-Filling Diatomite and Nanosized Silica Particles. *Mater. Sci. Eng. C* 2011, 31 (3), 600–605. <https://doi.org/10.1016/j.msec.2010.11.023>.
63. Rao, T. N.; Hussain, I.; Lee, J. E.; Kumar, A.; Koo, B. H. Enhanced Thermal Properties of Zirconia Nanoparticles and Chitosan-Based Intumescent Flame Retardant Coatings. *Appl. Sci.* 2019, 9 (17). <https://doi.org/10.3390/app9173464>.

64. Shaik, M. R.; Alam, M.; Adil, S. F.; Kuniyil, M.; Al-Warthan, A.; Siddiqui, M. R. H.; Tahir, M. N.; Labis, J. P.; Khan, M. Solvothermal Preparation and Electrochemical Characterization of Cubic ZrO₂ Nanoparticles/Highly Reduced Graphene (HRG) Based Nanocomposites. *Materials (Basel)*. 2019, 12 (5). <https://doi.org/10.3390/ma12050711>.
65. Sideridou, I. D.; Karabela, M. M. Effect of the Amount of 3-Methacyloxypropyltrimethoxysilane Coupling Agent on Physical Properties of Dental Resin Nanocomposites. *Dent. Mater.* 2009, 25 (11), 1315–1324. <https://doi.org/10.1016/j.dental.2009.03.016>.
66. Ansari, M. A.; Jahan, N. Structural and Optical Properties of BaO Nanoparticles Synthesized by Facile Co-Precipitation Method. *Mater. Highlights* 2021, 2 (1–2), 23. <https://doi.org/10.2991/mathi.k.210226.001>.
67. Shao, G.; Wu, X.; Kong, Y.; Cui, S.; Shen, X.; Jiao, C.; Jiao, J. Thermal Shock Behavior and Infrared Radiation Property of Integrative Insulations Consisting of MoSi₂/Borosilicate Glass Coating and Fibrous ZrO₂ Ceramic Substrate. *Surf. Coatings Technol.* 2015, 270, 154–163. <https://doi.org/10.1016/j.surfcoat.2015.03.008>.
68. Rao, T. G. V. M.; Rupesh Kumar, A.; Neeraja, K.; Veeraiah, N.; Rami Reddy, M. Optical and Structural Investigation of Eu³⁺ Ions in Nd³⁺ Co-Doped Magnesium Lead Borosilicate Glasses. *J. Alloys Compd.* 2013, 557, 209–217. <https://doi.org/10.1016/j.jallcom.2012.12.162>.